LOCAL ADAPTATION AND REPRODUCTIVE ISOLATION IN THE COPEPOD *TIGRIOPUS CALIFORNICUS*

Thiago G. Lima

A dissertation submitted to the faculty of the University of North Carolina at Chapel Hill in partial fulfillment of the requirements for the degree of Doctor of Philosophy in the Department of Biology.

Chapel Hill
2015

Approved by:

Christopher S. Willett

Maria R. Servedio

Corbin D. Jones

Todd J. Vision

Mohamed A. F. Noor

ABSTRACT

Thiago G. Lima: Local adaptation and reproductive isolation in the copepod *Tigriopus californicus*
(Under the direction of Christopher Willett)

The evolution of reproductive barriers between species, in many cases is a consequence of genetic divergence that evolves between populations that have become geographically isolated. In this case, processes such as local adaptation and genetic drift will contribute to this divergence, to the point where if the populations come into contact again, some form of reproductive isolation between them will have evolved. Understanding local adaptation, and how it affects a population's ability to deal with environmental changes has also become of interest to biologists, as way to assess how organisms will deal with predict climate changes. In chapter 2 of this dissertation I address how the evolution of reproductive isolation due to intrinsic postzygotic barriers (hybrid sterility and inviability) is affect by the presence/absence of sex chromosomes, which have been deemed important for the evolution of these reproductive barriers. I show that taxa that have heteromorphic sex chromosomes reach higher levels of intrinsic postzygotic isolation at lower levels of genetic divergence. On the other hand, taxa without sex chromosomes remain compatible until much higher levels of genetic divergence. In chapter 3, I look at genome-wide patterns of hybrid inviability in crosses of different levels of genetic divergence between populations of the copepod *Tigriopus californicus*. Theory and data in other species suggest that the more divergent cross should show higher levels of intrinsic reproductive isolation, caused by a larger number of genomic regions that are incompatible between the hybridizing populations. Results however show that the least divergent cross suffers the largest

effects due to hybrid inviability, suggesting that either this cross has a larger number of incompatibilities than the other two crosses, or that the architecture of these incompatibilities leads to a larger inviability effect. In chapter 4 I focus on the effects that differences in local adaptation play on a population's ability to deal with changes in thermal variability in their environment. The results show the populations studied have very different profiles of gene expression across the different temperature treatments, and changes in thermal variability elicited large differences in transcriptome wide expression changes, especially in the least thermal tolerant populations.

ACKNOWLEDGEMENTS

The work in this dissertation would not have been possible without the help of several individuals. I would like to thank my advisor, Chris Willett, for his guidance and incentive while allowing me to be independent in my research program. Maria Servedio, whose advice and suggestions improved the quality of my work, especially for the work in chapter 2. Todd Vision was vital to this work, especially early on, when he advised and helped me transition into a bioinformatics focused research program. Corbin Jones and Mohamed Noor were always willing to give me comments and feedback on ideas at all stages of my graduate career. These five committee members pushed me to be a better scientist, and their guidance has already helped my career immensely.

I would like to thank all the undergraduate students that helped me with my work (Lydia Hatfield, Inna Kovaleva, Judith Mendez-Segovia, Devon Allen and Stephanie Hopkins-Spencer), and Steven Morgan for helping with copepod collection from Bodega Bay. I want to thank Jack Weiss and James Umbanhower for the statistical advice, especially for the work in chapter 2. I am grateful for all the help that Toby Clarke, Eric Earley and Felipe Barreto provided early in my graduate career with analysis of large high-throughput sequencing data. This work would not have been possible without funding from NSF (to Chris Willett), and from the UNC Graduate School, and HHMI at UNC.

I would like to thank Ron Burton and everyone in his lab for hosting me at Scripps Institution of Oceanography during the last year of my Ph.D. Discussions with students and post-

docs in his lab (Ricardo Pereira, Felipe Barreto, Lani Gleason and Tessa Pierce) helped me both analyze and interpret my data.

Finally I would like to thank my friends and family for all their help and support. Sumit Dhole, Heidi MacLean, Rob Aldredge, Eric Earley, Audrey Kelly and Jeeyun Lee helped me with advice on my research, but maybe more importantly they helped me survive grad school, and were always there with a joke (or a beer) when I needed it. And lastly, I am grateful for all the support I received from my family, especially my wife Kerry Baumann, for always encouraging me. I certainly could not have done this without their support.

TABLE OF CONTENTS

LIST OF TABLES

LIST OF FIGURES

CHAPTER I: GENERAL INTRODUCTION

Populations of a species that live in isolation from each other (allopatry), where gene flow is either absent or low, will diverge due to natural selection and genetic drift. Genetic drift will be especially relevant if fluctuations in population size are common, and periods of small population sizes are common. Selection due to abiotic factors should lead to local adaptation of the different populations (Kawecki and Ebert 2004), and when these factors differ between populations, as is the case for species with wide range distribution, this should lead to divergence between the populations. The causes of this genetic divergence between allopatric populations, including which forces are important in different scenarios (e.g. selection versus genetic drift), as well as the consequence of this divergence to the populations, are of great interest to evolutionary biologists (Coyne and Orr 2004; Angilletta 2009). Understanding these processes is a major step in explaining how new species are formed (the process of speciation), which is how the incredible diversity of taxa that we observe today came to be. More recently, interest in understanding local adaptation has also been driven by predictions of global climate change, as a way to assess if species will be able to adapt to the predicted environmental changes.

While there are several definitions of what a "species" is, one of the most commonly used species concept is the biological species concept (BSC). The BSC defines species as groups of populations that are reproductively isolated from other such groups (Mayr 1942). In this concept, the study of the genetics of speciation involves understanding the genetic mechanisms that lead to reproductive isolation, or a decrease in gene flow between populations. These mechanisms can

be prezygotic (such as mate discrimination, or gametic incompatibility), or postzygotic (such as hybrid sterility and inviability). Chapters 2 and 3 of this dissertation focus on intrinsic postzygotic reproductive isolation, which evolve due to incompatibilities between the genomes of two hybridizing taxa. As the genomes of two populations of a species diverge through time, they become increasingly incompatible, and if these populations interbreed, the hybrid offspring may suffer from inviability and sterility. Studies in several groups of taxa show that the strength of intrinsic postzygotic isolation is correlated with the amount of divergence between the hybridizing taxa (e.g. Coyne and Orr 1989; Sasa et al. 1998; Presgraves 2002; Price and Bouvier 2002). A striking pattern regarding the evolution of intrinsic postzygotic isolation is the observation that, in hybrids, when one of the sexes suffers higher sterility or inviability, it is usually the heterogametic sex (males in mammals and *Drosophila*, females in birds and Lepidoptera). This was first described by J.B.S. Haldane, and is thus named Haldane's rule (Haldane 1922). A second important pattern regarding the evolution of intrinsic postzygotic isolation, called the Large-X effect, is the observation that the X chromosome (in XY systems; Z in ZW systems) contributes disproportionately to reproductive isolation (Tao et al. 2003; Masly and Presgraves 2007). These patterns are thought to be so widespread and important, that they were named "two rules of speciation" (Coyne and Orr 1989b), and they highlight the importance of sex chromosomes to the evolution of intrinsic postzygotic isolation.

As described in chapter 2, a large number of species do not have sex chromosomes, in which case these "rules of speciation" should not apply. However, these rules allow us to make predictions regarding how the evolution of intrinsic postzygotic isolation will differ depending on the presence of sex chromosomes as well as the amount of heteromorphism between the sex chromosomes when they are present. In chapter 2 I use predictions based on mechanisms that

lead to the "two rules of speciation" to formalize and test the hypothesis that hybrids between taxa with high levels of sex chromosome heteromorphism will display higher levels of intrinsic postzygotic isolation than species without sex chromosomes for the same amount of genomic divergence. The results of this chapter also show that while Haldane's rule is observed in taxa with heteromorphic sex chromosomes, in taxa without sex chromosomes males and females experience similar levels of intrinsic postzygotic isolation. This suggest that in the absence of sex chromosomes, incompatibilities between the nuclear genome and uniparentally inherited factors (such as the mitochondrial genome) may be of special importance for the evolution of intrinsic postzygotic isolation.

In animals most of what we know about how incompatibilities that cause intrinsic postzygotic isolation evolve comes from species with heteromorphic sex chromosome (such as *Drosophila*). Given that the presence of heteromorphic sex chromosomes has such a large impact on the expression of this reproductive barrier, it is important to study their evolution in animal taxa that lack sex chromosomes. It is worth noting that in plants, where a large number of species lack sex chromosomes, a lot of progress has been made towards understanding the evolution of reproductive isolation (see Baack et al. 2015 for a recent review). However, in many cases, postzygotic reproductive barriers in plants are caused by different mechanisms than in animals (such as chromosomal speciation), and it remains unclear if some of these differences are due to differences between plants and animals, or due to presence or absence of sex chromosomes.

The copepod *Tigriopus californicus* is an ideal system to study the evolution of local adaptation and intrinsic postzygotic isolation in an animal species lacking sex chromosomes. Several populations of this species occur in rocky outcrops, where they inhabit upper intertidal splash pools from Baja California, Mexico, to Alaska. These populations are isolated from each

other, and gene flow is extremely low even for populations that are only a few kilometers apart (Burton 1997; Willett and Ladner 2009), with high levels of local adaptation and genetic divergence between populations. These copepods have short generation time (< 1 month per generation), and they can be easily maintained in the laboratory where crosses between populations can be carried out.

With advances in sequencing technology, it is now possible to study the genome of most organisms, including non-model species. In chapter 3, we take advantage of whole genome sequencing, to survey the genome of hybrids from different *T. californicus* population crosses in an effort to find regions of the genome that are affect by hybrid inviability. The crosses studied were of increasing levels of divergence, and it was therefore expected that hybrids from the most divergent cross would have a higher proportion of their genome affected by hybrid inviability. However, this was not the case, as the least divergent cross had the largest proportion of its genome affected by inviability. This is likely a consequence of the placement of the incompatibilities across the genome, which differs between the crosses, as well as their strength, which need not be related to the amount of divergence. Therefore, at the genomic level, the level of divergence does not correlate with the effect size of hybrid inviability. Also, unlike in species with sex chromosomes, no one chromosome contributed more to hybrid inviability across populations, as would be expected since patterns similar to the Large-X effect are not expected.

Populations of *T. californicus* have also diverged in their ability to withstand different environmental conditions, supporting the idea that these populations show high levels of local adaptation. Thermal tolerance in particular has been well studied in this species, showing that southern populations are more thermal tolerant than northern ones (Willett 2010; Kelly et al. 2012). Furthermore, Willett (2010) showed that this adaptation to tolerate higher temperatures in

southern populations comes with a tradeoff at lower temperatures, and northern populations outcompete southern ones when raised at low temperatures, while southern populations outcompete northern ones at higher temperatures.

In the face of predicted global warming, organisms living in the intertidal zone are thought to be especially vulnerable, since in many cases they are already living close to their thermal limits (Somero 2010; Tomanek 2010). Furthermore, climate change is predicted to increases temperature variability, which has been shown to have a negative effect in certain life history traits in a number of organisms (Podrabsky and Somero 2004; Schaefer and Ryan 2006; Folguera et al. 2011). Therefore it is important to understand not simply how well organisms may be able to tolerate higher temperatures, but also to understand the effects that increases in thermal variability will have, since it may lead to trade-offs that affect an organism's competitive ability. In chapter 4, we look at the genetic effects that variable temperature environments (20^{o}C-28^{o}C) have on *T. californicus* in comparison to a constant temperature environment (20^{o}). As a comparison to the 28^{o} in the variable environment, some copepods from the constant environment were also exposed to a higher temperature (28^{o}), which should pose a moderate stress. We show that the more thermal tolerant populations (southern) display smaller transcriptome wide expression differences between these temperature treatments, while less thermal tolerant populations (northern) show larger expression differences. However, all four populations, independent of region, show very different profiles of gene expression across the treatments, especially when comparing the constant and variable temperature regimes. One of the northern populations in particular, appears to not respond as much to the 28^{o}C temperature in both constant and variable regimes, but displays a striking difference between the 20^{o}C treatments in both regimes. These results emphasize the importance of understanding the effects

that increases in thermal variability will have on organisms, as these changes may have a significant effect on a population's ability to survive, not simply due to their inability to deal with higher temperatures, but due to the trade-offs that thermal variability brings about.

The chapters in this dissertation contribute knowledge to our understanding of the genetic basis of local adaptation and reproductive isolation. In particular, chapter 2 demonstrates how intrinsic postzygotic isolation is strongly affect by the presence/absence of sex chromosomes, while chapter 3 gives us an overlook of the genomic structure of hybrid inviability at different stages of genetic differentiation. Finally, chapter 4 integrates the effects of local adaptation with increases in thermal variability, emphasizing that populations that appear to be similarly locally adapted, may do so by evolving different mechanisms, or co-adapting different sets of genes. These differences can lead to distinct responses to a changing environment.

CHAPTER II: HIGHER LEVELS OF SEX CHROMOSOME HETEROMORPHISM ARE ASSOCIATED WITH MARKEDLY STRONGER REPRODUCTIVE ISOLATION[1]

Summary

The two "rules of speciation" describe the genetic basis of postzygotic isolation, and have led to the realization that sex chromosomes play an important role in this process. However, a range of sex determination mechanisms exists in nature, not always involving sex chromosomes. Based on these "rules of speciation", I test the hypothesis that the presence of sex chromosomes will contribute to a faster evolution of intrinsic postzygotic isolation. I show that taxa that do not have sex chromosomes evolve lower levels of postzygotic isolation than taxa with sex chromosomes, at a similar amount of genetic divergence. Taxa with young homomorphic sex chromosomes show an intermediate pattern compared to taxa with heteromorphic sex chromosomes and taxa without sex chromosomes. These results are consistent with predictions from the two "rules of speciation", and emphasize the importance of sex chromosomes for the evolution of intrinsic postzygotic isolation.

Introduction

The evolution of postzygotic reproductive isolation, by the formation of maladaptive hybrids, can often be explained by the accumulation of Dobzhansky-Muller incompatibilities (DMIs) between incipient species (Dobzhansky 1936; Muller 1942). DMIs arise when alleles

[1] This chapter is based on Lima, T. G. 2014. Higher levels of sex chromosome heteromorphism are associated with markedly stronger reproductive isolation. Nat. Commun. 5.

that are neutral or beneficial on the parental genetic background lead to deleterious effects in a hybrid background. Two "rules of speciation" have been proposed to further describe patterns of the genetic basis of postzygotic isolation (Coyne and Orr 1989b). First, Haldane's rule (Haldane 1922) states that whenever a sex is absent, rare or sterile in a cross between two taxa, that sex is usually the heterogametic sex. This rule is obeyed by a wide range of animal taxa and at least one group of plants that possess sex chromosomes (Schilthuizen et al. 2011). The second rule is named the large X-effect, and is based on observation that the X (or Z) chromosome has a disproportionately high impact on hybrid fitness compared to autosomes. This has been shown, in *Drosophila*, to be due to a higher density of male sterility factors in the X chromosome (Tao et al. 2003; Masly and Presgraves 2007).

Both "rules of speciation" indicate sex chromosomes are important in the formation of intrinsic postzygotic isolation (IPI) (Presgraves 2008). However, a variety of sex determination mechanisms exist in nature, ranging from heteromorphic sex chromosomes, where one of the chromosomes is largely degenerate, to the absence of sex chromosomes, where sex is determined by the environment, and/or by a combination of genic factors that are not on the same chromosome (Bull 1983). The transition between an absence of sex chromosomes and heteromorphic sex chromosomes is observed in taxa bearing "young" sex chromosomes. Young sex chromosomes are usually homomorphic, where size and gene content are similar between the two chromosomes. As these chromosomes "age" recombination decreases and the Y (W) chromosome starts to degenerate (Bull 1983). Considering the importance of sex chromosomes in the evolution of IPI, it has been proposed that speciation and IPI should evolve more slowly in taxa lacking sex chromosomes (Rieseberg 2001; Levin 2012; Phillips and Edmands 2012), but

no empirical evidence exists showing that the amount of IPI suffered by taxa bearing heteromorphic sex chromosomes is higher than in taxa without sex chromosomes.

I therefore propose the following hypothesis: for a given amount of genetic divergence, higher sex chromosome heteromorphism will be accompanied by an increase in IPI. If taxa are classified based on their sex determination mechanism (as heteromorphic, homomorphic and no sex chromosomes), one would expect crosses between taxa in the heteromorphic sex chromosome group to display higher levels of IPI compared to the other two sex determination groups, and the homomorphic sex chromosome group should be intermediate. The homomorphic sex chromosome group spans a wide range of the sex chromosome evolution spectrum, so that taxa closer to the heteromorphic end of the spectrum should behave more like the heteromorphic sex chromosome group, while taxa on the opposite end of the spectrum should behave more like taxa without sex chromosomes.

Three theories that explain Haldane's rule and the large X-effect can further clarify the pattern proposed in the hypothesis. First, the dominance theory stems from the idea that DMIs are on average partially recessive (Orr 1993a; Turelli and Orr 1995, 2000), in a way that the average effect of an incompatibility when heterozygous is less than half of the effect of that incompatibility when hemizygous. Incompatibilities will be partially masked in F_1 hybrids, since they are heterozygous, except when they are X-linked (in taxa with sex chromosomes), in which case they will be fully expressed in the hemizygous sex, leading to Haldane's rule (but not the large X-effect). The amount of hemizygosity is relative to the amount of degeneracy between the sex chromosomes, so the dominance theory alone could lead to the pattern proposed above. Note that in this case the homogametic sex should suffer much lower levels of isolation in taxa where both copies of the X chromosome are active, such as *Drosophila*. In taxa where X inactivation

occurs (such as in mammals), the strength of isolation may be higher in the homogametic sex as well, compared to taxa without sex chromosomes, especially in marsupials where only the paternal X is silenced (Watson and Demuth 2012).

Second, the faster X (Z) theory (Charlesworth et al. 1987) predicts that genetic changes accumulate faster on the X chromosome than on autosomes, which occurs either because of efficient selection on hemizygous mutations when they are partially recessive (Charlesworth et al. 1987), or due to differences in effective population size between the X chromosome and autosomes (Mank et al. 2009), both of which are dependent on the amount of degeneracy between the sex chromosomes. This process could lead to the faster accumulation of hybrid incompatibilities on the X chromosome the more differentiated the sex chromosomes are, and both Haldane's rule and the large X-effect would be observed. Third, the faster-heterogametic-sex theory (Tao and Hartl 2003), explains the appearance of sterility in the heterogametic sex due to genomic conflicts, such as meiotic drive. If genomic conflicts affect sex ratio, there will be strong selection for suppressors to evolve. This evolutionary arms race will be stronger in the heterogametic sex, causing faster evolution of gametogenesis genes, and hence hybrid incompatibilities, leading to both Haldane's rule and the large X-effect. The rate of this process is again dependent on the amount of degeneracy between sex chromosomes. Here I separate the large X-effect from the effects of dominance, where a large X-effect is caused by a higher density of incompatibilities accumulating on the X (Z) chromosome (Tao et al. 2003; Masly and Presgraves 2007), and not due to the fact that hemizygosity exposes incompatibilities in this chromosome (dominance theory). Of course, if the incompatibilities that stem from both faster X and/or faster-heterogametic-sex (which lead to the large X-effect) are on average partially

recessive, we would observe an exaggerated pattern due to the combination of the large X-effect and the dominance theory (Orr 1997).

In this study I show that taxa bearing heteromorphic sex chromosomes suffer higher levels of IPI than taxa with homomorphic and without sex chromosomes. Taxa with homomorphic sex chromosomes display an intermediate pattern compared to the other sex chromosome groups. The cause of this is likely a combination of the dominance theory and the large X-effect, and emphasizes the importance of sex chromosomes for the evolution of postzygotic reproductive isolation.

Results

Total intrinsic postzygotic isolation is stronger with higher sex chromosome heteromorphism

To test the proposed hypothesis, data on F_1 hybrid IPI was surveyed from the literature, for crosses between taxa with heteromorphic sex chromosomes, homomorphic sex chromosomes, and taxa without sex chromosomes (Table 2.1 and Appendix 2.1). Postzygotic isolation was measured as in Coyne and Orr (1989a), with values of 0, 0.25, 0.5, 0.75 and 1.0, with a slight modification when sexes were analyzed separately (see Methods). I analyzed the data in 4 different ways: heterogametic and homogametic sexes were analyzed separately for total postzygotic isolation, and for inviability alone; and both sexes were analyzed together for the same two measures of reproductive isolation.

I first analyzed the data separating the heterogametic and homogametic sexes. To avoid confusion between the words hetero-/homogametic and hetero-/homomorphic, I refer to the heterogametic and homogametic sexes as XY and XX respectively. For this analysis the IPI index was adapted to have three different values (0, 0.5, 1.0), where a score of 0 indicates

individuals of that sex are fertile and viable in both directions of the cross, a score of 0.5 indicates that sex is sterile or inviable in one direction of the cross, and a score of 1.0 indicates that sex is sterile or inviable in both directions of the cross. For the no sex chromosome group, which does not have XY and XX sexes, the scores are the same independent of which sex is analyzed, since the cross with a score of 0.5 has unidirectional compatibility (both males and females are inviable in one direction of the cross, but viable and fertile in the other).

For the XY sex dataset the heteromorphic sex chromosome group reached higher levels of postzygotic isolation at lower genetic divergence than the homomorphic sex chromosome group (*t*-test, $P = 0.0042$, FDR adjusted $P = 0.0252$, $n = 19$), and the no sex chromosome group (*t*-test, $P = 0.0001$, FDR adjusted $P = 0.0009$, $n = 17$). The homomorphic sex chromosome group was intermediate and different from the other two groups (homomorphic vs no sex chromosome groups: *t*-test, $P = 0.0346$, but the difference is not significant when multiple comparisons are account for: FDR adjusted $P = 0.0967$, $n = 16$; Table 2.2 and Fig. 2.1a).

When considering only the XX sex, however, the same pattern is not expected. If we assume incompatibilities appear at the same rate in both autosomes and sex chromosomes, and they are on average partially recessive (dominance theory, without any effect of sex chromosomes), crosses from all three sex chromosome groups should show similar amounts of postzygotic isolation for a given amount of genetic divergence since all individuals are heterozygous throughout their entire genome. Two conditions would lead to higher levels of isolation in the XX sex of taxa with sex chromosomes in this case: in a faster X scenario changes would accumulate faster on the X chromosome versus autosomes, which could increase the total number of incompatibilities (including X-X incompatibilities); and in some cases where dosage compensation inactivates one of the X chromosomes (as in mammals) making it effectively

hemizygous. In this case however, the effect will not be as strong as in the heterogametic sex because there will be a mosaic pattern of inactivation of either of the X chromosomes across cells. In the XX sex dataset, the heteromorphic and homomorphic sex chromosome groups were not significantly different from each other, and nor was the homomorphic and no sex chromosome groups. The heteromorphic sex chromosome group did however experience higher level of IPI than the no sex chromosome group (*t*-test, $P = 0.0457$, $n = 17$), but this difference was not significant when multiple comparisons were accounted for (FDR adjusted $P = 0.1028$; Table 2.2 and Fig. 2.1b).

The main hypothesis, however, states that higher sex chromosome heteromorphism will be accompanied by an increase in IPI, and this should hold if the effects on both sexes are combined. When the sexes are analyzed together, the resulting pattern is somewhat intermediate to the one we see when the sexes are analyzed separately, and all groups are different from each other (the difference between homomorphic and heteromorphic sex chromosome groups however is marginally insignificant when FDR adjusted, $P = 0.0706$; Table 2.2; Fig. 2.1c).

Haldane's rule occurs at lower genetic distances with increased sex chromosome heteromorphism

A comparison between the XY and XX sex datasets within each sex determination group shows that the difference between the two sexes is higher for the heteromorphic sex chromosome group (the difference between the intercepts of both sexes is 5.53 for the logit transformed data, where the XY sex is significantly higher, *t*-test, $P = 0.0331$, $n = 20$) than for the homomorphic sex chromosome group (1.53 intercept difference, and the two sexes are not significantly different, *t*-test, $P = 0.3218$, $n = 18$; Fig. 2.2); as stated before there is no difference between the sexes for the no sex chromosome group. These results show that Haldane's rule evolves more

readily with higher sex chromosome heteromorphism, while unidirectional incompatibility becomes more common with lower sex chromosome differentiation.

Inviability by itself does not contribute significantly to a difference in the strength of IPI for the different sex chromosome groups

Total IPI can be caused by both sterility and inviability, and there is evidence that sterility evolves more quickly than inviability (Orr et al. 2004). Also, while evidence supports the dominance theory as an explanation of Haldane's rule for both inviability and sterility, evidence for the large X-effect is restricted to cases of sterility (Masly and Presgraves 2007; Presgraves 2008). I therefore analyzed the data considering only viability (Appendix 2.1), as we would expect the difference between the sex chromosome groups to be smaller if the pattern observed in Fig. 2.1 is being driven by a combination of the dominance theory and the large X-effect. Note that since we cannot observe if inviable individuals are also sterile, the same analysis cannot be performed for sterility only. When only viability was considered, in the XY dataset, the regression lines for the homomorphic and no sex chromosome groups were estimated to be nearly identical, while the difference between the heteromorphic sex group and the other two groups was larger but non significant (Table 2.3; Fig. 2.3a). In the XX dataset there were no differences between the groups (Fig. 2.3b), and when both sexes were analyzed together, again the pattern is intermediate compared to when the sexes are analyzed separately, and only the difference between the heteromorphic and no sex chromosome groups was significant (*t*-test, $P = 0.0376$, $n = 17$), but not when multiple comparisons are accounted for (FDR adjusted $P = 0.0967$; Table 2.3; Fig. 2.3c). For the entire dataset there are 20 cases where a sex is sterile, and 15 where a sex is inviable. The heteromorphic sex chromosome group has 10 sterile and 8

inviable sexes; the homomorphic sex chromosome group has 8 sterile and 3 inviable sexes; and the no sex chromosome group has 2 sterile and 4 inviable sexes (Appendix 2.1).

Discussion

In this study I showed that for a given amount of genetic divergence between two hybridizing species, increasing sex chromosome heteromorphism is accompanied by a disproportionate increase in IPI (Fig. 2.1). The effects of the dominance theory are clearly an important driver of this pattern, although these results suggest the large X-effect also contributes to the observed pattern. Some support for this comes from a trend for higher levels of IPI suffered by the XX sex of the heteromorphic sex chromosome group compared to the no sex chromosome group (although this difference is not significant when multiple comparisons are accounted for [Table 2.2]). But more importantly, the presence of a large X-effect explains why inviability by itself does not separate the sex chromosome groups (Fig. 2.3 and Table 2.3); this process appears to only lead to incompatibilities affecting sterility (Tao et al. 2003; Masly and Presgraves 2007). The present results also show that the prevalence of Haldane's rule increases with increasing degeneracy of sex chromosomes, which means unidirectional incompatibility should become more common when the converse is true, as chromosomes between the two sexes are more similar (Fig. 2.2).

No single process is thought to cause Haldane's rule by itself (Coyne and Orr 2004) and this is also likely to be true for the large X-effect (Presgraves 2008). While evidence for the dominance theory is widespread (Coyne and Orr 2004) cases supporting a large X-effect are less common at this point; but evidence exists in *Anopheles* (Slotman et al. 2004), *Mus* (Good et al. 2008) and *Drosophila* (Turelli and Begun 1997; Masly and Presgraves 2007). The best evidence

for a large X-effect comes from crosses between *Drosophila mauritiana* and *D. sechellia* (Masly and Presgraves 2007), where a higher density of incompatibilities causing hybrid male sterility were found to occur on the X chromosome than on autosomes, and these incompatibilities were found to be on average recessive. The mechanisms leading to a large X-effect are still debated, and both faster X (due to efficient selection of recessive mutations due to hemizygosity, or because of reduced effective population size of the hemizygous chromosome) and the faster-heterogametic-sex (due to genomic conflicts) could lead to a higher density of incompatibilities in the X chromosome.

Evidence supporting a faster X as the cause of the large X-effect is contradictory in *Drosophila* depending on the cross and dataset used, but is stronger in mammals, birds and moths (reviewed in Pregraves (Presgraves 2008) and Meisel and Connallon (2013). On the other hand, evidence that faster-heterogametic-sex (genomic conflict) can lead to the large X-effect is still rare, but two cases are known in *Drosophila* where a correlation between genes that are involved in drive or suppression within species also lead to male hybrid sterility (Tao et al. 2001; Orr and Irving 2005), suggesting these processes occur at least in some cases. Interestingly the large X-effect only contributes to the evolution of sterility incompatibilities, which is evident in the results from Masly and Presgraves (Masly and Presgraves 2007), where the majority of incompatibilities that are X-linked contribute to sterility and not inviability. The same appears to be true for the results presented here, where inviability alone is not enough to explain the difference in total IPI between the different sex chromosome groups. Therefore, inviability may evolve at a similar rate in the different sex chromosome groups, and if they are not often X-linked their expression will also be more similar across the different sex chromosome groups. These results also appear to agree more with predictions from the faster-heterogametic-sex

theory than with the faster X theory, since the former will lead only to sterility incompatibilities, while the later, in theory, could lead to both sterility and inviability. Although given the current data set, where extremely divergent taxa are analyzed together, this assertion should be taken with caution as different processes might be contributing to the evolution of DMIs in each group of taxa.

The present study suggests Haldane's rule becomes prevalent with higher sex chromosome heteromorphism, while unidirectional incompatibilities are more important in taxa without sex chromosomes. This is consistent with what was observed in crosses between *Drosophila* species where the X chromosome makes up a larger portion of the genome (large X), and obey Haldane's rule at lower genetic distances than taxa with small X chromosomes (Turelli and Begun 1997). Here this pattern is extended to the entire sex chromosome evolution spectrum, and it is observed that in taxa without sex chromosomes males and females are affected by DMI at similar rates. In this case, because incompatibilities are on average partially recessive, haploid uniparentally inherited factors may become especially important for the appearance of postzygotic barriers. If we consider the current results, where the IPI index depends on hybrids crossing a threshold (where one of the sexes is completely inviable or sterile) to reach a value of 0.25, there is no a priori reason to think that either sex would become inviable faster than the other in taxa without sex chromosomes. Similarly, hybrid sterility evolves at similar rates in both sexes in some taxa without sex chromosomes (Moyle and Graham 2005; Willett 2008a) despite the fact that sterility incompatibilities usually involve different loci for males and females (Orr 1993b). If both sterility and inviability evolve at similar rates in both sexes, the IPI index will remain at zero, and either go to 0.5 due to uniparentally inherited factors or 1 due to autosomal incompatibilities, mostly skipping IPI of 0.25 and 0.75. This is precisely

what is seen in *Tigriopus californicus*, where crosses between any two populations are either fully compatible (IPI index of 0), unidirectionally compatible (IPI index of 0.5), or fully incompatible (IPI index of 1) in which case F_1 hybrids of both sexes are sterile in one direction and inviable in the other (Ganz and Burton 1995; Peterson et al. 2013). Such a pattern indicates uniparentally inherited factors (likely cyto-nuclear incompatibilities in this case [Ellison and Burton 2008]) may be of special importance for the formation of IPI in taxa without sex chromosomes.

The different sex determination mechanisms form a continuum that goes from the complete absence of sex chromosomes to the presence of highly heteromorphic ones. This continuum is shown here to correlate with the level of IPI experienced between two taxa: increasing sex chromosome differentiation increases the severity of postzygotic isolation. Predictions from the two "rules of speciation" are consistent with this pattern, and the current results accentuate the importance of sex chromosomes for the evolution of IPI, and highlight patterns that may be important in taxa that lack sex chromosomes.

Methods

Crosses selection

This survey included any crosses for which information was published for reciprocal crosses, sex determination mechanisms, and Nei's *D* genetic distances (Table 2.1 and Appendix 2.1). I used the same index of IPI as in Coyne and Orr (Coyne and Orr 1989a), where a score of 1 is assigned for every sex that is completely sterile or inviable in both reciprocal crosses. This sum is divided by 4, giving five possible scores 0, 0.25, 0.50, 0.75 and 1. A score of zero therefore indicates both males and females are viable and fertile in both directions of the cross,

while a score of 1 indicates both males and females are either sterile or inviable. When analyzing the XX and XY sexes separately, the IPI index was adapted to take three scores (0, 0.5, and 1), where a score of zero indicates all individuals from this sex are fertile and viable in both directions of the cross, and a score of one indicates that sex is completely sterile or inviable in both directions of the cross.

To avoid that the pattern in any of the sex chromosome groups was driven by a single taxon group, all cases where information was available for more than three crosses (i.e. *Drosophila* (Coyne and Orr 1989a), Lepidoptera (Presgraves 2002), frogs (Sasa et al. 1998), and *Tigriopus californicus* (Ganz and Burton 1995)), only three crosses with different IPI indexes were chosen. A large number of *Drosophila* crosses meet all the criteria outlined in the previous paragraph, however, some species of *Drosophila* have a neo-Y chromosome (Bachtrog 2013), therefore, I only included crosses for which I could confirm the Y chromosome was degenerate. For Lepidoptera, only 11 crosses from Presgraves (Presgraves 2002) met all criteria, 7 of which had an isolation index of 0. Three crosses with different isolation indexes were randomly chosen in this case. In frogs, both male and female heterogamety exist, and the degree of sex chromosome differentiation as well as which sex is XY varies even in closely related species (Hillis and Green 1990). Of the crosses presented in Sasa et al. (1998), I included three crosses where information on sex chromosomes exists. Crosses from *Tigriopus californicus* were randomly chosen for three different isolation index values from Ganz and Burton (1995).

Data that meet all the criteria are largely lacking for birds (mostly due to a lack of Nei's *D* genetic distance for cases where reciprocal cross information exists), and only one cross was included. This is unfortunate since birds, in general, follow Haldane's rule, but are known to

evolve IPI much slower than other groups of animals (Price and Bouvier 2002). The inclusion or omission of this single cross does not change the results presented here.

In one cross, two types of sex determination mechanisms exist. *Xiphophorus maculatus* has multi factor sex determination mechanism (X, Y, and W sex chromosomes), with male and female heterogamety, while *Xiphophorus helleri* has polyfactorial sex determination, and neither sex is heterogametic (Bull 1983). The results are the same independent of assigning this cross to the no sex chromosome group or the homomorphic sex chromosome group.

Genetic Distance

In order to compare strength of isolation between these diverse groups of taxa, I only included taxa with published Nei's *D* genetic distance (Nei 1972). This metric was chosen because it has been previously used in studies of this sort (i.e Coyne and Orr 1989a, 1997; Sasa et al. 1998; Presgraves 2002; Yukilevich 2013) and it maximized the number of crosses in the analysis. Nei's *D* measures the accumulation of codon differences at a locus between two taxa. Even if the molecular clocks are not the same between all the taxa analyzed here, Nei's *D* would still be a good metric as long as it approximates how divergent the genomes of the two hybridizing taxa are (Nei's *D* are usually calculated based on information of at least 10 loci). If the genomes are not diverging at the same rate in distantly related taxa, we might expect DMIs to accumulate at different rates with respect to time as well. Here I am interested in how divergent the genomes are more so than time since divergence, as IPI should be a by product of genomic divergence. Several other methods were attempted, such as calculating *Ks*, or four-fold degenerate transversions (4DTv) from DNA sequences. However, all of these methods yielded a very small number of potentially comparable crosses due to the lack of appropriate DNA

sequences for many species, and in none of them was it possible to include the no sex chromosome group.

Phylogenetic corrections

Due to the small amount of data available, performing a traditional correction for phylogenetic dependence would render the dataset too small for analysis. Therefore, the dataset contains two groups of taxa with non-phylogenetically independent crosses (*Mus*, and *Tigriopus californicus*). To ameliorate this issue in these two groups the following criteria were applied: For *Mus,* the two crosses used are of increasing phylogenetic distance, which insures that the two crosses only shared a small portion of phylogenetic branch. Also, these crosses have different IPI indexes, meaning that even if a portion of the phylogenetic branch is not independent (certain incompatibilities may be part of both comparisons), we know that independent incompatibilities have evolved in each lineage since they last shared an ancestor leading to the difference in IPI. For *Tigriopus californicus*, the phylogenetic relationship of some of the populations is still unresolved, however, since this is the only group of crosses that yields IPI indexes greater than 0 in the no sex chromosome group, I decided to include three crosses that span the different IPI index classes observed in this group (0, 0.5, 1.0).

Statistical analysis

All statistical analyses were performed in R 2.15.1 (R Core Team 2012). Due to the nature of the IPI index, which is bounded by 0 and 1, analysis using an ordinary linear regression is inappropriate. However, when a logit transformation is applied to these values, this problem is eliminated. The IPI index values were logit transformed, and treated as a continuous variable.

The logit function is undefined for values of 0 and 1, therefore I changed boundary values to 0.001 and 0.999 prior to logit transformation. Due to the small sample size in each sex chromosome group I used a logistic-normal model, which is an ordinary linear regression that uses the logit transformed IPI index as the response variable. This test is appropriate for small sample sizes because it uses an *F*-distribution (and a *t*-distribution for the post-hoc pairwise comparisons) with degrees of freedom that are a function of the sample size. An additive model was used, as there was not enough power to determine if the slopes were different (in an interactive model). This method was used in all comparisons presented in this study. In the present study, I am interested in the difference between the estimated regressions between each of the sex chromosome groups, therefore, the reported *P-values* in the results section refer to the post-hoc *t*-test for each pairwise comparison. To account for multiple comparisons a false discovery rate (FDR) set at 5% (Benjamini and Hochberg 1995) was used to adjust the *P*-values.

Bootstrap confidence intervals

Bootstrap confidence intervals for the predicted logit curves were obtained for each individual value of genetic distance using 1000 bootstrap samples of the actual observations. This means that for each single combination of the predictors "genetic distance" and "sex determination group" we are 95% confident that the true inverse mean logit lies within the displayed interval for those specific predictor values.

Influential observations

Given the small number of observations in each sex chromosome group, I used standard diagnostic statistics to identify possible influential observations in the regression analysis. These

were tests of leverage, Cook's distance, DFFITS, and DFBETAS, all of which were run in R 2.15.1 (R Core Team 2012). The output of these tests is displayed in Appendix 2.2-2.7. None of the observations are influential given commonly used threshold values for these statistics.

Figure legend

Figure 2.1. Strength of total intrinsic postzygotic isolation versus Nei's *D* genetic distance. Regression lines were calculated through a logistic normal model. Logit values were transformed back to the reproductive isolation index values (from 0 to 1) for purpose of visualization. Het = heteromorphic sex chromosomes (n = 10); Hom = homomorphic sex chromosomes (n = 9); NS = no sex chromosomes (n = 7). a) F_1 hybrids of the XY sex. b) F_1 hybrids of the XX sex. c) Both sexes analyzed together. For both a) and c): Taxa with heteromorphic sex chromosomes experience higher levels of intrinsic postzygotic isolation at lower genetic distances compared to the other two groups (*t*-test, FDR adjusted P = 0.0252 for Het vs Hom, n = 19; FDR adjusted P = 0.0009 for Het vs NS, n = 17). Species without sex chromosomes remain compatible until much higher levels of genetic differentiation (*t*-test, Hom vs NS: P = 0.0346; FDR adjusted P = 0.0967, n = 16). In b): The heteromorphic sex chromosome group is significantly higher than the no sex chromosome group (*t*-test, P = 0.0457, n = 17), but the difference is not significant if corrections for multiple comparisons are carried out (FDR adjusted P = 0.1028) while all other comparisons are not significantly different. All comparisons are post-hoc pairwise *t*-tests with 22 degrees of freedom.

Figure 2.2: Strength of intrinsic postzygotic isolation versus Nei's *D* genetic distance for XY and XX sexes in heteromorphic and homomorphic chromosome taxa. Regression lines were calculated through a logistic normal model. Logit values were transformed back to the reproductive isolation index values (from 0 to 1) for purpose of visualization. a) Crosses between taxa with heteromorphic sex chromosomes. The XY sex reaches higher levels of intrinsic postzygotic isolation at lower genetic distances than the XX sex (difference between intercepts = 5.53; *t*-test, $t(17)$ = 2.32; P = 0.0331, n = 20); b) Crosses between taxa with homomorphic sex

chromosomes. Intrinsic postzygotic isolation is not significantly different between the two sexes (difference between intercepts = 1.53; *t*-test, *t(15)* = 1.02; *P* = 0.3218, *n* = 18).

Figure 2.3: Strength of intrinsic postzygotic isolation versus Nei's *D* genetic distance considering only viability. Regression lines were calculated through a logistic normal model. Logit values were transformed back to the reproductive isolation index values (from 0 to 1) for purpose of visualization. Het = heteromorphic sex chromosomes (*n* = 10); Hom = homomorphic sex chromosomes (*n* = 9); NS = no sex chromosomes (*n* = 7). a) F_1 hybrids of the XY sex b) F_1 hybrids of the XX sex. c). Both sexes analyzed together. None of the comparisons are significantly different, except for the comparison Het vs NS in (c), when both sexes are analyzed together, where Het reaches higher levels of postzygotic isolation at lower genetic distance than NS (*t*-test, *P* = 0.0376, *n* = 17), although this difference is not significant when multiple comparisons are accounted for (FDR adjusted *P* = 0.0967). All pairwise comparisons are post-hoc *t*-tests with 22 degrees of freedom.

Tables

Table 2.1. Cross data.

Cross	Total IPI	Inv. IPI	ND	SD
Drosophila melanogaster x *D. sechellia*	1.00	0.50	0.620	Het
Drosophila yakuba x *D. santomea*	0.50	0.00	0.300	Het
Drosophila p. pseudoobscura x *D. p. bogotana*	0.25	0.00	0.194	Het
Mus m. musculus x *M. m. domesticus*	0.50	0.00	0.180	Het
Mus musculus x *M. caroli*	1.00	0.75	0.300	Het
Anopheles gambiae x A. arabiensis	0.50	0.00	0.150	Het
Papilio eurymedon x *P. glaucus*	0.25	0.25	0.418	Het
Heliconius himera x *H. erato*	0.00	0.00	0.280	Het
Yponomeuta cagnagellus x *Y. padellus*	0.50	0.50	0.099	Het
Anas platyrhynchos x *A. fulvigula*	0.00	0.00	0.011	Het
Hyla cinerea x *H. versicolor*	1.00	0.00	0.900	Hom
Rana berlanderi x *R. forreri*	0.50	0.50	0.380	Hom
Hyla japonica (Tsushima) x *H. japonica* (Korea)	0.00	0.00	0.060	Hom
Silene latifolia x *Silene dioica*	0.00	0.00	0.038	Hom
Triturus cristatus x *T. marmoratus*	0.75	0.25	0.750	Hom
Gasterosteus aculeatus (PA) x *G. aculeatus* (JA)	0.25	0.00	0.732	Hom
Gasterosteus aculeatus (Limnetic) x *G. aculeatus* (Benthic)	0.00	0.00	0.018	Hom
Wyeomyia smithii (ON,ME) x *W. smithii* (FL)	0.00	0.00	0.330	Hom
Aedes triseratus x *A. hendersoni*	0.25	0.00	0.315	Hom
Tigriopus californicus (SD) x *T. californicus* (SC)	0.00	0.00	0.699	NS
Tigriopus californicus (PLA) x *T. californicus* (PMO)	0.50	0.50	1.290	NS
Tigriopus californicus (AB) x *T. californicus* (PLA)	1.00	0.50	1.600	NS
Oryza sativa (Japonica) x *O. sativa* (Indica)	0.00	0.00	0.112	NS
Mimulus guttatus x *M. nasutus*	0.00	0.00	0.200	NS
Dubautia latifolia x *D. sheriffiana*	0.00	0.00	0.473	NS
Xiphophorus maculatus x *X. helleri*	0.00	0.00	0.400	NS

Note - Intrinsic postzygotic isolation index (IPI), postzygotic isolation index considering only inviability (Inv. IPI), Nei's *D* genetic distance (ND), and sex determination mechanism (SD). Het = heteromorphic sex chromosomes; Hom = homomorphic sex chromosomes; NS = no sex chromosomes. References to original sources are in Appendix 2.1 and 2.17.

Table 2.2. Results from the linear model with the response variable (total IPI) logit transformed.

Comparison	Estimate	Std. err.	*t*-stat	*P*-value (22 d.f.)	*FDR adjusted P-value*
XY sex					
(*Intercept)*	-0.567	1.355	-0.419	0.6795	-
ND	10.343	2.228	4.643	0.0001	-
Hom vs Het	-5.783	1.810	-3.190	**0.0042**	**0.0252**
NS vs Het	-10.433	2.140	-4.876	**0.0001**	**0.0009**
NS vs Hom	-4.650	2.060	-2.252	**0.0346**	0.0967
XX sex					
(*Intercept)*	-6.038	1.440	-4.193	0.0004	-
ND	10.129	2.367	4.279	0.0003	-
Hom vs Het	-1.764	1.930	-0.916	0.3698	0.4438
NS vs Het	-4.816	2.270	-2.118	**0.0457**	0.1028
NS vs Hom	-3.053	2.190	-1.392	0.1780	0.2465
Both sexes					
(*Intercept)*	-2.936	1.085	-2.706	0.0129	-
ND	10.647	1.784	5.968	0.0000	-
Hom vs Het	-3.655	1.450	-2.518	**0.0196**	0.0706
NS vs Het	-8.272	1.710	-4.827	**0.0001**	**0.0009**
NS vs Hom	-4.616	1.650	-2.792	**0.0106**	**0.0477**

Note - The three datasets have the same degrees of freedom. XY and XX sex comparisons refer to analysis where the sexes are considered separately. ND = Nei's *D* genetic distance; Het = heteromorphic sex chromosomes; Hom = homomorphic sex chromosomes; NS = no sex chromosomes. The comparison between NS vs Hom was attained by re-running the model with Hom as the reference group.

Table 2.3. Results from the linear model with the response variable (IPI for viability only) logit transformed.

Comparison	Estimate	Std. err.	*t*-stat	*P*-value (22 d.f.)	*FDR adjusted p-value*
XY sex					
(*Intercept)*	-4.595	1.207	-3.807	0.0010	-
ND	4.475	1.984	2.255	0.0344	-
Hom vs Het	-3.296	1.610	-2.041	0.0534	0.1048
NS vs Het	-3.390	1.910	-1.778	0.0891	0.1458
NS vs Hom	-0.094	1.840	-0.051	0.9595	0.9595
XX sex					
(*Intercept)*	-6.064	0.973	-6.229	0.0000	-
ND	4.817	1.600	3.010	0.0064	-
Hom vs Het	-1.193	1.300	-0.916	0.3694	0.4438
NS vs Het	-2.155	1.540	-1.402	0.1750	0.2465
NS vs Hom	-0.961	1.480	-0.648	0.5236	0.5891
Both sexes					
(*Intercept)*	-4.672	1.007	-4.641	0.0001	-
ND	4.776	1.655	2.886	0.0086	-
Hom vs Het	-2.691	1.350	-1.998	0.0582	0.1048
NS vs Het	-3.519	1.590	-2.213	**0.0376**	0.0967
NS vs Hom	-0.827	1.530	-0.540	0.5950	0.6300

Note - The three datasets have the same degrees of freedom. XY and XX sex comparisons refer to analysis where the sexes are considered separately. ND = Nei's D genetic distance; Het = heteromorphic sex chromosomes; Hom = homomorphic sex chromosomes; NS = no sex chromosomes. The comparison between NS vs Hom was attained by re-running the model with Hom as the reference group.

Figures

Figure 2.1:

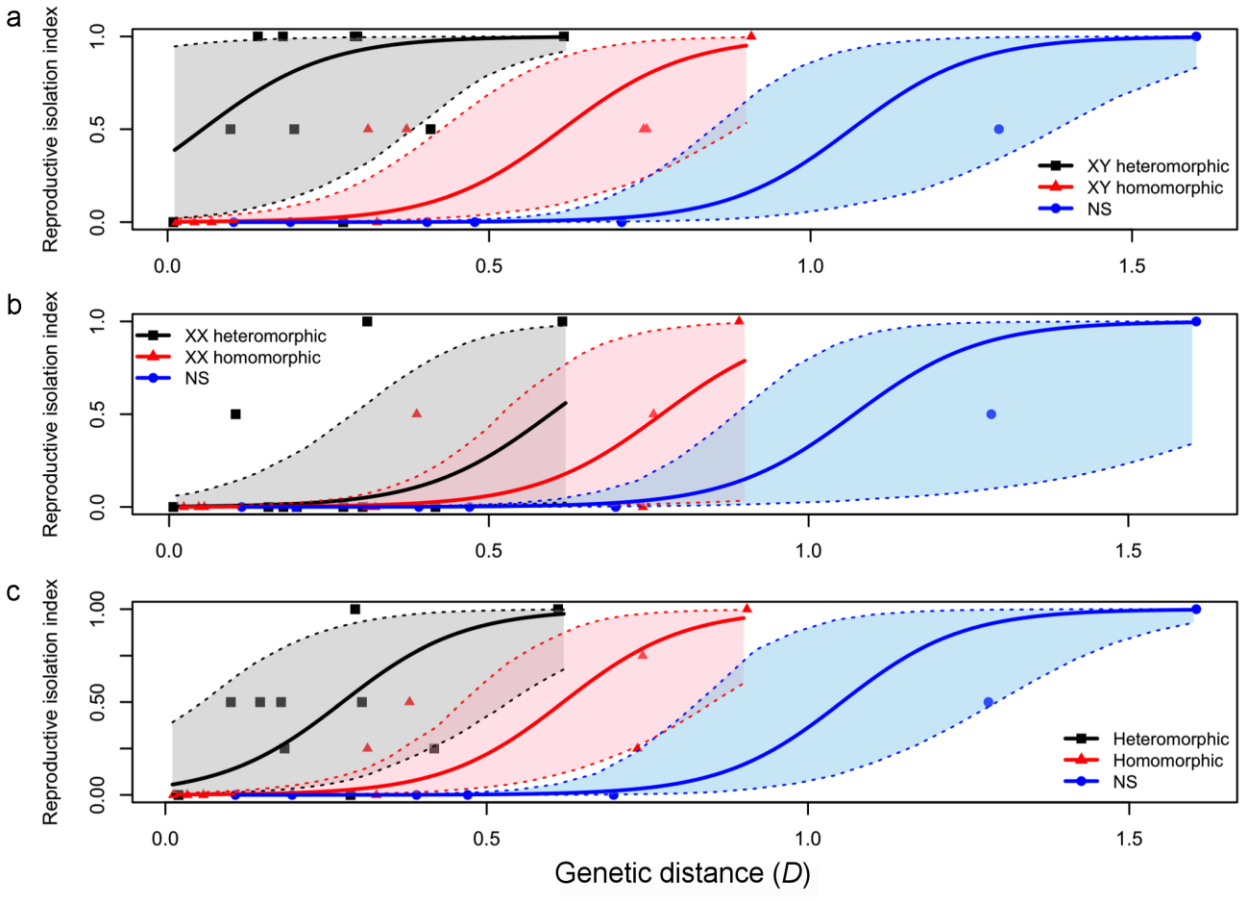

Figure 2.2:

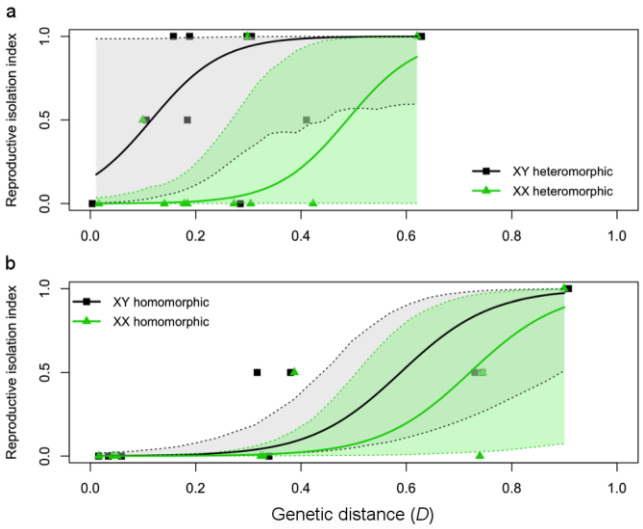
a
Reproductive isolation index
1.0
0.5
0.0
XY heteromorphic
XX heteromorphic
0.0
0.2
0.4
0.6
0.8
1.0
b
Reproductive isolation index
XY homomorphic
XX homomorphic
Genetic distance (D)

Figure 2.3:

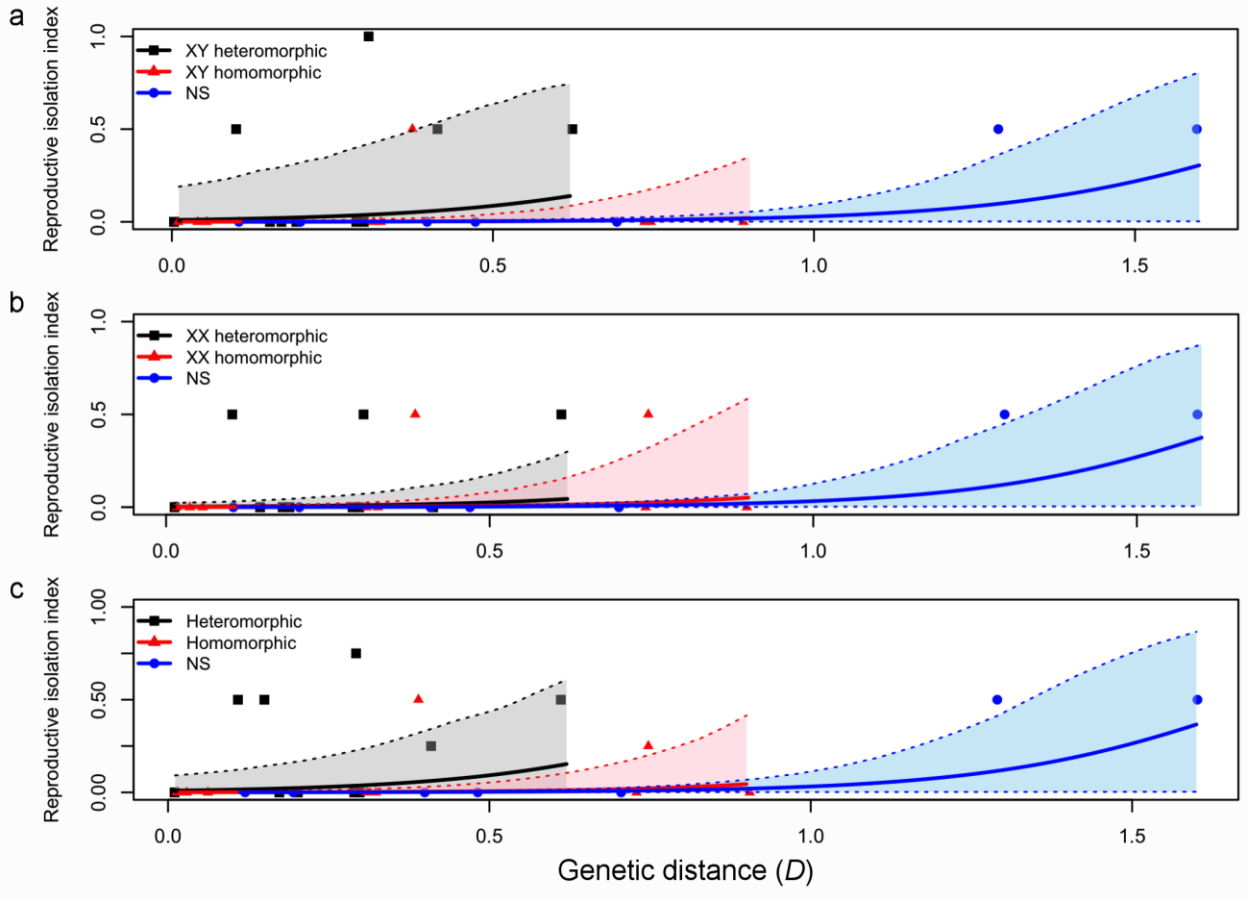
a
Reproductive isolation index
XY heteromorphic
XY homomorphic
NS
b
Reproductive isolation index
XX heteromorphic
XX homomorphic
NS
c
Reproductive isolation index
Heteromorphic
Homomorphic
NS
Genetic distance (D)

CHAPTER III: GENOME-WIDE PATTERNS OF HYBRID INVIABILITY IN POPULATION CROSSES OF THE COPEPOD *TIGRIOPUS CALIFORNICUS*

Summary

The formation of reproductive barriers between populations living in allopatry usually involves the accumulation of genic incompatibilities that lead to intrinsic postzygotic isolation. The evolution of these incompatibilities is usually explained by the Dobzhansky-Muller (DM) model, where positive or neutral epistatic interactions that arise within the diverging populations, lead to deleterious interactions when they come together in a hybrid genome. Other forms of incompatibilities, brought about due to differences in chromosomal structure between the populations (such as inversions), may also lead to hybrid dysfunction. In both cases the number of incompatibilities should increase relative to the amount of divergence between the populations, but the number of DM incompatibilities should increase faster than the number of incompatibilities due to chromosomal inversions. We introduce a method that uses PoolSeq of F_2 hybrids to scan the genome for regions associated with hybrid inviability. We analyzed three crosses of increasing levels of divergence between populations of the copepod *Tigriopus californicus*. Surprisingly, the cross with the lowest level of divergence showed the most drastic allele frequency deviations from expected null frequencies. This was the case for both the magnitude of the deviations as well as for the proportion of the genome that was skewed. Between the other two crosses, the more divergent one had more deviations than the less divergent one. Our results suggest that in the early stages of speciation, when divergence between different populations is similar, the strength and position of incompatibilities within the

genome may be more important in determining the strength of intrinsic postzygotic isolation than the actual number of incompatibilities.

Introduction

The formation of new species is a product of reproductive barriers that evolve between diverging populations, and can occur by a number of different mechanisms that decrease gene flow. One of the key forms of reproductive isolation is intrinsic postzygotic isolation, under which the hybrids between two incipient species suffer from lower fitness due to partial or complete sterility or inviability. The evolution of these postzygotic barriers to gene flow is usually explained by the accumulation of deleterious epistatic genic incompatibilities between the hybridizing taxa, known as Dobzhansky-Muller (DM) incompatibilities (Dobzhansky 1936; Muller 1942). In the DM model, for two populations living in allopatry, different portions of their genomes may diverge due to natural selection or drift, forming novel alleles that have beneficial or neutral effects in the populations they evolved in. When these novel alleles (generally at different loci) come together in a hybrid genome, their interactions, which have never been tested in the same genetic background, can have deleterious effects leading to lowered hybrid fitness.

The DM model also predicts that the number of incompatibilities will increase faster than linearly with time, in what is known as the "snowball effect" (Orr 1995). Because DM incompatibilities involve two or more interacting loci, the number of possible deleterious interactions will increase at least with the square of time. This has been shown in *Drosophila* for incompatibilities causing inviability (Matute et al. 2010), and *Solanum* for hybrid seed sterility (Moyle and Nakazato 2010) but see Städler et al. (2012). Other forms of incompatibilities may

also lead to sterility and inviability in hybrids, which will not "snowball" with divergence, namely chromosomal rearrangements (Noor et al. 2001; Lowry and Willis 2010; Charron et al. 2014). The number of non-epistatic incompatibilities due to chromosomal rearrangements should increase linearly with divergence between the incipient species, as they do not involve interactions between multiple loci.

Several studies, mostly in animal taxa, have determined that when comparing hybrids from both sexes, the heteromorphic sex (XY in mammals and *Drosophila*) is affected disproportionately by intrinsic postzygotic isolation, which led to the formulation of "two rules of speciation" to describe this pattern (i.e. Haldane's rule and the Large-X effect [Coyne and Orr 1989; detailed in chapter 2]). On the other hand, studies that consider taxa without sex chromosomes, or with homomorphic sex chromosomes suggest that the presence of heteromorphic sex chromosomes can speed up the appearance of these postzygotic barriers (Presgraves 1998; Lima 2014), and may increase speciation rates (Phillips and Edmands 2012). In fact, it has been postulated that in plants a lack of sex chromosomes may increase the importance of chromosomal speciation, because these taxa do not accumulate genic incompatibilities as fast as taxa with heteromorphic sex chromosomes, increasing the chance that chromosomal differences will evolve and contribute to reproductive isolation (Rieseberg 2001).

Tigriopus californicus, an intertidal copepod that lives in upper intertidal pools on the west coast of North America, is an ideal system in which to study the early stages of intrinsic postzygotic isolation. Populations of these copepods are allopatric, with highly restricted gene flow amongst them (Burton 1997; Willett and Ladner 2009), and different populations can be crossed in the laboratory to generate hybrids. Crosses between several of these populations have shown that first generation hybrids (F_1) are usually equal in fitness, or even superior, to the

parental populations, while second generation hybrids (F_2) have on average lower fitness (Burton 1987; Edmands 1999; Willett 2008b), indicating that most of the incompatibilities are at least partially recessive. These copepods lack sex chromosomes, and sex determination in *T. californicus* is thought to be polygenic with an environmental component (Voordouw and Anholt 2002, Alexander et al. 2014). Several unlinked factors are thought to contribute to sex determination, and processes that lead to the faster appearance of intrinsic postzygotic barriers due to the present of heteromorphic sex chromosomes (such as in the "two rules of speciation"), should not apply in this system. This is likely one of the reasons *T. californicus* populations remains compatible despite the fact that genetic divergence can be extremely high between them (mitochondrial DNA divergence can be as high as 20%).

Here we used a PoolSeq approach (Schlötterer et al. 2014) to sequence the genome of *T. californicus* F_2 hybrids from three crosses of increasing phylogenetic relationship. This method allowed us to sequence a large number of hybrid individuals (300) for each cross at high coverage, and to use deviations in allele frequency to determine regions of the genome that are affected by hybrid inviability. We were interested in estimating the genome-wide effects of hybrid inviability in these three crosses, with the expectation that as divergence increased between the populations, so too should the amount of the genome that is affected by hybrid inviability. Our results were surprising however, as of the three crosses, the most closely related one showed the most extreme deviations in allele frequencies, and had the largest proportion of its genome skewed as well. We were also interested in determining if any of the chromosomes or chromosome regions contributed to hybrid inviability across all three crosses. We found that this is not the case, and different chromosomes and chromosomal regions were most highly skewed in each of the three different crosses.

Methods

Population sampling, crossing design, DNA isolation and sequencing

Tigriopus californicus were collected from intertidal rocky pools at four sites in California, Abalone Cove (AB, 33°44' N, 118°22' W), Catalina Island (CAT, 33°27' N, 118°29' W), San Diego (SD, 32°44' N, 117°15' W), and Santa Cruz (SC, 36°57' N, 122°03' W). Animals were maintained in mass cultures in 400 mL beakers in artificial seawater close to natural saltwater concentrations (35 ppt, Instant Ocean, Aquarium Systems), and fed powdered commercial flake fish food as well as natural algae growth. Cultures were kept in incubators at 20°C with 12h light:dark cycle. Males and females used in crosses were randomly sampled from culture beakers (and not from isofemale lines), so different crosses between the same populations included some of the genetic diversity of natural populations. Females from SD, SC and CAT were crossed to males from AB in 24 well plates, with a single pair of copepods in each well. *Tigriopus californicus* females mate only once in their lives, and males will guard females by clasping onto them until they reach reproductive maturity (Burton 1997). Virgin females were obtained by separating females from clasped pairs, and their non-mated status was confirmed by monitoring them in individual wells over a week, at which point AB males were added to each well. F_1 hybrids were separated into individual wells before they reached sexual maturity, to prevent siblings from mating with each other. F_1 x F_1 crosses were setup with a single pair per well again, and outcrossing was insured by avoiding crossing siblings with each other. In both parental and F_1 x F_1 crosses, male fathers were removed from the cross as soon as nauplii were observed. In *T. californicus,* egg sacs turn reddish right before the nauplii hatch, and if the egg sac is removed from the female at this point, nauplii will hatch normally. Given the small size of *T. californicus,* it is necessary to pool individuals to acquire enough DNA for high-throughput

sequencing. For the SD x AB cross, we collected 300 red egg sacs and 300 adults F_2 hybrids (150 males and females), while for the SC x AB and CAT x AB crosses we collected 300 adult F_2 hybrids (150 males and females). Animals were kept frozen at -80^{o}C until all individuals were collected for each cross. For the SD x AB and SC x AB crosses, DNA was isolated using the Qiagen DNeasy blood and tissue kit, with the suggested modification for extraction from insects (Qiagen). These samples were extracted in May and July 2012 respectively. For the CAT x AB cross, DNA was isolated using a Phenol:Chloroform (Sambrook and Russel 2006) procedure in February 2015.

One microgram of DNA per sample was submitted to the UNC High Throughput Sequencing Facility where sequencing libraries were prepared using the KAPA library preparation protocol for SD x AB and SC x AB, and KAPA Hyper protocol for CAT x AB (KAPA Biotechnology). Samples were sequenced as 100-bp paired-end libraries on the Illumina HiSeq 2000 for the SD x AB and SC x AB crosses, and as 125-bp paired-end libraries on the Illumina HiSeq 2500 for the CAT x AB cross. Illumina reads were trimmed for quality using PoPoolation (Kofler et al. 2011a) discarding bases with Phred quality scores lower than 25, and keeping reads of at least 50-bp after trimming.

Parental reference genome assembly, and SNP identification

When using a PoolSeq approach in hybrids, it may be difficult to differentiate within population polymorphism from between population polymorphism, which can affect allele frequency estimation. Therefore, we created a "high confidence" single nucleotide polymorphism (SNP) list using the parental reference genomes, where it is possible to confidently determine SNPs that are fixed between populations. The SD reference genome is

published online (https://i5k.nal.usda.gov/Tigriopus_californicus; v1.0), and is the highest quality reference for this species. To create reference genomes from the other three parental populations used in this study, we used an approach that involved mapping Illumina reads to the SD genome using BWA (Li and Durbin 2009), and then extracting a consensus reference using SAMtools and BCFtools (Li et al. 2009) (Supplemental Methods). We identified SNPs between the parental populations by mapping their reads to both parental reference genomes using BWA, and SNPs were called using SAMtools and BCFtools. Therefore, for each pair of parental populations (AB plus one of the other three populations) four SNP lists resulted; two from mapping across populations (divergence), and two from mapping to the their own populations (polymorphism). We first compared the two divergence SNP lists and only reciprocal SNPs were kept. The result of this was then compared to the two polymorphism SNP lists, keeping only SNPs that were not in these two lists. This procedure should yield only SNPs that are fixed (or nearly so) between each pair of populations.

Hybrid read mapping, SNP identification, and allele frequency calculation

For the hybrid datasets, reads from each cross were mapped to both parental genomes using BWA, SNPs were called using Samtools, and read counts for each SNP, as well as population specific allele counts were determined using PoPoolation 2 (Kofler et al. 2011b). The resulting list of SNPs with allele counts was compared to the high confidence SNP list and only SNP that occurred in this list were retained. Allele frequencies were calculated in relation to the AB population for each of the three crosses. Due to the large amount of noise in the allele frequency data (likely due to stochastic differences in coverage between SNPs, as well as the sampling of alleles from a pool), a sliding bin that averages over 3000 consecutive SNPs was

performed, moving the bin 600 SNPs in each step. If a scaffold had less than 3000 SNP it was excluded from any further analyses. This bin size was chosen as it was a good compromise between how much noise remained in the allele frequency estimates and the number of scaffolds that were excluded because of their size.

Determination of genome-wide patterns of hybrid inviability

We tested for deviations from the expected allele frequency across the genome to determine if hybrid inviability caused skews from this expectation. An artifact of mapping hybrid reads to each parental genome, is that allele frequencies will tend to be skewed towards the population they are mapped to on average. This is a consequence of alleles of one population being more similar to their own population's reference, and mapping with better alignment scores. This bias will cause the expected allele frequency for the hybrids (null expectation) to be different than 0.5 when mapped to either individual parental population. To minimize this bias, we averaged the allele frequencies for each bin when mapped to each of the two parental genomes.

Significant deviations from the expected allele frequencies were determined by calculating Z-scores for each allele frequency bin from each cross. Z-scores give the number of standard deviations that each bin deviates from the genome-wide allele frequency mean; a Z-score of 1 indicates the allele frequency in that bin is 1 standard deviation away from the mean. The change in allele frequency that is expected due to inviability by the F_2 generation in pooled individuals is relatively small (compared to later generation hybrids as in "evolve and resequence" studies [e.g. Burke et al. 2014]). Therefore, we considered a Z-score greater than 1 to indicate a significant deviation from the null allele frequency. Z-scores for each cross will

vary depending on the amount of variation in allele frequency within that cross, and a Z-score of 1 will not translate to same difference in allele frequencies across crosses. A major aim of this study is to compare the size and magnitude of skewed regions between crosses, therefore, we chose to use the most conservative Z-score threshold of the three crosses, in all crosses; this was the cross with the highest variance in allele frequency across the genome. Although our method cannot separate individual DM incompatibilities we can calculate the proportion of the genome that is skewed from the expected Mendelian ratio. For this calculation, we divided the number of bins that exceeded the threshold by the total number bins in each cross.

Genotyping of chromosome markers and candidate hybrid inviability regions

To verify and extend the results obtained in the genome-wide comparisons, we genotyped individual F_2 hybrids from the SD x AB cross at one marker per chromosome as well as one marker for each region that showed markedly skewed allelic frequencies. To do this, a second set of SD x AB crosses was setup in the same way as above, except that DNA was isolated from individual F_2 hybrids using a proteinase-K cell lysis buffer method (as in Willett and Berkowitz 2007) rather than individuals being pooled. Genotypes for individual F_2 hybrids were determined through PCR reactions with population specific fragment sizes (see Appendix 3.1 for primer sequences), using an annealing temperature of 56^{o}C for all markers. We genotyped 227 F2 adult individuals at 16 loci, and deviations from expected 1:2:1 Mendelian ratios were determined through a χ^2-test for each marker, with significance determined after a Bonferroni correction for multiple comparisons. Deviations were calculated for the entire dataset, as well as for males and females separately, to check for sex specific effects.

To test for epistatic interactions between genomic regions, we used the same procedure as in Willett (2006). Briefly, it is a multiplicative model that accounts for the observed single-locus effects (in inter-chromosomal comparisons) to test whether the loci are behaving as if they are independent from each other. The test asks if the observed numbers in the two- or three-locus genotypic classes deviate from expected numbers, accounting for the deviations at each locus. The significance of the deviations was assessed through a χ^2-test followed by a false discovery rate (FDR) correction at 5% (Benjamini and Hochberg 1995). Again, we analyzed males and females combined and separately.

Phylogenetic relationship estimation

Previously published *T. californicus* phylogenies that include the populations used in the present study have low support for branches between SD, AB and CAT (Willett and Ladner 2009; Peterson et al. 2013), and their relationship is not well defined. We took advantage of the annotated *T. californicus* genome to build a phylogeny using more than a single gene sequence. Coding sequences for all annotated genes in the *T. californicus* genome were extracted for all four populations used in this study, in addition to a population from San Roque (SRQ, 27°11' N, 114°24' W), known to be an outgroup to the other populations. Alignments were done for each gene separately using PRANK (Loytynoja 2014), and positions where the quality of the alignment was low were removed with Gblocks (Castresana 2000). Alignments for all genes were then concatenated, and two independent stretches of 99 Kbp of sequence were randomly chosen for phylogeny reconstruction. Phylogenies were reconstructed in MrBayes (Huelsenbeck and Ronquist 2001), using the GTR substitution matrix model (nst = 6), with gamma-distributed rate variation across sites (rates = gamma). The chain was run for 1 million generations,

sampling every 10,000 generations discarding the first 25% of the samples as burn-in. We determined convergence was achieved by examining the maximum standard deviation of split frequencies, which was 0.000, and potential scale reduction factors between 1.0000-0.9998.

We also calculated the number of synonymous changes per synonymous sites (dS) for all genes annotated in the *T. californicus* genome (13,447 genes). Estimation of dS was done in PAML 4.8 (Yang 2007) in the program yn00, in pairwise comparisons between AB and the other populations. Values were averaged across all genes for each pairwise comparison, excluding genes with a dS = 0 (which only occurred in the CAT x AB and SC x AB comparisons), and were likely a consequence of the lower quality reference genome. However, only a small number of genes had dS = 0, which should not affect the estimate (45 in CAT x AB, 63 SC x AB).

Results

Descriptive analysis and validation of method

The average depth of coverage ranged from 77.78 (SC x AB) to 234.61 (CAT x AB), which yielded between 4.4-3.7 million SNPs and 3,967-3,134 SNP bins per cross (Table 3.1). The higher depth of coverage in the CAT x AB cross is the result of using the Illumina HiSeq 2500 and new chemistry for library preparation (instead of HiSeq 2000). Note that even though AB is more closely related to SD than it is to CAT and SC (Fig. 3.3), there are more SNPs between SD x AB than the other two crosses. This however is a consequence of SD having a higher quality reference genome than the other populations, and does not indicate it is more divergent from AB than CAT and SC. The phylogeny of these populations shows that the split between AB, SD and CAT is very close together, and previous publications were unable to resolve it. While our phylogeny has high probability support for all branches, we also calculated

genome-wide dS, as this measure should approximate the amount of genomic divergence between AB and the other populations. Values for dS show that indeed the difference in divergence between AB-SD and AB-CAT is very similar, and in this case AB and CAT are slightly more closely related (Table 3.1).

When mapping hybrid reads to one of the parental population's genome, the allele frequency will be skewed towards that parental population on average. By averaging allele frequencies from mappings to both populations, this problem was in general alleviated. After this correction, genome-wide allele frequency for SD x AB and SC x AB F_2 adults was 0.50, while for SD x AB F_2 nauplii it was 0.49, and it was 0.48 for CAT x AB F_2 adults (Table 3.1). We used these values as the expected allele frequency from which deviations were measured. Next, we ran a sliding bin analysis that averaged the allele frequency of 3000 consecutive SNPs, followed by the calculation of Z-scores across all bins to determine a threshold for considering a SNP bin significantly skewed from the expected frequency. We chose to use a Z-score of one (one standard deviation away from the mean) to indicate a SNP bin was significantly skewed from the expected allele frequency. Z-scores are calculated using the distribution of the allele frequency data in each cross, and a Z-score of one will not translate to the same allele frequency in the different crosses. In order to use the same allele frequency threshold to determine skewed SNPs, we used the Z-score = 1 from the adult SD x AB cross, which had the highest variance, and therefore the more conservative threshold (± 0.05 allele frequency change from the expected frequency; Table 3.1). Another reason to use the SD x AB threshold is that we have genotyping data for this cross, and we could directly compare if the allele frequency of a specific locus was skewed both in the genome-wide sequencing (GWS) data as well as in the genotyping data.

Given this threshold of ± 0.05 allele frequency change, we compared the F_2 nauplii and F_2 adult datasets for the SD x AB cross. Our results showed that no chromosome regions exceeded the threshold in the nauplii dataset, while several large regions of the genome were skewed in the adult dataset (Fig. 3.1a-b).

Before comparing the different crosses we were interested in testing if genomic regions that were skewed in the WGS dataset, were also skewed when copepods were individually genotyped at these loci. We focused on the same SD female x AB male cross, genotyping 227 individuals at 16 loci, with at least one marker per chromosome. Deviations from expected genotypic ratios were determined through a χ^2-test, and results for each marker were compared to their respective position in the genome-wide plot. All 16 loci generally showed the same pattern as the genome-wide plot, where loci that had skewed genotypic ratios also had skewed allele frequency in the WGS data (Fig. 3.2a; Table 3.2). Four markers in particular showed the strengths and weaknesses of the allele frequency method: chromosome 2 shows that the allele frequency method has enough power to detect even weak effect incompatibilities. The marker in chromosome 2 did not significantly deviate from the 1:2:1 ratio when individuals were genotyped but had somewhat less AB homozygous individuals than expected. The allele frequency at this position in the WGS plot reached the threshold line but did not cross it. Allele frequency calculated using the genotyping data is below 0.5, but not quite as low as for the WGS data (Table 3.2), which is likely due to a difference in the sex ratio between the two datasets (males appear to show a slightly stronger skew in this chromosome). Therefore, this appears to be an incompatibility (or more than one) of weak effect, and the pattern in the WGS plot, while not exceeding the threshold line, clearly suggests a non-neutral skew. The chromosome 5 marker has skewed genotypic ratios, but the corresponding allele frequency in the WGS plot is not

significantly skewed (allele frequency = 0.47, threshold = 0.45). In this case, there is a lack of homozygous AB individuals, but there is also a small deficit of SD homozygous individuals, so the WGS approach will miss cases where both homozygotes are selected against (i.e. there are excess heterozygotes). For chromosomes 8 and 10, the PCR markers were purposely designed close to where the WGS plot crosses the threshold line. Both of these markers had significantly skewed genotypic ratios at this position, but not after Bonferroni correction was applied. These results combined suggest our method has enough power to detect relatively small skews in allele frequency, but will have low power when both homozygous classes are selected against.

In four cases, makers c1-1718, c6_CYC, c8-3336, c10-1464, the allele frequency is either skewed in WGS data and not in the genotyping data (c1-1718 and c8-3336), or skewed in the genotyping but not in the WGS data (c6_CYC and c10-1464). This is because these markers show sex specific effects, and the sex ratio in the two datasets is not the same (detailed in the next section). The genotyping dataset has 137 females and 87 males, while the WGS pool was extract from a mix of approximately the same number of males and females.

Sex specific inviability

We took advantage of the genotype data to look at sex specific effects. We considered a locus to have a sex specific effect if it was skewed from the 1:2:1 ratio in one sex only (and not if the ratio between the sexes was significantly different). Nine of the 16 markers showed some kind of sex specific effect. Males were affected more in chromosome 8, while females were affected more in seven chromosomes (1, 4, 6, 7, 10, 11, 12) (Fig. 3.2b-c). It is worth noting however that the number of males is a lot smaller than that of females, and therefore we have less power to detect deviations from Mendelian ratios. For example, markers c1-c4L and c7_37

are significantly skewed in both sexes before Bonferroni correction, however they remain significant only in females after correction for multiple comparisons. Given the current dataset females have a stronger skew for these markers, but that effect may disappear if more males were genotyped. (Appendix 3.2).

Epistasis between genomic regions

We tested for two- and three-locus epistatic interactions in the SD x AB cross, analyzing males and females separately and combined. Only a small number of significant interactions were detected in each case, none of which remained significant after FDR correction for multiple comparisons at 5% (Appendix 3.3). The signal of possible interactions were stronger when the sexes were analyzed separately, which is not surprising considering we observed sex specific effects in several chromosomes.

Patterns of hybrid inviability across different population crosses

In an effort to assess how incompatibilities accumulate between populations as they become more divergent, we compared the proportion of the genome, from three different population crosses, that deviate from expected Mendelian ratios. The phylogenetic relationship between these crosses indicates that SC x AB is more divergent than the other two crosses, while SD and AB are more closely related than the other populations (Fig. 3.3). This allowed us to test if the more divergent cross had a larger proportion of its genome skewed, as would be expected. Our results did not agree with our expectations, as the SD x AB cross had a much higher proportion of its genome skewed (32%) than the SC x AB cross (14%) and the CAT x AB cross (4%) (Table 3.1). Not only was a higher proportion of the genome of SD x AB F_2 hybrids

skewed, but also the magnitude of the skews were in general much higher than in either of the other two crosses. The most extreme allele frequencies observed in the SC x AB dataset are 0.415 and 0.572, and 0.406 and 0.591 in CAT x AB cross, while in the SD x AB cross frequencies are as low as 0.380 and as high as 0.651. In fact, the SD x AB cross has a large number of bins with allele frequencies more extreme than the most extreme frequencies in the other crosses (121 bins are less than 0.406 and 335 are greater than 0.591).

The SD x AB cross showed several regions with skewed allele frequencies in five different chromosomes (1, 3, 7, 8, and 10), and four other chromosomes had allele frequencies that reached the threshold line, but either never crossed it (chromosomes 2 and 11), or only crossed it for one (chromosome 12), three (chromosome 5) and four (chromosome 9) bins (Fig 3.1b and Table 3.3). Chromosome 3 and 10 were entirely skewed (or nearly so) towards either an excess of AB alleles (chromosome 3) or SD alleles (chromosome 10). Allele frequencies in these two chromosomes are also the most extreme we observed for any chromosome in all crosses. Chromosomes 1 and 8 are skewed for half of their length, with an excess of AB alleles in chromosome 1, and SD alleles in chromosome 8. Chromosome 7 has a small part of the chromosome skewed with an excess of SD alleles, and the magnitude of the skew is high, close to that of chromosome 10. Chromosome 5 only has a small number of bins that exceed threshold line, and the magnitude of the skew is low, but the genotyping data for this region supports it as being skewed. For chromosome 5, the effect is stronger in males, where both homozygous classes are observed less than expected, but both males and females have lower numbers of AB homozygous genotypes (Appendix 3.2). Chromosome 11 has three consecutive bins that reach the threshold line, showing an excess of AB alleles. The genotyping data suggest this effect is significant only in females, which may explain why the magnitude of the skew is low (Appendix

3.2). Chromosomes 2 and 12 are marginally skewed however the effect is weak even in the genotyping data, and only chromosome 12 in females shows significant skew at $P < 0.05$ (but not after Bonferroni correction at $P < 0.003$; Fig. 3.2 and Appendix 3.2).

The CAT x AB cross has the lowest proportion of bins showing a significant deviation from expected ratios, and has four chromosomes where multiple bins exceed the threshold lines. Chromosome 2 is skewed towards and excess of CAT alleles, while chromosomes 7, 8 and 12 are skewed towards an excess of AB alleles (Fig 3.1c and Table 3.3). The skew in chromosome 2 is the strongest in magnitude in this cross, reaching allele frequencies of 0.415, but it only affects the left end of the chromosome for less than 3 Mbp, after which the allele frequency remains within the threshold lines. Chromosome 7 is the only one that shows a strong deviation towards an excess of AB alleles, however this may be a consequence of a misassembled scaffold (see below). As whole however, chromosome 7 and 8 are marginally skewed towards an excess of AB alleles for most of the chromosome length. Chromosomes 11 and 12 are also marginally skewed in the same direction, although only for a small portion towards the center of the chromosome. In comparison with SD x AB, chromosomes 5, 10, 11 and the left portion of chromosome 2 are skewed (or nearly skewed) in the same direction, while chromosomes 6, 7, 8, 9 and 12 are skewed in opposite direction, although not all significantly so (Fig 3.1b-c).

The SC x AB cross only has three chromosomes with skewed allele frequency (3, 5, 7), and a fourth one that approaches the threshold line for some bins (chromosome 12 allele frequency = 0.544) (Fig 3.1d and Table 3.3). Chromosomes 3 and 7 both have an excess of AB alleles for a large portion of the chromosome, however the magnitude of the skews is very low. In comparison to the SD x AB cross, the skew in chromosome 3 is in the same direction, however it is not nearly as extreme in the SC x AB cross, and it does not affect the entire

chromosome. Chromosome 7 is skewed in the same direction in SC x AB and CAT x AB, but in the opposite direction in SD x AB. However, the scaffold that is skewed in the SD x AB cross, is one of the few regions in chromosome 7 that is not skewed in the SC x AB cross. Our genotyping data suggests this scaffold is anchored to the correct region of the chromosome, and that it is skewed in the SD x AB cross. But allele frequencies for this scaffold in SC x AB and CAT x AB indicate it may contain a misassembled portion in the middle of the scaffold (*de novo* assembly of the SD genome incorrectly joined certain contigs in this scaffold). Rapid shifts in allele frequency should not be expected in F_2 hybrids, and they may indicate the presence of misassembled scaffolds such as in chromosome 7 and in chromosome 5 (evident in the SC x AB cross. Fig 1d).

Chromosome 5 is the only one that has a more extreme skew in the SC x AB cross than in the SD x AB cross (of those skewed in the same direction). It has the highest magnitude skew of any SC x AB chromosomes, however this magnitude of skew is still low in comparison to several SD x AB chromosomes. Chromosome 12 shows a similar pattern between CAT x AB and SC x AB, especially at the right end of the chromosome, where in both crosses allele frequencies are close to the 0.550 threshold line. In SD x AB, this chromosome is skewed in the opposite direction, towards an excess of SD alleles. Chromosomes 5, 10 and 11, while not significantly skewed in all crosses, show the same trend, with excess of AB alleles in the c11, and a lack of AB alleles in c5 and c10 (Fig 3.1 and Table 3.3).

Discussion

We compared genome-wide patterns of hybrid inviability in *T. californicus* in three crosses of increasing phylogenetic relationship. Our results generally did not agree with

expectations from the DM model, since the more closely related cross had the highest proportion of its genome affected by hybrid inviability. Below, we discuss possible explanations for the patterns we observed, and how it fits in with previously published theories regarding the evolution of intrinsic postzygotic isolation. First though we will explore how well the pooled method works in detecting departures from expected patterns of inheritance in comparison to individual genotyping.

Validation of method

Comparisons between nauplii and adult F_2 hybrid pools from the SD x AB cross indicates there are no deviations from expected Mendelian ratios in nauplii (Fig. 3.1a), as has been previously observed in this cross for most markers (Willett and Berkowitz 2007). The average allele frequency across the entire genome was 0.49 for nauplii and 0.50 for adults, suggesting that there may be small deviations in nauplii when they hatch, as previously observed (Pritchard et al. 2011). This observation also agrees with the pattern observed in chromosome 3 markers in Willett et al (unpublished), where newly hatched nauplii have low numbers of homozygous AB genotypes in this chromosome, but as they develop ~90% of individuals that are homozygous SD at these markers die (Willett and Berkowitz 2007; Willett 2011; Willett et al [unpublished]).

Genotyping individuals can give you more power to detect deviations from Mendelian ratios, while WGS allele frequency scans allows you to scan the genome of a very large number of individuals, at a much higher density of markers (between 3,134-3,967 in this study), with very little effort, and low cost per marker. Deviations from expected Mendelian genotypic ratios (1:2:1) agreed with deviations from Mendelian allele frequency ratios (1:1) at all markers (Fig. 3.1b and Fig. 3.2). Some discrepancies appeared when we transformed the genotype data to

allele frequencies, but in all cases this was due to sex specific effects, which were more pronounced in the genotyping data.

Hybrid inviability in a phylogenetic context

The nature of DM incompatibilities has led to the prediction that the number of hybrid incompatibilities will increase faster than linear with time [snowball effect (Orr 1995)]. Evidence for this exists for inviability incompatibilities in *Drosophila* (Matute et al. 2010), and for seed sterility in *Solanum* (Moyle and Nakazato 2010). Chromosomal rearrangements may also contribute to intrinsic postzygotic isolation (Noor et al. 2001; Lowry and Willis 2010; Charron et al. 2014), however such incompatibilities should increase linearly with divergence. Even though we cannot separate individual incompatibilities in the present study, the results are surprising independent of which types of incompatibilities are causing the deviations. Our most closely related cross (SD x AB) had a much larger portion of its genome skewed due to inviability than the other more divergent crosses as well as more extremely skewed allele frequencies in three of the twelve chromosomes. While this does not necessarily mean the SD x AB cross has more incompatibilities than the other crosses (this could be caused by a smaller number of large effect incompatibilities), it indicates that when comparing crosses with low levels of divergence, the number of incompatibilities between two taxa may not be as important as the strength and positioning of the incompatibilities.

One mechanism through which this could happen even if SD x AB cross had a smaller number of incompatibilities is through incompatibilities that occur due to chromosomal changes, such as repeats, heterochromatin blocks, centromeres, and inversions (reviewed in Brown and O'Neill 2010). Large chromosomal inversions would be especially prone to cause long stretches

of chromosome to be skewed. In their review on the impact of inversions in evolution, Hoffmann and Rieseberg (2008) point out that chromosomal evolution is high in annual plants due to high levels of population turnover and size fluctuations, which increase the effects of genetic drift, allowing for chromosomal rearrangements to establish. Genetic drift is also high in *T. californicus* (Pereira et al [unpublished]), likely due to large populations size fluctuations, which may facilitate the establishment of inversions.

However, we do not think large chromosomal changes are needed to explain our observed patterns. Given that there is no recombination in *T. californicus* females, and that we are surveying second-generation hybrids, the amount of recombination that we would expect is small in each chromosome. We are able to detect skewed regions of fairly small sizes (< 2Mbp in chromosome 7 for SD x AB; < 3Mbp in chromosome 2 in CAT x AB), which are likely a consequence of the position of the incompatibility, the structure of the chromosome, and the fact that we sampled alleles from a pool of 300 individuals. For these cases, we hypothesize that a small number of incompatibilities of moderate effect, maybe just one, occur at an end of the chromosome in an area where recombination is high, and this allows us to detect such a small region. In the case of chromosome 1 and 8 in SD x AB, where a larger portion is skewed towards one end of the chromosome, the same may be the case, except that recombination rates may be lower in these regions. Such a pattern would be observed if these incompatibilities occurred near chromosomal features that decrease recombination (e.g. centromeres or telomeres). An alternative explanation would be that these chromosomes have an incompatibility of large effect in one end of the chromosome, and one or more incompatibilities of small effect towards the other end of the chromosome, shifting the allele frequency of the entire chromosome. If incompatibilities occur towards the center of the chromosome a larger portion of the

chromosome will appear skewed, as regions on both sides of the incompatibility will be dragged due to linkage (Fig. 3.1).

On the other hand, the extreme allele frequencies that we observe in chromosome 3 in SD x AB are likely the result of multiple incompatibilities, of moderate to large effect, in the same chromosome. In a backcross study (Willett et al [unpublished]) between F1 hybrids of this cross and SD males, where an intact SD (and AB) chromosome is passed on by female hybrids (because there is no recombination in females), the same high mortality was observed for this chromosome for individuals that were homozygous SD. However, when F1 hybrids were backcrossed to SD females, where there is recombination in the F1 male hybrid, the same skews were not observed. This suggests that there are two factors in chromosome 3 contributing to this, and they are far enough from each other that recombination can separate them in one generation of mating. The incompatibilities involved are likely partially recessive, and in backcrosses only when both chromosome 3 factors are present as SD homozygous do we observe the full effect. This is because these incompatibilities likely involve AB alleles in other chromosome, which in a backcross will never appear as homozygous AB. However, in F2 hybrids, where homozygous-homozygous incompatibilities are observed, the effects of these incompatibilities will be stronger, and a large change in allele frequency will be observed even in the face of recombination. Therefore, most individuals that are homozygous SD for any part of this chromosome will experience some combination of these incompatibilities, which should be enough to make them inviable.

Sex specific inviability

We observed higher deviations from expected genotypic ratios in females than in males, even though the sex ratio was female biased, which may indicate higher male mortality. Since we cannot differentiate sex in nauplii, it is difficult to determine if this female biased sex ratio is due to higher mortality of males due to incompatibilities, or if the sex ratio is already skewed once sex is determined due to sorting of sex determining alleles. *Tigriopus californicus* does not have differentiated sex chromosomes, and sex is thought to be determined by genic factors that are not necessarily in the same chromosome (Voordouw and Anholt 2002; Alexander et al. 2014). One characteristic of polygenic sex determination is the large variation in sex ratios between families (Bull 1983), which may be exacerbated in hybrids, if sex-determining loci have diverged between the populations. The stronger deviations in females are in part due to the higher number of individuals of this sex in our dataset, which gives us more power to detect deviations. However, stronger deviation in females for 6 chromosomes are unlikely to be due to this difference in number, as the difference in ratios is large. Males show stronger deviations in only two chromosomes compared to females (Fig 3 b-c and Appendix 3.2).

Our findings stand in contrast to those of Foley et al. (2013) who saw stronger hybrid inviability effects in males in a SD x SC cross. However, this is not surprising as *T. californicus* does not have differentiated sex chromosomes, and it is not expected that one of the sexes will always suffer stronger inviability. Even though we observe some sex specific effects in these F_2 hybrids, sex specific effects appear to have little importance for the formation of complete reproductive isolation in *T. californicus*. In F_1 hybrids, when sterility or inviability is complete, it affects not a specific sex, but both sexes with the same mitochondrial background (Ganz and Burton 1995; Peterson et al. 2013). This pattern is likely the consequence of incompatibilities

between the mitochondrial genome of one population and the nuclear genome of the other (mito-nuclear incompatibilities). Therefore, effects of sex specific incompatibilities observed in F_2 hybrids may eventually be swamped by the stronger effects of mito-nuclear incompatibilities affecting F_1 hybrids.

Conclusion

Here we surveyed the genome of pooled F_2 hybrids from different population crosses for regions affected by hybrid inviability. Results show that the least divergent of the three crosses had the highest amount of allele frequency deviations, which could indicate it accumulated more incompatibilities than the other more genetically divergent crosses. However, a more likely scenario is that at these early stages of divergence, the number of incompatibilities between two taxa is less important in determining the level of isolation than the strength of the incompatibilities and their location within specific chromosomes. Both strength and location of an incompatibility may be stochastic between populations of a species, but will determine the strength of postzygotic isolation more than overall genomic divergence.

Figure legend

Figure 3.1. Allele frequency plots for F_2 hybrids from three population crosses of *T. californicus*. Allele frequencies are in relation to the AB populations (y-axis). The x-axis indicates the relative position across each chromosome. Data points are the average allele frequency for a bin of 3000 consecutive SNPs. Data points above the top dashed line indicate the allelic ratio is skewed towards an excess of AB alleles, while data points below the bottom dashed line indicate the allelic ratio is skewed towards a deficit of AB alleles. Dashed line thresholds are ± 0.05 from the mean genome-wide allele frequency for each cross. **a.** SD x AB F_2 nauplii; **b.** SD x AB F_2 adults; **c.** CAT x AB F_2 adults; **d.** SC x AB F_2 adults. Asterisks in SD x AB adults plot (b.) indicate the positions that were genotyped. Straight lines connecting groups of allele frequency points refer to chromosomal positions where scaffolds have not been anchored to.

Figure 3.2. Relative genotypic frequencies for SD x AB adult F_2 hybrids. Each bar represents a genotyped marker, and x-axis label refer to the chromosome the makers map to. Asterisks indicate markers for which the genotypic ratio deviates significantly from the expected 1:2:1 Mendelian ratio after Bonferroni correction ($P < 0.003$). Dots indicate deviations from this ratio with $P < 0.05$. **a.** Males and females combined; **b.** Males only; **c.** Females only.

Figure 3.3. Bayesian phylogeny of the four *T. californicus* populations used in this study, with the San Roque (Mexico) population as outgroup. Branch lengths were calculated using the GTR+gamma model with two independent sets of 99 Kbp stretches of concatenated coding sequences. Numbers above branches are the Bayesian posterior probabilities.

Table

Table 3.1. Summary statistics for the three crosses of *T. californicus* populations. SNP bins are the average allele frequency for 3000 consecutive SNPs, moving the bin 600 SNP each time. Mean genome-wide allele frequency and Z-scores were calculated using the allele frequencies averaged across the SNP bins.

Cross	Average depth of coverage	Number of SNP	SNP bins	dS	Mean genome-wide allele frequency	Z-score = 1 around genome-wide mean	Bins > 0.050 from average	Bins < 0.050 from average
SD x AB nauplii	89.55	4,358,490	3967	0.0492	0.49	0.016	6	16
SD x AB adults	87.49	4,214,453	3774	0.0492	0.50	0.050	637	565
CAT x AB adults	234.61	4,017,719	3559	0.0488	0.48	0.024	63	69
SC x AB adults	77.68	3,695,662	3134	0.0530	0.50	0.030	208	216

Table 3.2. Allele frequencies from SD x AB F_2 adults calculated from the genotyping data and from the whole-genome sequencing (WGS) data for the same genomic regions. In bold are skewed allele frequencies based on the Z-score threshold of ± 0.05 from the mean genome-wide allele frequency. Italics in the genotyping data indicate significant deviation from the 1:2:1 genotypic ratio.

Allele Frequency	c1-1718	c1-c4L	c2-5	3fblrr	3qcr8	c4R	c5-P5C	c6-CYC	c7-2776	c7-37	c8-3336	c9-2203	c10-1464	c10-c11	c11-septub	c12-ME1
Genotyping	*0.548*	***0.551***	0.484	***0.645***	***0.648***	0.544	*0.454*	**0.551**	0.482	***0.427***	0.476	0.545	**0.444**	***0.406***	***0.562***	0.476
WGS	**0.577**	**0.569**	0.467	**0.607**	**0.631**	0.509	0.471	0.506	0.462	**0.417**	**0.437**	0.546	0.472	**0.430**	**0.554**	0.469

Note – PCR markers in c1, c7-2776, c10, c11-septub and c12-ME1 map to scaffolds that have less than 3000 SNP, and were therefore excluded during the SNP bin averaging for other analyses. Thus, the allele frequencies shown for these markers for the WGS data were calculated based on the allele frequency average for all SNP in these scaffolds.

Table 3.3. Percentage of skewed SNP bins for F2 hybrids for each chromosome for each cross. Extreme frequency displays the allele frequency SNP bin that deviates the most from the mean genome-wide allele frequency. Anchored scaffolds are the number of scaffolds that are anchored to each chromosome based on the linkage map from Foley et al (2011) and Willett et al (unpublished), followed by the total number of base pairs in these scaffolds.

Chromosome	Anchored scaffolds	Base pairs anchored	SD x AB		CAT x AB		SC x AB	
			% skewed	Extreme frequency	% skewed	Extreme frequency	% skewed	Extreme frequency
1	15	5,273,807	86.6	0.610	0.0	0.457	0.0	0.516
2	12	6,196,910	0.0	0.450	14.7	0.415	0.0	0.480
3	13	5,870,172	99.4	0.651	0.0	0.517	29.6	0.564
4	8	3,956,900	0.0	0.526	0.0	0.508	0.0	0.520
5	14	6,664,514	2.7	0.436	0.0	0.447	75.1	0.415
6	7	2,036,135	0.0	0.530	0.0	0.444	0.0	0.518
7	10	6,460,330	10.4	0.403	4.5	0.591	38.9	0.572
8	10	4,125,445	50	0.422	13.8	0.535	0.0	0.478
9	10	4,456,974	3.3	0.563	0.0	0.454	0.0	0.520
10	10	4,339,135	85.7	0.380	0.0	0.439	0.0	0.468
11	7	2,056,121	0.0*	0.547	0.0	0.530	0.0	0.526
12	5	2,225,762	6.1	0.444	1.4	0.541	0.0	0.544

Note- *Chromosome 11 has a skewed region in the middle of the chromosome based on genotyping. However, the scaffold where this marker maps to has less than 3000 SNP, and is therefore excluded from the bin averaging.

Figures

Figure 3.1:

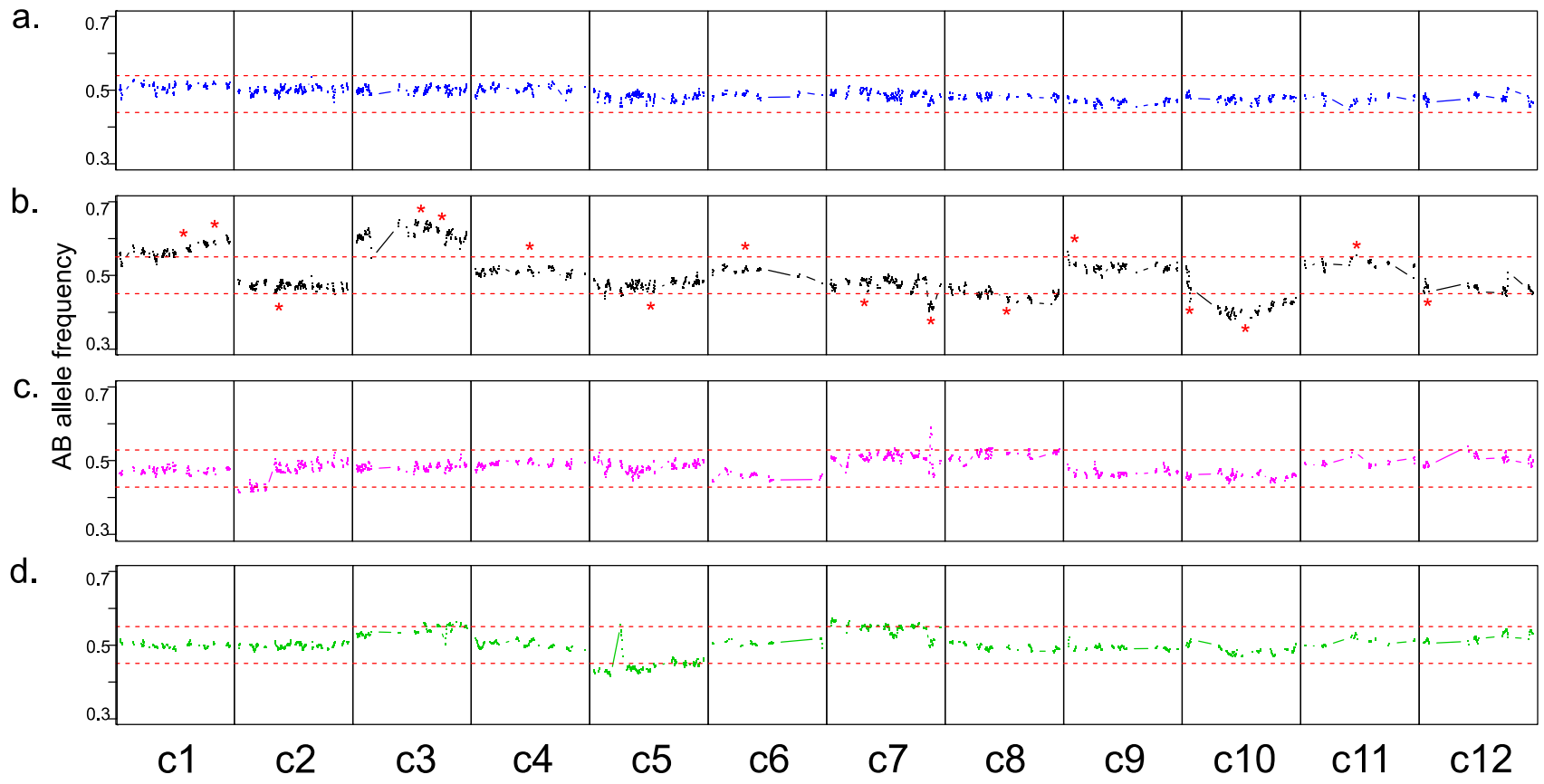

Note- Chromosome 11 has a skewed region in the middle of the chromosome based on genotyping. However, the scaffold where this marker maps to has less than 3000 SNP, and is therefore excluded from the bin averaging. The data point shown under the asterisk in this chromosome was calculated using 602 SNP

Figure 3.2:

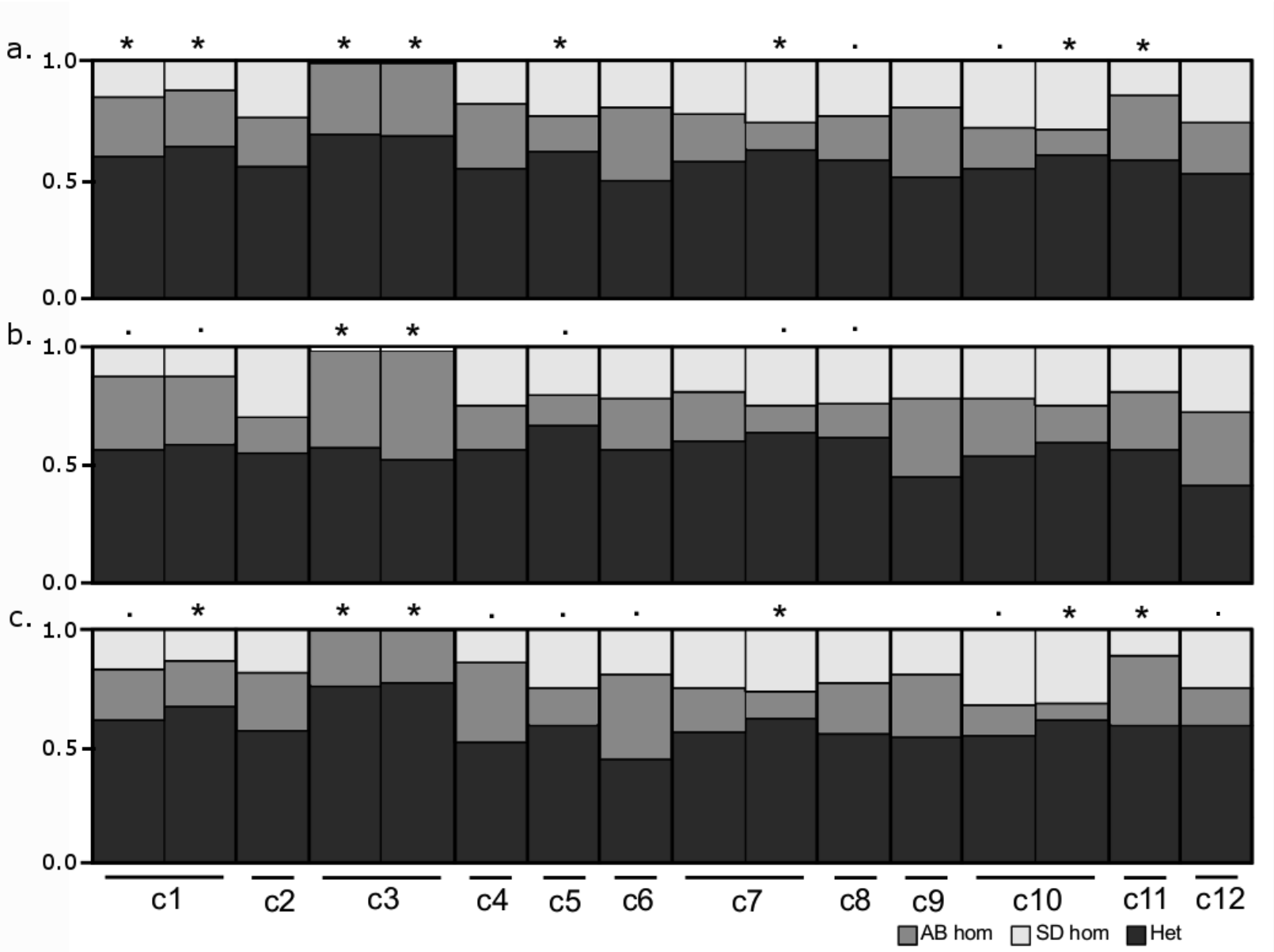

Figure 3.3:

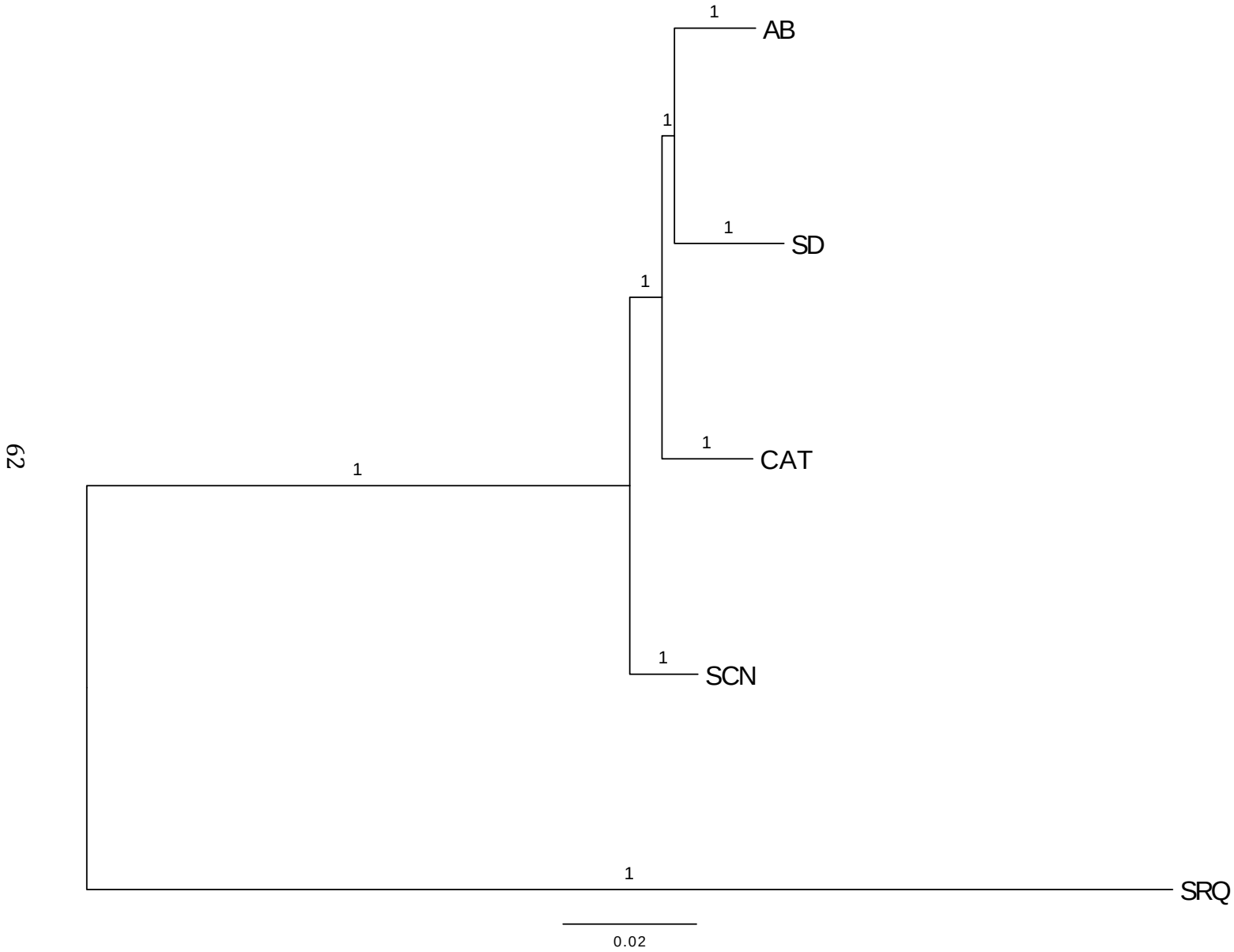

CHAPTER IV: TRANSCRIPTOME-WIDE GENE EXPRESSION RESPONSES TO CONSTANT AND VARIABLE THERMAL ENVIRONMENTS

Summary

Understanding the genetic basis of adaptation and phenotypic plasticity is of interest to evolutionary biologists and physiologist as these mechanisms can contribute divergence between populations. Predictions of climate change have also made this area of research important as a way to assess how organisms will respond to these changes. Several recent studies have greatly improved our understanding of how local adaptation to thermal tolerance affects an organism's ability to withstand increases in mean and maximum temperatures. However, one of the predicted consequences of climate change is the increase in thermal variability in many environments. We still know very little about how increases in thermal variability will affect organisms, and a few studies have showed that exposure to fluctuating temperatures may increase an organism's ability to withstand higher temperatures, but with a trade-off that decreases other fitness measures such as growth rate and fertility. Here we used the copepod *Tigriopus californicus* to investigate transcriptome-wide expression responses to constant and variable thermal regimes, and looked at how locally adapted populations differed in the genetic basis of their response to these different regimes. Our results show that the genetic basis of the response to these temperature treatments differed drastically between all populations, even for populations that are geographically close. Also, less thermally tolerant populations showed markedly different expression profiles from each other, but in both populations, the genetic

signature of their response indicates potential trade-offs between increasing response to heat stress and lowering expression of genes involved in basic cellular processes.

Introduction

Studies on the ability of organisms to adjust to changing environments through time (adaptation), or within a generation (phenotypic plasticity), have been of interest to evolutionary biologists and physiologists for some time. The selective pressures imposed by these scenarios, especially for ectotherms, can be a driver of divergence between closely related populations (Angilletta 2009). This line of research has also become increasingly important as a way to assess the likelihood that species will be able to persist in the face of predicted future climate change. How important evolutionary adaptation versus phenotypic plasticity will be in response to climate change is especially important for predicting the ability of organisms that have limited dispersal to persist (Hoffmann and Sgrò 2011). More recently, it has become evident that understanding the effects of increases in thermal variability may be as important as understanding the impacts of increases in mean or maximal temperatures for determining how well an organism will fare in future climates (Petavy et al. 2004; Podrabsky and Somero 2004; Schaefer and Ryan 2006; Tomanek 2010; Folguera et al. 2011).

Differences in local adaptation between populations (or species) and how it contributes to difference in thermal tolerance are becoming better understood. Studies that exposed organisms to a constant high temperature stress demonstrate that more heat tolerant populations show a correlation between their ability to survive higher temperatures and their ability to display a strong molecular response of the well characterized heat shock response mechanism (Tomanek and Somero 1999; Angilletta 2009; Schoville et al. 2012; Barshis et al. 2013; Gleason and

Burton 2015). In comparison, studies that exposed organisms to fluctuating temperatures find that while experiencing higher non-lethal temperatures before a thermal stress is applied may increase their ability to tolerate higher temperatures, there is usually a trade-off that decreases the organism's performance in other traits such as growth rate and fertility (Schaefer and Ryan 2006; Folguera et al. 2011). These trade-offs may have a stark impact on an organism's ability to compete with other organisms, and it may indicate that increases in thermal variability can have a greater impact on a population's ability to survive than an increase in mean or maxima temperatures.

The ability on an organism to deal with differences in thermal variability will depend on the degree of phenotypic plasticity that they can express, which can differ between different locally adapted populations. Our understanding of the genetic basis of responses associated with an increase in thermal variability is still largely unknown. In this study we were interested in determining the transcriptome-wide responses that different locally adapted populations from the same species would have when exposed to variable temperature environments compared to constant temperature environments. More specifically, we wanted to determine if there are differences in the genetic basis of phenotypic plasticity between the locally adapted populations. And finally, we wanted to investigate if differences in the genetic response to cycling temperature environments can give us clues as to how organisms cope with increases in thermal variability in their environment.

We used the copepod *Tigriopus californicus* to address these issues, as this species gives us the opportunity to compare a number of locally adapted populations. Populations of this species inhabit splash pools on the Pacific coast of North America, and can be exposed to large changes in temperature on a daily basis. Gene flow between populations is extremely low, even

for populations that are only a few kilometers apart (Burton 1997; Willett and Ladner 2009). These populations show some significant differences in local adaptation, particularly for thermal tolerance where thermal tolerance increases as latitude decreases with lethal temperatures ranging from 35˚ in the north to 38˚ in the south (Willett 2010; Kelly et al. 2012). Kelly et al. (2012) showed that this range of tolerance across the entire species range is much wider than the range within any one individual population, implying that models that only consider species-wide tolerance ranges can be incorrectly estimating the ability of populations to survive. Willett (2010) showed that at higher non-lethal daily cycling temperatures (20-28^{o}), southern populations outcompete northern ones, and the opposite is true for colder cycling temperatures (16-25^{o}) or lower constant temperatures (16^{o}). One study to date has looked at the genetic response to high stressful temperatures in this species (Schoville et al. 2012) but no studies have examined gene expression under more moderate temperatures. Schoville et al. (2012) in their study of acute thermal stress (35^{o}), found that *T. californicus* from a southern population (San Diego, CA) showed much greater up-regulation of genes that are known to respond to heat stress, such as heat shock proteins, than did individuals from a northern population (Santa Cruz, CA) (Schoville et al. 2012).

In the present study we compare patterns of transcriptome-wide gene expression for four populations of *T. californicus* (two southern and two northern) under two different temperature regimes (constant 20^{o} and cycling 20-28^{o}). Our results show that the molecular response to these temperature treatments varies widely across the four populations, even between populations separated by < 10 km (the two southern populations). The less thermally tolerant northern populations show markedly different expression profiles from each other, but in both populations, the genetic signature of their response can potentially explain why they are

outcompeted by the more thermal tolerant southern populations at these non-lethal cycling temperatures.

Methods

Copepod collection, culture and thermal treatments

Copepods were collected in May 2103 from rocky intertidal pools from four sites, the two southern populations of San Diego (SD-S, 32°44’ N, 117°15’ W) and Bird Rock (BR-S, 32°48’ N, 117°16’ W), and the two northern populations of Santa Cruz (SC-N, 36°57’ N, 122°03’ W) and Bodega Bay (BB-N, 38°19’ N, 123°04’ W). Copepods were maintained *en masse* cultures in petri dishes in 35ppt artificial seawater (Instant Ocean, Aquarium Systems), and fed commercial fish food, as well as natural algae growth. Cultures were kept in incubators with 12 hour light:dark cycle at 20^{o} for 2-3 generations before beginning the experiment. Copepods were exposed to two thermal regimes: a) a constant 20^{o} and b) a cycling environment with 12h at 20^{o} and 12h at 28^{o} each day. For both regimes for all populations, 25 gravid females were transferred to petri dishes (4 dishes per population per treatment), and randomly assigned to one of the thermal regimes. Mothers were removed when offspring reached the copepodid stage. On the day before RNA isolation, 100 copepods from each petri dish were transferred to a new petri dish, without food added. For each treatment all populations had two dishes with 100 copepods and a separate mRNA library was created from the pool of 100 copepods for each population/treatment replicate. As shown in Fig. 4.1, there were two sampling points for both the 20-28^{o} daily cycle, the first at the end of the 20^{o} period and the second two hours after the temperature shift to 28^{o}. For the 20^{o} constant environment samples were taken at the same point in the diurnal light cycle (end of the dark cycle) and from the other dishes that had been moved

to the 28º environment at the same two hour point as for the cycling samples (2 hours after the start of the light cycle).

RNA extraction, and Illumina sequencing

For each treatment at the appropriate sampling time, copepods from each dish (~100 individuals) were collected onto filter paper, rinsed with filtered seawater, and immediately transferred to 250µL of Tri-reagent (Sigma). RNA isolation was done following the manufacturer's protocol. RNA samples were quantified using Qubit 2.0 fluorometer (Life Techonologies), and 2µg of total RNA per sample were submitted to the UNC High-Throughput Sequencing Facility for library preparation and sequencing. RNAseq libraries were prepared using the TruSeq Sample Prep kit (Illumina), and samples were sequenced as 100-bp single-end unstranded mRNA libraries in the Illumina HiSeq 2000 (for one replicate of SD-S and SC-N, and both replicates of BR-S and BB-N) and HiSeq 2500 (for the second replicate of SD-S and SC-N). Each Illumina sequencing lane contained two populations (SD-S and SC-N; BR-S and BB-N), with all treatments barcoded. Replicates were sequence in the same manner in separate lanes, for a total of four lanes. Illumina reads were trimmed for quality using CLC Genomics Workbench (CLC GW) 7.0.4 (CLC Bio) discarding bases with Phred score lower than 20, and keeping reads with at least 15-bp remaining after trimming.

Transcriptome assembly and annotation

An annotated reference genome for the SD-S populations has been published online (https://i5k.nal.usda.gov/Tigriopus_californicus), and it was used to build transcriptome references for all populations in this study as follows. Annotated genes from the SD-S reference

genome were extracted, and alternative splice variants were removed keeping only the longest splice variant of a gene. To avoid a bias in mapping of reads from SD-S to its own high quality reference with reads from the other populations likely to have some SNP differences, we built references from each of the four populations by mapping them to the SD-S genes, and extracting a consensus reference for each one. Trimmed reads from all treatments were combined for each single population, and mapped to the SD-S genes using BWA MEM using default parameters (Li and Durbin 2009). Following mapping, reads with low mapping quality (MAPQ < 20, likely the result of incorrect alignment) were removed, and the consensus sequences for each population were extracted using SAMtools and BCFtools (Li et al. 2009; Li 2011). We assessed the quality of the references by calculating the total number of "N's" in the reference transcript set of each population. We also compared the sizes of the orthologus contigs and the number of "N's" in each contig for all transcripts that occurred in all four populations. Since our gene expression analysis only compared within population differences in treatment reads mapped to their own reference, no further action was taken at this stage of the analysis to remove short transcripts with high percentage of "N", as these were removed during gene expression analysis (see below).

The published SD-S genome assembly is thought to include ~80% of the entire genome, and certain genes are known to not be in this reference (including at least 1 heat shock protein). To avoid excluding these genes from our analysis, we used *de novo* transcriptome assemblies from Pereira et al (unpublished) to complement the pool of genes in our analysis (see below). To avoid confusion, we will refer to the set of genes relating to the reference genome as genomic-transcripts (GT), and from the *de novo* transcriptome assembly as *de-novo*-trancripts (DNT). Transcripts originating from the different references can be differentiated based on their ID,

where GT transcript IDs begin with "TCALIF", while DNT transcript IDs begin with either "Contig" or "comp".

BLAST2GO (Conesa et al. 2005) was used to annotate transcripts from the references. We used the SD-S reference for annotation as it had slightly higher quality than the others. BLASTX searches were performed against the "nr" NCBI protein database, retaining hits with $E \leq 10^{-3}$. Gene Ontology (GO) terms (Ashburner et al. 2000) were retrieved for contigs with positive BLAST hits, with an $E \leq 10^{-3}$.

Mapping and identification of differentially expressed genes

Trimmed reads for each treatment were mapped to their respective population's GT references in CLC GW (mapping parameters: similarity fraction = 0.99; length fraction = 0.8; mismatch cost = 2; insertion cost = 3; deletion cost = 3). Unmapped reads were retained and mapped to the DNT references using the same mapping parameters. Only unique mapped reads from the two sets of mapping files were used in further analyses. Only orthologous genes that occurred in all four populations were considered. Orthologous genes from the GT reference already had the same ID, while those from the DNT reference were extracted from the orthologous list in Pereira et al (unpublished), and were given the SD-S ID for ease of comparison in later steps.

Differential expression was determined using the Bioconductor package edgeR (Robinson et al. 2010), in pairwise comparisons between treatments within each population. Since the pairwise comparisons were not simply "control vs treatment", separate files for each pairwise comparison for each population were created, and analyzed separately. Genes with very low levels of expression in both treatments were removed by retaining only those that

accumulated at least two counts per million in at least two out of four samples, allowing for both replicates of a treatment to have zero mapped reads, if both replicates in the other treatments had enough reads mapped to them. This also removed all genes that had zero mapped reads in the DNT reference, because the appropriate reads for these transcripts had already mapped to the GT reference. Compositional differences between the libraries were normalized using the trimmed mean of M-values method (Robinson and Oshlack 2010). For each population, all treatments were examined for possible batch effects between the replicates. A multidimensional scaling (MDS) plot was used to visualize the level of similarity between each RNA sample for each population (Appendix 4.1). To account for batch effects between the replicates, a negative binomial generalized linear model (GLM) was fit, where "batch" was used as a blocking factor. Likelihood ratio tests were used to determine genewise expression differences between two treatments, followed by a false discovery rate (FDR) correction of *P*-values set to 5% (Benjamini and Hochberg 1995). Genes that were detected as differentially expressed (DE), but had 0 reads mapped to both replicates in one of the treatments, were considered DE but were excluded in comparisons of the magnitude of their relative expression, as they showed abnormally high levels of fold change.

Pairwise comparisons of relative gene expression

Three pairwise comparisons between treatments were done in edgeR, each aimed at answering a specific question (Fig. 4.1). To determine how populations respond to potentially low levels of thermal stress, relative expression between the constant 20^{o} (co20) and stress 28^{o} (st28) treatments was calculated. To determine how populations respond to daily fluctuations in temperature, relative expression between the cycling 20^{o} (cy20) and cycling 28^{o} (cy28) was

calculated. Differences between these two comparisons (co20-st28 vs cy20-cy28) should then reflect the effects of phenotypic plasticity responses to exposure to 28^{o}C. To determine if genes were being differentially expressed between cycling and constant regimes, relative expression between co20 and cy20 was calculated.

Gene ontology enrichment analysis and Fisher's exact test

Enrichment of Gene Ontology (GO) terms was assessed in Blast2GO using Fisher's exact tests for every GO term that appeared in a subset of genes, compared to all genes used in the analysis for each population (reference set). *P*-values were adjusted for multiple comparisons using a FDR set at 5%. GO enrichment analysis was performed for up- and down-regulated genes separately for each pairwise comparison, as well as, for each cluster of covarying genes in each population. In many cases redundant GO terms were significantly enriched in a dataset, in which case only one of these terms was included in our results using the following criteria: a) if the terms associated with the same transcript belonged to different GO categories (i.e. biological process (P), molecular function (F), or cellular component (C)) they were all kept; b) the most specific term was kept if it included approximately the same number of genes as the more broad term (e.g. response to stress (more specific) had 13 genes, response to stimulus (broader) also had 13 genes, response to stress was kept); c) when multiple more specific terms combined included most of the genes in their common broader term, the specific ones were kept.

Fisher's exact tests were also used to compare the magnitude of the fold-change between different pairwise comparisons, or between the same comparison across populations. In this case, four different treatments (or two different treatments in two populations) were compared, and we

used the averaged normalized read counts for both replicates of a treatment as a measure of expression for each treatment.

Clustering of expression patterns

In order to get a clearer picture of the pattern of gene expression across the different treatments, we clustered genes based on how they were behaving in the three different pairwise comparisons (co20-st28, cy20-cy28, co20-cy20). For each of the three comparisons we asked if genes were DE or not, and for the DE genes whether they were up- or down-regulated. For example, all genes that were up-regulated in all three comparisons were clustered together (i.e up-up-up in Fig. 4.2).

Results

Illumina sequencing, RNAseq mapping and differential expression analysis

RNA sequencing yielded ~7.6-29 million reads per sample after trimming (Table 4.1). The GT references created by mapping RNAseq reads to the genome transcriptome yielded 13,839 orthologous transcripts, while the DNT *de novo* assembly from Pereira et al. (unpublished) included 12,576 orthologous transcripts, for a total of 26,415 transcripts. Of these, 20,211 (76%) had a significant BLAST hit, and were assigned a gene name. GO terms were retrieved for 17,422 transcripts (66%). The roughly 26,000 transcripts is an overestimate of the number that factored in the analyses for several reasons. First, the two transcriptomes are redundant (redundant DNT transcripts were dropped after mapping reads as described in the methods), and second, several transcripts were filtered out during differential expression analysis due to low number of mapped reads. The resulting datasets varied slightly for each population

because the transcripts with low coverage were not always the same; the number of transcripts used for the remainder of the study were: SD-S: 18,560 (11,747 GT, 6,813 DNT); BR-S: 18,168 (11,720 GT, 6,448 DNT); SC-N: 19,021 (11,584 GT, 7,437 DNT); BB-N: 18,480 (11,569 GT, 6,911 DNT).

Response to moderate thermal stress from constant temperature regime (co20-st28)

Southern populations have been shown to be more tolerant to higher temperatures, and to be able to up-regulate thermal stress genes (such as HSPs) to higher levels when exposed to acute thermal stress (Willett 2010; Kelly et al. 2012; Schoville et al. 2012). Here we exposed *T. califonicus* from two southern and two northern California populations, that had been raised at a constant 20^{o} (co20), to a moderate thermal stress [28^{o} (st28)], which allowed us to assess not the limits of each populations' ability to up-regulate certain genes (as in acute stress), but rather to determine whether they would differentially regulate these genes to cope with mild thermal stress. One potential hypothesis is that the southern populations, which are more thermal tolerant, will need to change gene expression less than northern populations between these temperatures, since this thermal regime presents a less stressful environment to them. This means southern populations may regulate expression of a smaller number of genes, and/or change expression to a lesser extent than northern populations. This is what we observe between the two southern populations and BB-N, however SC-N had a lower number of differentially expressed (DE) genes than all other populations for this treatment (Fig 3a). DE genes were those with a *P*-value < 0.05 after correction for multiple comparisons using a FDR of 5%. SD-S had 107 DE genes (100 up, and 7 down), and BR-S had 85 DE genes (74 up, 11 down), while BB-N showed

differential expression in 237 genes (204 up, 33 down), and SC-N had 54 DE genes (52 up, 2 down).

In order to determine if northern populations increased the expression of certain genes to a higher magnitude than southern ones, we looked at genes that were DE in all four populations for the co20-st28 comparison, and performed Fisher's exact tests for all pairwise combinations. All of the 25 genes that were DE in all populations are up-regulated between co20-st28. All 25 genes are up-regulated to a higher magnitude in BB-N than in SD-S based on fold-change, and 11 of these are significantly so based on the Fisher's test. Twenty genes had higher fold change in BB-N than in BR-S, 9 of them were significantly higher, while 5 genes have higher fold-change in BR-S compared to BB-N, none of them however were significantly higher (Table 4.2). SC-N has higher magnitude of change in 18 genes compared to SD-S, three of these are significantly higher; compared to BR-S, 17 genes are up-regulated to a higher magnitude in SC-N, only one of them significantly so, while two have significantly higher magnitude of change in BR-S (Table 4.2). In comparisons within region, BR-S had higher magnitude of fold-change of 14 genes, three were significantly so compared to SD-S, and BB-N had higher up-regulation of 22 genes, three being significantly so compared to SC-N (Table 4.2). Overall, SD-S in average up-regulated these 25 genes less than the other populations, and this increased as you moved north, with BB-N having the highest magnitude of change in expression in the majority of these genes.

In all four populations GO enrichment analysis found that terms associated with "response to stress" and "unfolded protein binding" were enriched in DE genes that were up-regulated (Table 4.3). Heat shock protein genes contributed to the enrichment of both these terms and were the most common class of up-regulated genes (16 in SD-S, 13 in BR-S, 14 in SC-N and

15 in BB-N). BB-N also had enriched GO terms for down regulated genes as well ("structural molecule activity" and "extracellular region"), and cuticle protein genes contributed to this enrichment, although these genes were DE in both directions (7 up, 3 down) (Table 4.3).

Response to moderate thermal stress in cycling versus constant temperature regimes (co20-st28 vs cy20-cy28)

Next, we compared genes that were DE in co20-st28 and cy20-cy28. The total number of DE genes for cy20-cy28 in SD-S was 128 (94 up, 34 down), in BR-S it was 100 genes (66 up, 34 down), in SC-N 32 (28 up, 4 down), and in BB-N there were 491 DE genes (107 up, 384 down) (Fig. 4.3b). Except for SC-N, there were more DE genes in cy20-cy28 comparison than in the co20-st28, however, this was due to a larger number of down regulated genes in all populations. The number of up-regulated genes was smaller in all populations, especially in the northern ones, where there were approximately half as many up-regulated genes; in southern populations the number of up-regulated genes was approximately the same (Fig. 4.3).

We then looked at the magnitude of the fold change for DE genes, comparing genes that were DE in both co20-st28 and cy20-cy28 for each population using Fisher's exact test (we consider genes that are uniquely DE in only one of the comparisons in the clustering section below). Of the 42 genes that were DE in both comparisons for SD-S, 35 have a lower fold change in cy20-cy28 (11 are HSP genes), 9 of which are significantly so. Two genes are up-regulated in co20-st28 and down-regulated in cy20-cy28 (one of these is an HSP beta 1 gene) (Appendix 4.2). In BR-S, of the 27 genes (4 are HSP genes), 21 have lower fold change in cy20-cy28, of which 9 are significantly lower. Three genes are down-regulated in cy20-cy28 but up-regulated in co20-st28 (Appendix 4.3). In SC-N, 18 genes are DE in both comparisons (7 are HSP genes), and 11 have lower fold change in cy20-cy28, but only one is significantly so (an

HSP 70). One gene has significantly higher fold change in co20-st28, something that is not observed in either southern population (Appendix 4.4). BB-N has 128 genes that are DE in both comparisons, of which 117 have lower fold change in cy20-cy28 (13 are HSP genes), and 85 are significantly lower. Three genes have significantly higher fold change in co20-st28 (Appendix 4.5).

The difference in fold change for genes with a lower magnitude of change between these comparisons ranges from 25.71-0.02 in SD-S, 35.86-0.10 in BR-S, 40.76-0.05 in SC-N, and 328.63- 0.11 in BB-N. Two HSP 70 (TCALIF_04517 and TCALIF_06728) are the top genes with highest change in magnitude in all populations (in SC-N they are in the top 3). In southern populations TCALIF_04517 has the highest change in magnitude, while in northern populations it is TCALIF_06728 (Appendix 4.2-4.5).

GO enrichment analysis for the cy20-cy28 comparison again finds that terms associated with "unfolded protein biding" were enriched in DE genes that were up-regulated in all populations. While terms associated with "response to stress" are enriched in SD-S, SC-N and BB-N, but not BR-S. Terms associated with "structural molecule activity" also appear in SD-S, BR-S and BB-N, however they occur in up-regulated genes in SD-S, but down-regulated genes in BR-S and BB-N. This enrichment occurs mostly due to cuticle protein genes, and their expression pattern appears to be population specific, and not region specific. Genes associated with "extracellular region" are enriched in down-regulated genes in SD-S and BB-N only, while "hydrolase activity" and "carbohydrate metabolic process" terms are enriched in down-regulated genes in BR-S (Table 4.3).

Differential expression between thermal regimes

In the previous section we showed that the fold change of genes from the cycling treatment is often smaller than when individuals are raised at a constant temperature and shifted to a novel temperature, as would be expected as a form of plastic response. One hypothesis for why the fold change in HSPs, and other genes associated with thermal tolerance, was lower in the cy20-cy28 comparison may be due to the up-regulation of these genes while at 20^{o}, in "anticipation" to the higher temperature they experience in a daily basis (frontloaded). This would maintain higher levels of expression of certain genes compared to individuals raised at a constant 20^{o}. Considering our results so far, where northern populations show stronger responses to both st28 as well as 28^{o} in a cycling environment, we would expect them to also show more change in gene expression when co20 is compared to cy20.

The co20-cy20 comparison shows that 224 genes are DE in SD-S (172 up, 52 down), 83 genes are DE in BR-S (45 up, 38 down), 2089 genes are DE in SC-N (1369 up, 720 down), and 1015 genes are DE in BB-N (437 up, 578 down) (Fig. 4.2c). The number of DE genes in northern populations are therefore between 4.5 to 25 times more numerous than in southern populations for this comparison. In terms of number of DE genes this comparison differentiates southern and northern populations the most. GO enrichment analysis (Table 4.3) finds that "structural molecule activity" genes are enriched in up-regulated genes in SD-S, while "peptidase activity" genes are enriched in down-regulated genes in this populations. In BR-S, "extracellular region", "carbohydrate metabolic process" and "hydrolase activity" terms are enriched in up-regulated genes, and "peptidase activity" terms are enriched in down-regulated genes. In SC-N 8 terms are enriched for up-regulated genes, while 9 are enriched for down-regulated genes (Table 4.3). In BB-N, genes associated with "structural molecule activity" are

overrepresented in up-regulated genes, while 3 catalytic activity terms, as well as, “extracellular region” and “carbohydrate metabolic process” genes are enriched in down-regulated genes.

Clustering of covarying genes.

To better understand how genes behave in the different treatments, we clustered genes based on their expression pattern across the three pairwise comparisons discussed above (Fig. 4.2; Dataset S1-S4). We focused on clusters that have DE genes in co20-st28, cy20-cy28 and co20-cy20, and highlight clusters that may have biological relevance to phenotypic plasticity to thermal tolerance.

SD-S (2 genes), SC-N (2 genes) and BB-N (13 genes), but not BR-S, have genes that are up regulated across all 3 comparisons (up-up-up in Fig. 4.2), having in common an HSP 70 (TCALIF_06728). Both genes in SD-S and SC-N are HSP genes, as are 7 of the 13 genes in BB-N including HSP 70, 90, beta-1 and small HSPs. In all three populations GO terms related to response to stress are enriched in this cluster (Table 4.4). Genes in this cluster are not only being up-regulated at 28^{o}, but are also being frontloaded at 20^{o} when in the cycling treatment. Our results therefore suggest that BB-N may be affected the most when exposed to 28^{o}, but also for the cycling regime compared to the constant one. In the cluster where genes are up-regulated in co20-st28 and cy20-28, but not in co20-cy20 (up-up-NDE in Fig. 4.2), HSP genes feature prominently in all populations, with southern populations having 9/35 (SD-S) and 4/22 (BR-S) HSP genes, while northern populations have 6/14 (SC-N) and 6/42 (BB-N) HSP genes in this cluster. Northern populations have enriched GO terms for “response to stress” and “unfolded protein binding”, while SD-S has the same two enriched terms, in addition to 5 other terms (Table 4.4); there are no enriched term in BR-S. Genes in this cluster are responding to the

change from 20ºC to 28ºC in the same manner, independent of thermal regime; the clustering however does not differentiate the magnitude of change between these comparisons.

Genes that are up-regulated for co20-st28 and co20-cy20, but not for cy20-cy28 (up-NDE-up in Fig.2), represent a plastic response, where in the cycling treatments they are maintained at a constantly higher level compared to co20. The number of genes in this cluster is not region specific (SD-S: 12; BR-S: 7; SC-N: 2; BB-N: 13), and all populations have at least one small HSP in this cluster (Dataset S1-S4). Genes associated with "structural molecule activity" and "response to stress" are enriched in this cluster in SD-S, but no GO terms are enriched in the other populations (Table 4.4).

Genes that are up regulated at co20-st28, but not differentially expressed in cy20-cy28 or co20-cy20 (up-NDE-NDE in Fig. 4.2), show strong plastic response. These genes are being up-regulated when exposed to a novel moderate thermal stress, but when in a cycling temperature environment their expression is similar to that at co20. This cluster contains the largest proportion of the genes that are up-regulated at co20-st28 for all populations (SD-S: 45/100, BR-S: 40/74, SC-N: 24/52, BB-N: 73/204). Both BR-S and SC-N have enrichment in GO terms associated with "response to stress", "unfolded protein biding" and "protein folding" (Table 4.4), mostly due to the presence of HSP genes (Dataset S2-S3). SD-S and BB-N do not have any enriched GO terms, but a few genes associated with stress response are present in this cluster (Dataset S1 and S4).

Genes that are up regulated at co20-st28, down regulated at cy20-cy28 and up-regulated at co20-cy20 (up-down-up in Fig. 4.2) also show strong plastic response, as they are up-regulated when individuals are exposed to a higher novel temperature (co20-st28), as well as at cy20 (compared to co20), but the expression goes down at cy28. Southern populations have a

small number of genes in this cluster (SD-S: 4; BR-S: 3), while SC-N has none. BB-N on the other hand has 58 genes including cuticle proteins and lectins (Dataset S4). Both BR-S and BB-N have enrichment in GO terms associate with "structural molecule activity" (Table 4.4).

Next we focus on genes that are not differentially expressed at co20-st28, but are DE in at least one of the other two comparisons (cy20-cy28 or co20-cy20). Genes that are up-regulated at cy20-cy28, and down-regulated or not DE at co20-cy20 (NDE-up-down and NDE-up-NDE in Fig. 4.2) are responding to the change in temperature in the cycling environment, but their expression levels at cy20 is the same or lower than at co20 and st28. It is interesting that both southern populations have an HSP 40, and that BR-S and BB-N also have the same ubiquitin gene in this cluster (Dataset S1-S4). Both these genes are known to be involved in response to thermal stress, but in this case they are only being up regulated at cy28 (but not at st28). Therefore variable temperature environment can elicit some heat shock responses that are not observed in individuals that are stressed at that same temperature after being raised at a constant 20^{o}C. In these two clusters SD-S is enriched for "structural molecule activity" terms and SC-N has no enrichment in the NDE-up-NDE cluster, but enriched terms in the NDE-up-down cluster include genes associated with nuclease, hydrolase and structural molecule activities. BR-S and BB-N have no enriched GO terms (Table 4.4).

Genes that are DE only in co20-cy20 either have overall higher expression at the cycling regime (NDE-NDE-up), or overall lower expression (NDE-NDE-down). It is worth noting that since we have not compared the two 28^{o}C treatments to each other, we cannot say that cy28 has significantly different expression levels than st28. The NDE-NDE-up cluster has 146 in SD-S genes, 23 in BR-S genes, 1360 in SC-N genes (including one HSP gene, and one ubiquitin gene), and 205 in BB-N genes (including two ubiquitin genes) (Dataset S1-S4). This cluster is enriched

for “structural molecule activity” genes in SD-S, and for 11 GO terms in SC-N, including terms related to catalytic activity (3 different terms), extracellular region (2 terms), structural molecule activity, cell wall biogenesis, carbohydrate metabolic process, and sulfur compound metabolic process (Table 4.4). The NDE-NDE-down cluster has 40 genes in SD-S, 25 genes in BR-S; 703 genes in SC-N, and 540 genes in BB-N. GO enrichment exists for “peptidase activity” terms in SD-S, no enriched terms in BR-S, while 9 terms are enriched in SC-N most of them related to basic cell processes, components and functions (Table 4.4). In BB-N GO terms are enriched for three different catalytic activities, as well as for “carbohydrate metabolic process” and “extracellular region” (Table 4.4).

Discussion

We used RNAseq to determine transcriptome-wide patterns of gene expression for differently locally adapted populations in four different temperature treatments. The molecular response to these treatments varied across the different populations, and was especially different when comparing constant and variable thermal regimes. Our results emphasize the importance of considering thermal variability when assessing an organism’s ability to deal with climate change.

Molecular signature of local adaptation

Exposing individuals from the different populations to a moderately high novel temperature, should lead to different levels of response between southern and northern populations. These temperatures should pose less of a stress to southern populations, which should translate in fewer genes being DE as well as lower changes in expression levels

(especially for genes related to heat shock response). A number of studies that have looked at changes in gene expression following acute or chronic thermal stress (e.g. Schoville et al. 2012; Barshis et al. 2013; Gleason and Burton 2015), have found that the least thermal tolerant population (or species) differentially expresses a larger number of genes than more tolerant ones when exposed to these high temperatures. In the present study however, we only observe this between BB-N and the southern populations but not for SC-N, which has the lowest number of DE genes of the four populations in the co20-st28 comparison. Of course, here we exposed individuals to a moderate stress, and the same expectations are not necessarily anticipated. The southern populations in this study survived acute stress up to 38-39^{o}, while the northern populations survived up to 36-37^{o} (Willett 2010; Willett unpublished). Even though the northern populations appear to have a very similar upper thermal limit, SC-N differentially expresses a smaller number of genes, even less than both southern populations. This may indicate that 28^{o} may not be affecting them any more than, or even less than the more thermal tolerant southern populations.

The composition of DE genes in the co20-st28 comparison indicates that each population deals with this moderate thermal stress somewhat differently at the molecular level. The four populations only share 25 DE genes in this comparison (Table 4.2), and while the majority of these genes are well-characterized genes in heat shock response (including 12 HSP genes), they only makes up between 10-46% of all DE genes in each population. Even in pairwise comparisons the populations share only a few more genes than these 25 common DE genes, but southern and northern populations do not share more DE genes within themselves. SD-S and BB-N however, share approximately twice as many genes as they do with the other populations (64 genes; this is also true for the cy20-cy28 comparison; Table 5). This is a between region

comparison, and suggests that sharing more DE genes does not mean having the same phenotype in thermal tolerance. The magnitude of the fold change of these genes, however, may be more informative for determining this phenotype; for example, of the 64 DE genes that are shared between SD-S and BB-N in co20-st28, 51 (80%) have higher fold change in BB-N. GO enrichment analysis finds that terms associated with "response to stress" and "unfolded protein biding" are enriched in up-regulated genes in all four populations, with 14 of the 25 common DE genes making up many of these. The other 11 common DE genes are either HSPs that did not pass the annotation quality cutoff (and were therefore excluded from GO enrichment analysis), or genes whose annotation was too broad or un-annotated. Therefore, besides sharing well-characterized heat shock response genes, the populations are largely responding in unique form.

Molecular signature of phenotypic plasticity

Differently from other studies (Kelly et al. 2012), which looked at the effects of phenotypic plasticity on the ability of organisms to survive acute thermal stress, we looked at the effects that raising individuals in a cycling temperature regime (20^{o}-28^{o}) would have compared to the effects of raising them at a constant 20^{o}C and exposing them to 28^{o}C as adults. This comparison elucidates differences in gene expression profile that are due to differences in phenotypic plasticity. The temperatures used in the present study were the same as those in Willett (2010), conditions under which southern populations outcompeted northern ones. Again, based on previous studies (Schoville et al. 2012; Barshis et al. 2013; Gleason and Burton 2015) we would expect northern populations to have a larger number of DE genes than southern ones between the cycling temperatures. These expectations are met between the southern populations and BB-N, but not for SC-N, which has a much lower number of DE genes than the other

populations (as was observed for co20-st28) (Fig. 4.3b). Most genes that are DE in both co20-st28 and cy20-cy28 have lower fold change in the cycling regime (between cy20 and cy28), indicating that in general all populations show signs of a plastic response to cy28 compared to st28. This is especially true for HSPs where in all but one case (an HSP 90 in SC-N) the fold change is lower in cy20-cy28 (although not always significantly so) (Appendix 4.2-4.5). BB-N shows the most change between co20-st28 and cy20-cy28, indicating it experiences the greatest degree of plasticity in gene expression, with HSPs 70 and 90 going from 333.38-8.88 fold change in co20-st28 to 4.85-2.30 fold change in cy20-cy28. Several other genes go from being up-regulated in co20-st28 to down-regulated in cy20-cy28, including several cuticle proteins and lectins (Appendix 4.5). Even though SC-N has a much smaller number of DE genes than any of the other populations, the magnitude of the potentially plastic gene expression change was high for several genes. For example, fold change between three HSP 70 (TCALIF_06728, TCALIF_04517, comp38417), decreases from 54.94, 24.16, and 22.90, to 14.18, 12.69 and 12.55 respectively. However, even though the fold change decreases in the cycling regime, these increases in expression in SC-N are the highest for all HSP in all populations in the cycling regime. Southern populations also show plastic response with HSP fold change decreasing anywhere from 7.07-1.16 times in SD-S, and 6.47-2.22 times in BR-S.

GO terms that are enriched in the cy20-cy28 comparison include “response to stress” and “unfolded protein binding” for up-regulated genes in SD-S, SC-N and BB-N, while BR-S only has “unfolded protein biding” term enriched. These two terms were enriched in all population for the co20-st28 comparison as well. Terms associated with “structural molecule activity” and “extracellular region” are also enriched in up-regulated genes in SD-S, and down-regulated genes in BB-N. BR-S has enrichment of “structural molecule activity” on down-regulated genes

as well (Table 4.3). As mentioned before, these terms are over-represented in large part due to the large number of cuticle proteins that are DE (especially in BB-N), however, the direction of the difference in expression is not the same across populations (they are up-regulated in SD-S, but down-regulated in BR-S and BB-N). Over-representation of cuticle protein has been observed in studies of thermal adaptation in *Drosophila* (Zhao et al. 2015), and in previous studies of acute thermal stress in *Tigriopus californicus* (Schoville et al. 2012), where a difference in the direction of expression change was also observed between SD-S (up-regulated) and SC-N (down-regulated). While we do not know the function these genes are serving in this case, one of these genes (Contig59_58; homologous to agap006369-pa in *Anopheles gambiae*) is annotated with a GO term associated with stress response. Therefore it is possible that these cuticle proteins are part of thermal response in arthropods.

Molecular signature of constant versus cycling regimes

One consistent difference between southern and northern populations was the difference in the number of up-regulated genes between co20-st28 and cy20-cy28. While all populations have a larger number of down regulated genes in cy20-cy28, the number of up-regulated genes in this comparison is approximately the same for the southern populations (in relation to co20-st28), while they are approximately half for northern populations (Fig. 4.3a-b), indicating that northern populations display a stronger plastic response between the thermal regimes. It is interesting that even though SC-N has a much smaller number of DE genes between the cycling treatments, the average fold change for these genes is much higher than for any of the other populations. Average fold change for DE genes in cy20-cy28 in SC-N is 9.74, but 3.95 in SD-S, 3.68 in BR-S, 2.89 in BB-N. If we consider only the top 10 genes with the highest fold changes

in each populations, SC-N average fold change is 15.73, while it is 10.76 in SD-S, 7.83 in BR-S, and 7.85 BB-N. This higher difference in fold change in SC-N is at least in part because of high fold change in HSPs. Therefore, even though SC-N has a smaller number of DE genes between cy20-cy28, it is up-regulating these genes to a higher extent daily, which may be contributing at least in part to their lower competitive ability against the southern populations (i.e. Willett 2010). One reason for this is that while increasing expression of HSP increases an organism's ability to withstand higher temperature, the continued production of these proteins can have negative effects in other fitness components (Feder et al. 1992; Tomanek 2010).

The biggest difference in the pattern of gene expression between southern and northern populations is in the comparison between co20 and cy20, which measures how the levels of gene expression differ when the populations are at 20^{o}C in the constant versus the cycling regimes. Northern populations differentially express a much larger number of genes (both up and down) than southern populations (Fig. 4.3c), and unlike the previous comparisons, SC-N differentially expresses many more genes than any of the other populations. Within southern populations, SD-S differentially expresses more genes in both directions; however, it does so to a lower magnitude, especially in up-regulated genes (SD-S average fold change: 4.48 up- and 2.10 down-regulated; BR-S average fold-change 10.95 up- and 2.22 down). One reason for genes to be up-regulated at cy20 compared co20 would be an "anticipation" to the higher temperatures individuals in the cycling regime experience daily (frontloading). Studies in *Chlorostoma* snails and a species of *Acropora* corals show that more thermal tolerant populations or species in these groups have higher constitutive levels of HSP gene expression, that may enable them to more readily respond to thermal stress (Tomanek and Somero 1999; Dong et al. 2010; Barshis et al. 2013; Gleason and Burton 2015). The same may be expected in individuals that were raised in a

cycling environment compared to a constant one, where some genes that respond to thermal stress in the constant temperature environment, are up-regulated at 20^{o} in the cycling environment compared to 20^{o} in the constant environment.

In the present study these frontloaded genes would be genes that are up-regulated in co20-st28 as well as in co20-cy20 (genes in clusters up-up-up, up-NDE-up and up-down-up; Fig 2 and Dataset S1-S4). SD-S has 18 frontloaded genes (6 HSP and 1 cuticle protein), BR-S has 10 frontloaded genes (one small HSP, and 2 cuticle proteins), SC-N has 4 frontloaded genes (3 HSP), and BB-N has 84 frontloaded genes (8 HSP and 7 cuticle proteins). Frontloading genes can be seen as a form of plastic response, in which case BB-N is demonstrating the highest response between the two regimes, also suggesting it is being affected the most by these high temperatures. SC-N again is behaving in a manner more similar to the southern populations than to BB-N when we look at frontloaded genes. However, while it may seem like the cycling regime is not stressful to SC-N, based on the observation that it does not change expression of a large number of genes, this may come with a trade-off of having to down-regulate important genes related to cell maintenance in this regime. The large number of DE genes in co20-cy20 that are not frontloaded in SC-N (1364 up, 703 down) are a likely reason why this population is outcompeted by southern ones at this cycling regime (i.e. Willett 2010). The reason being both the metabolic cost of up-regulating so many genes, as well as the trade-off of having to down-regulate genes that are important to basic cellular processes. Therefore, SC-N may have lower fitness at these cycling temperatures not because of their level of heat shock response, as appears to be the case for BB-N, but because of the changes to its metabolic framework when in these cycling temperatures.

Over-represented GO terms for the co20-cy20 comparison in SD-S and BR-S include "structural molecule activity" (SD-S up-regulated genes), "peptidase activity" (SD-S and BR-S down-regulated genes), and "carbohydrate metabolic process" and "hydrolase activity" (BR-S up-regulated genes). GO terms are enriched in BB-N for "structural molecule activity" in up-regulated genes, and for "hydrolase activity", "extracellular region", "oxireductase activity", carbohydrate metabolic process", and "lyase activity" in down-regulated genes. All of the terms enriched in down-regulated genes in these populations have been observed in a heat stress study in *Drosophila melanogaster* (Sorensen et al. 2005), although in flies they were down-regulated following thermal stress. It seems that in the comparison between 20^{o} in constant versus cycling regimes, genes that are down-regulated at cy20 compared to co20 have similar function as those that are down-regulated during thermal stress in *Drosophila* (Sorensen et al. 2005). SC-N shows a much larger number of enriched GO terms in the co20-cy20 comparison (8 for up-regulated and 9 for down-regulated genes; Table 4.3). It shares the same enriched terms the other populations have (except for lyase activity), but it has several other ones related to basic cellular processes that suggests the changes it has to make in gene expression between co20 and cy20 have a negative effect on their fitness compared to southern populations (and maybe even BB-N).

Conclusion

The present study highlights some key ways that local adaptation can impact the manner in which an organism deals with environmental variability. First, it is clear that locally adapted populations of the same species display different responses to different thermal regimes at the molecular level. This is particularly striking between SD-S and BR-S, which are only 8 km apart.

Therefore, even for closely related populations (both genetically and geographically) the molecular mechanisms they use to deal with temperature changes can be different. Second, as seen in the northern populations the molecular response to variable temperature environments (i.e. co20-cy20 comparison) may be drastically different, even though their upper thermal limit is very similar. This means that studies that look at taxa with similar upper thermal limits, may wrongfully estimate their ability to deal with climate change by simply looking at their ability to deal with increases in mean or maximum temperatures. Given our results, it seems that the consequences associated with changes in thermal variability may be as important as increases in mean or maximum temperatures in determining an organism's ability to survive in the face of climate change.

Figure legend

Figure 4.1. Experimental design. Populations were exposed to two thermal regimes (constant and cycling). RNA was isolated from both regimes at 20^{o}C, at the end of the 20^{o}C portion of the cycling regime. Plates from the constant regime were moved to 28^{o}C (stress 28^{o}C). RNA was isolated from both regimes at 28^{o}C, after two hours at this temperature. Dashes indicate pairwise comparisons that were made to calculate relative gene expression between treatments. In red: constant at 20^{o}C (co20) compared to stress at 28^{o}C (st28); in blue: cycling at 20^{o}C (cy20) compared to cycling at 28^{o}C (cy28); in dark grey: co20 compared to cy20.

Figure 4.2. Example diagrams of gene clustering. Genes were grouped based on their relative expression in the three different pairwise comparisons (co20-st28, cy20-cy28, co20-cy20). Up = up-regulated; down = down-regulated; NDE = not differentially expressed. Red arrows refer to the co20-st28 comparison; blue arrows refer to the cy20-cy28 comparison; dark grey arrows refer to the co20-cy20 comparison. Y-axis depicts relative expression.

Figure 4.3. Differentially expressed genes for the three pairwise treatment comparisons. **a.** constant 20˚ (co20) versus stress 28˚ (st28); **b.** cycling 20˚ (cy20) versus cycling 28˚ (cy28); **c.** constant 20˚ (co20) versus cycling 20˚ (cy20). X- and y-axes are expression values for the different treatments, measured as the $\log_2$ count of reads mapped to each transcript, normalized for the library size, averaged between replicates.

Tables

Table 4.1. Number of reads for each sample after trimming, and the number of reads and percentages that were mapped to the references.

Treatment	Trimmed reads	Mapped to GT	Mapped to DNT	Total mapped	% mapped
			SD-S		
co20-1	12,872,554	4,555,835	3,543,925	8,099,760	62.92
co20-2	17,143,308	8,474,716	4,879,581	13,354,297	77.90
st28-1	16,408,726	5,664,363	4,729,381	10,393,744	63.34
st28-2	17,179,316	8,178,326	5,228,211	13,406,537	78.04
cy20-1	14,355,582	5,145,499	4,020,190	9,165,689	63.85
cy20-2	17,083,468	8,095,867	5,083,644	13,179,511	77.15
cy28-1	11,892,344	4,099,376	3,476,360	7,575,736	63.70
cy28-2	20,240,034	11,182,234	5,004,946	16,187,180	79.98
			BR-S		
co20-1	9,352,537	2,955,978	2,361,620	5,317,598	56.86
co20-2	22,293,237	9,983,751	7,060,271	17,044,022	76.45
st28-1	16,225,920	5,396,336	3,798,957	9,195,293	56.67
st28-2	21,841,078	9,858,588	6,955,168	16,813,756	76.98
cy20-1	7,698,444	2,419,610	1,956,037	4,375,647	56.84
cy20-2	12,793,717	5,672,030	3,853,155	9,525,185	74.45
cy28-1	11,750,350	3,596,306	3,207,364	6,803,670	57.90
cy28-2	29,073,232	10,074,266	5,208,716	15,282,982	52.57
			SC-N		
co20-1	11,428,402	3,705,020	3,275,656	6,980,676	61.08
co20-2	16,766,684	6,963,207	6,079,277	13,042,484	77.79
st28-1	10,208,731	3,300,905	2,865,960	6,166,865	60.41
st28-2	10,532,089	4,441,460	3,686,869	8,128,329	77.18
cy20-1	11,688,633	3,545,760	3,431,916	6,977,676	59.70
cy20-2	17,887,164	7,834,548	5,695,801	13,530,349	75.64
cy28-1	11,179,377	4,083,251	2,397,768	6,481,019	57.97
cy28-2	23,762,493	10,456,973	7,434,340	17,891,313	75.29
			BB-N		
co20-1	13,127,029	4,179,023	3,535,189	7,714,212	58.77
co20-2	18,095,437	8,154,582	6,013,711	14,168,293	78.30
st28-1	8,567,321	2,776,597	2,182,853	4,959,450	57.89
st28-2	12,944,412	5,779,006	4,327,404	10,106,410	78.08
cy20-1	11,378,699	3,750,432	2,845,145	6,595,577	57.96
cy20-2	15,814,360	7,492,404	4,820,856	12,313,260	77.86
cy28-1	13,509,632	4,475,930	3,469,773	7,945,703	58.82
cy28-2	14,105,530	6,780,762	4,245,735	11,026,497	78.17

Note – SD-S, San Diego; BR-S, Bird Rock; SC-N, Santa Cruz; BB-N, Bodega Bay.

Table 4.2. Genes that are differentially expressed in all four populations in the comparison between constant 20 (co20) and stress 28 (st28). Fold change refers to the expression in st28 compared to co20 within each population. Fisher's exact tests were calculated for all pairwise population comparisons, using the normalized read counts for each treatment (co20 and st28). *P*-values in bold indicate that the magnitude of the fold change is significantly different between the indicated populations, corrected for multiple comparisons with a false discovery rate of 5%.

Gene ID	Description	Fold Change				Fisher's test *P*-value (FDR corrected)					
		SD	BR	SC	BB	SD-BR	SD-SC	SD-BB	BR-SC	BR-BB	SC-BB
comp51313_c0_seq1_44507	N/A	9.85	13.18	9.21	10.42	**0.0302**	0.3350	0.6806	0.2912	0.2582	0.9041
Contig20_19	N/A	4.32	3.37	4.41	5.10	0.6806	1.0000	1.0000	0.9041	0.9157	1.0000
TCALIF_03375	N/A	22.30	29.35	16.15	16.14	1.0000	1.0000	1.0000	1.0000	1.0000	1.0000
TCALIF_03376	N/A	21.99	14.99	10.44	14.61	0.6684	0.4291	0.6806	0.7281	1.0000	0.9041
TCALIF_00753	78 kda glucose-regulated partial	3.89	5.13	5.67	4.91	0.1429	**0.0176**	0.1791	0.6806	0.9041	0.4200
comp32704_c0_seq2_17919	78 kda glucose-regulated protein precursor	3.69	5.27	5.20	4.57	0.9041	0.8160	0.8736	1.0000	0.9439	0.9826
TCALIF_01534	a chain orally active 2-amino thienopyrimidine inhibitors of the hsp90 chaperone	4.49	8.04	5.44	6.86	**1.56E-12**	**0.0328**	**1.10E-08**	**0.0001**	0.1681	**0.0138**
TCALIF_01814	adhesion lipoprotein	5.24	4.02	5.14	7.37	0.3636	0.6806	**0.0091**	0.2633	**2.71E-05**	0.3813
TCALIF_09395	bag domain-containing protein samui-like isoform x3	2.53	2.79	3.68	5.93	0.9041	0.4291	**0.0091**	0.6781	**0.0234**	0.2250
TCALIF_02439	cd63 antigen	5.33	4.49	6.25	7.11	0.8688	0.9041	0.7983	0.5802	0.5071	0.9157
TCALIF_05614	heat shock protein 40	2.22	2.83	2.48	3.88	0.5802	0.9041	**0.0471**	0.9002	0.4358	0.1791
TCALIF_04517	heat shock protein 70	30.90	42.41	22.90	67.36	0.2924	0.4200	**0.0010**	**0.0422**	0.1791	**2.41E-05**
TCALIF_06728	heat shock protein 70	28.22	19.63	54.94	333.38	0.6714	0.8160	**0.0069**	0.4200	**0.0001**	0.1824
TCALIF_09482	heat shock protein 70	4.59	2.79	5.48	8.88	0.5802	0.9041	0.3883	0.2582	**0.0234**	0.5802
comp46685_c0_seq1_33583	heat shock protein 90	5.14	8.34	9.72	14.89	**0.0471**	0.2318	**0.0443**	0.8160	0.4358	0.9209

TCALIF_07011	heat shock protein beta-1	3.10	2.68	3.34	3.94	0.9041	0.9949	0.8036	0.7983	0.4532	0.9041
TCALIF_10081	heat shock protein beta-1	15.59	18.03	6.78	18.74	1.0000	0.2731	0.9244	0.9041	1.0000	0.3030
TCALIF_13714	heat shock protein beta-1	3.85	4.40	6.15	7.80	0.9949	0.5237	0.1791	0.5842	0.2181	0.8646
TCALIF_13715	heat shock protein beta-1	4.05	4.96	12.47	12.95	0.8650	**0.0138**	**0.0091**	**0.0422**	**0.0302**	1.0000
TCALIF_04918	heat shock protein hsp16-	4.74	4.22	5.00	9.13	1.0000	1.0000	0.5237	0.9458	0.5032	0.5802
TCALIF_00957	protein isoform b	2.72	1.96	2.85	5.14	0.6800	1.0000	0.1824	0.5842	**0.0227**	0.1791
TCALIF_06394	small heat shock protein	6.80	6.21	6.35	10.42	0.6781	0.9041	**0.0302**	0.9041	**0.0115**	**0.0328**
TCALIF_13523	small heat shock protein	4.25	5.63	6.63	9.39	1.0000	0.3618	**0.0115**	0.6806	0.2452	0.4200
TCALIF_05480	unkown protein	2.68	2.83	3.48	4.55	0.9041	0.2969	**0.0091**	0.4360	**0.0138**	0.1681
TCALIF_09115	x-box binding protein 1	3.52	3.11	5.12	5.81	1.0000	0.3231	0.1102	0.2559	**0.0462**	0.8646

Note – SD-S, San Diego; BR-S, Bird Rock; SC-N, Santa Cruz; BB-N, Bodega Bay.

Table 4.3. Enriched Gene Ontology (GO) terms for differentially expressed genes in the three treatment comparisons. 'Category' refers to the GO categories: C = cellular component; F = molecular function; P = biological process. *P*-values are corrected for multiple comparisons using a false discovery rate of 5%.

Term	Category	*P*-value	# genes with term	Regulation change	GO-ID
co20-st28					
SD-S					
response to stress	P	1.47E-12	23	up	GO:0006950
unfolded protein binding	F	1.02E-07	7	up	GO:0051082
BR-S					
response to stress	P	7.37E-08	16	up	GO:0006950
unfolded protein binding	F	7.54E-07	6	up	GO:0051082
SC-N					
response to stress	P	2.29E-11	17	up	GO:0006950
unfolded protein binding	F	6.26E-06	5	up	GO:0051082
BB-N					
response to stress	P	3.75E-08	26	up	GO:0006950
unfolded protein binding	F	1.93E-04	6	up	GO:0051082
structural molecule activity	F	0.00147	4	down	GO:0005198
extracellular region	C	0.02583	3	down	GO:0005576
cy20-cy28					
SD-S					
structural molecule activity	F	1.73E-09	15	up	GO:0005198
response to stress	P	1.08E-08	18	up	GO:0006950
unfolded protein binding	F	1.44E-06	6	up	GO:0051082
extracellular region	C	3.68E-02	7	up	GO:0005576
BR-S					
unfolded protein binding	F	0.0301	3	up	GO:0051082
structural molecule activity	F	4.24E-03	5	down	GO:0005198
hydrolase activity, acting on carbon-nitrogen (but not peptide) bonds	F	4.24E-03	3	down	GO:0016810
carbohydrate metabolic process	P	2.08E-02	4	down	GO:0005975
SC-N					
response to stress	P	3.35E-07	10	up	GO:0006950
unfolded protein binding	F	1.73E-03	2	up	GO:0051082
BB-N					
response to stress	P	1.16E-06	17	up	GO:0006950

unfolded protein binding	F	2.60E-03	4	up	GO:0051082
structural molecule activity	F	3.79E-51	71	down	GO:0005198
extracellular region	C	4.69E-06	27	down	GO:0005576
co20-cy20					
SD-S					
structural molecule activity	F	3.07E-13	21	up	GO:0005198
peptidase activity	F	2.94E-04	8	down	GO:0008233
BR-S					
extracellular region	C	3.28E-03	6	up	GO:0005576
carbohydrate metabolic process	P	3.40E-02	4	up	GO:0005975
hydrolase activity	F	3.40E-02	8	up	GO:0016787
peptidase activity	F	4.64E-02	4	down	GO:0008233
SC-N					
extracellular region	C	2.43E-12	78	up	GO:0005576
cell wall organization or biogenesis	P	2.50E-06	10	up	GO:0071554
carbohydrate metabolic process	P	4.10E-05	48	up	GO:0005975
structural molecule activity	F	2.45E-04	42	up	GO:0005198
hydrolase activity	F	1.73E-03	129	up	GO:0016787
oxidoreductase activity	F	6.66E-03	66	up	GO:0016491
sulfur compound metabolic process	P	2.39E-02	15	up	GO:0006790
cytoskeletal protein binding	F	2.42E-02	22	up	GO:0008092
nucleus	C	2.52E-06	100	down	GO:0005634
chromosome	C	7.13E-04	29	down	GO:0005694
cellular nitrogen compound metabolic process	P	2.26E-02	114	down	GO:0034641
DNA binding	F	1.04E-02	44	down	GO:0003677
protein binding transcription factor activity	F	1.04E-02	11	down	GO:0000988
cell cycle	P	1.04E-02	32	down	GO:0007049
external encapsulating structure	C	2.26E-02	3	down	GO:0030312
peptidase activity	F	3.07E-02	36	down	GO:0008233
microtubule organizing centera	C	3.92E-02	11	down	GO:0005815
BB-N					
structural molecule activity	F	6.46E-15	38	up	GO:0005198
hydrolase activity	F	1.90E-03	59	down	GO:0016787
extracellular region	C	3.59E-02	22	down	GO:0005576
oxidoreductase activity	F	3.59E-02	29	down	GO:0016491
carbohydrate metabolic process	P	3.59E-02	18	down	GO:0005975
lyase activity	F	3.59E-02	9	down	GO:0016829

Note – SD-S, San Diego; BR-S, Bird Rock; SC-N, Santa Cruz; BB-N, Bodega Bay.

Table 4.4. Enriched Gene Ontology (GO) terms for differentially expressed (DE) genes in each cluster. 'Category' refers to the GO categories: C = cellular component; F = molecular function; P = biological process. *P*-values are corrected for multiple comparisons using a false discovery rate of 5%. '-' indicates a population did not have any DE genes in that cluster.

Cluster	# genes in cluster	Term	Category	*P*-value (FDR)	# genes with term	GO-ID
		SD-S				
up-up-up	**2**	response to stress	P	1.66E-02	2	GO:0006950
up-up-NDE	**35**	response to stress	P	4.21E-09	13	GO:0006950
		unfolded protein binding	F	1.46E-06	5	GO:0051082
		protein folding	P	1.55E-03	4	GO:0006457
		protein targeting	P	5.58E-03	3	GO:0006605
		ion binding	F	1.56E-02	12	GO:0043167
		cell motility	P	1.71E-02	3	GO:0048870
		anatomical structure development	P	4.13E-02	7	GO:0048856
up-NDE-up	**12**	structural molecule activity	F	3.42E-03	3	GO:0005198
		response to stress	P	1.08E-02	3	GO:0006950
up-NDE-NDE	**45**	No enriched terms	-	-	-	-
up-down-up	**4**	No enriched terms	-	-	-	-
NDE-up-NDE	**48**	structural molecule activity	F	2.93E-11	12	GO:0005198
NDE-up-down	**8**	structural molecule activity	F	2.03E-02	2	GO:0005198
NDE-NDE-up	**146**	structural molecule activity	F	3.13E-11	18	GO:0005198

NDE-NDE-down	**40**	peptidase activity	F	4.14E-05	8	GO:0008233
		BR-S				
up-up-up	**0**	-	-	-	-	-
up-up-NDE	**22**	No enriched terms	-	-	-	-
up-NDE-up	**7**	No enriched term	-	-	-	-
up-NDE-NDE	**40**	response to stress	P	1.36E-05	10	GO:0006950
		unfolded protein binding	F	6.71E-05	4	GO:0051082
		protein folding	P	2.32E-02	3	GO:0006457
up-down-up	**3**	structural molecule activity	F	1.01E-02	2	GO:0005198
NDE-up-NDE	**34**	No enriched terms	-	-	-	-
NDE-up-down	**9**	No enriched terms	-	-	-	-
NDE-NDE-up	**23**	No enriched terms	-	-	-	-
NDE-NDE-down	**25**	No enriched terms	-	-	-	-
		SC-N				
up-up-up	**2**	response to stress	P	1.64E-02	2	GO:0006950
up-up-NDE	**14**	response to stress	P	1.01E-07	8	GO:0006950
		unfolded protein binding	F	8.36E-03	2	GO:0051082
up-NDE-up	**2**	No enriched terms	-	-	-	-

up-NDE-NDE	**24**	unfolded protein binding	F	2.68E-03	3	GO:0051082
		response to stress	P	5.87E-03	6	GO:0006950
		protein folding	P	1.08E-02	3	GO:0006457
up-down-up	**0**	-	-	-	-	-
NDE-up-NDE	**4**	No enriched terms	-	-	-	-
NDE-up-down	**5**	nuclease activity	F	7.46E-03	2	GO:0004518
		hydrolase activity, acting on ester bonds	F	1.92E-02	2	GO:0016788
		structural molecule activity	F	1.92E-02	2	GO:0005198
NDE-NDE-up	**1360**	hydrolase activity, acting on glycosyl bonds	F	1.50E-07	31	GO:0016798
		extracellular space	C	2.25E-06	19	GO:0005615
		cell wall organization or biogenesis	P	2.33E-06	10	GO:0071554
		peptidase activity	F	6.79E-06	70	GO:0008233
		carbohydrate metabolic process	P	3.50E-05	48	GO:0005975
		structural molecule activity	F	2.14E-04	42	GO:0005198
		hydrolase activity, acting on carbon-nitrogen (but not peptide) bonds	F	3.06E-03	15	GO:0016810
		proteinaceous extracellular matrix	C	4.08E-03	9	GO:0005578
		oxidoreductase activity	F	5.77E-03	66	GO:0016491
		cytoskeletal protein binding	F	2.24E-02	22	GO:0008092
		sulfur compound metabolic process	P	2.24E-02	15	GO:0006790
NDE-NDE-down	**703**	nucleus	C	8.82E-07	100	GO:0005634
		chromosome	C	5.06E-04	29	GO:0005694
		DNA binding	F	7.08E-03	44	GO:0003677
		cell cycle	P	9.00E-03	32	GO:0007049
		protein binding transcription factor activity	F	9.00E-03	11	GO:0000988
		external encapsulating structure	C	2.44E-02	3	GO:0030312

		peptidase activity	F	3.51E-02	35	GO:0008233
		cellular nitrogen compound metabolic process	P	3.51E-02	110	GO:0034641
		microtubule organizing center	C	3.51E-02	11	GO:0005815
		BB-N				
up-up-up	**13**	response to stress	P	6.34E-10	9	GO:0006950
up-up-NDE	**42**	unfolded protein binding	F	9.77E-03	3	GO:0051082
		response to stress	P	1.18E-02	7	GO:0006950
up-NDE-up	**13**	No enriched terms	-	-	-	-
up-NDE-NDE	**73**	No enriched terms	-	-	-	-
up-down-up	**58**	structural molecule activity	F	7.75E-04	7	GO:0005198
NDE-up-NDE	**27**	No enriched terms	-	-	-	-
NDE-up-down	**22**	No enriched terms	-	-	-	-
NDE-NDE-up	**205**	No enriched terms	-	-	-	-
NDE-NDE-down	**524**	peptidase activity	F	2.43E-05	34	GO:0008233
		oxidoreductase activity	F	3.34E-02	28	GO:0016491
		lyase activity	F	3.34E-02	9	GO:0016829
		extracellular region	C	4.03E-02	20	GO:0005576
		carbohydrate metabolic process	P	4.08E-02	17	GO:0005975

Note – SD-S, San Diego; BR-S, Bird Rock; SC-N, Santa Cruz; BB-N, Bodega Bay. In cluster names: up = up-regulated; down = down-regulated; NDE = not differentially expressed. Cluster names refer relative expression from co20-st28, cy20-cy28, co20-cy20 respectively.

Table 4.5. Number of shared differentially expressed (DE) genes between populations, for comparisons constant 20 to stress 28 (co20-st28) and cycling 20 to cycling 28 (cy20-cy28). Bolded in the diagonal are the number of DE genes in each population. In bold italic: SD-S and BB-N share significantly more DE genes between themselves than any of the other pairwise population comparisons (Fisher's exact test, FDR corrected *P*-value < 0.001).

co20-st28				
	SD-S	**BR-S**	**SC-S**	**BB-S**
SD-S	**107**	35	37	64
BR-S	-	**85**	31	39
SC-N	-	-	**54**	36
BB-N	-	-	-	**237**

cy20-cy28				
	SD-S	**BR-S**	**SC-S**	**BB-S**
SD-S	**128**	22	15	***70***
BR-S	-	**100**	15	36
SC-S	-	-	**32**	20
BB-S	-	-	-	**491**

Note – SD-S, San Diego; BR-S, Bird Rock; SC-N, Santa Cruz; BB-N, Bodega Bay.

Figure 4.1

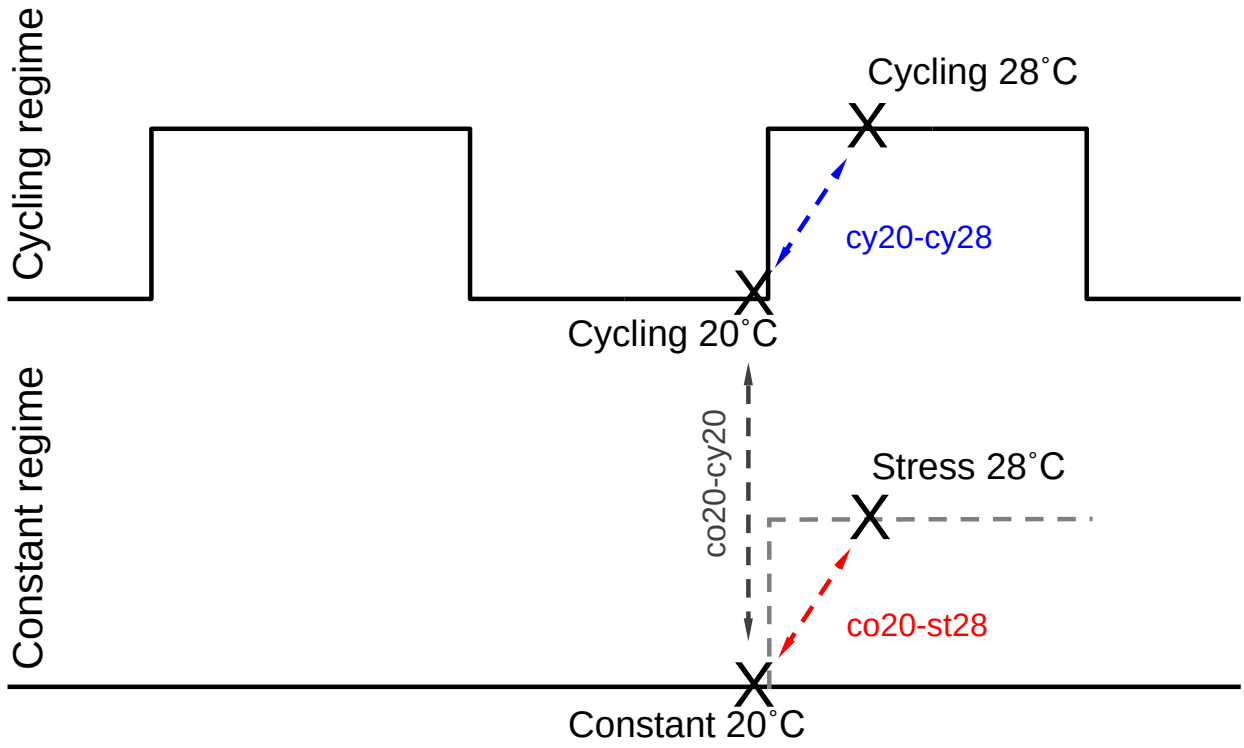
Cycling regime
Cycling 28˚C
cy20-cy28
Cycling 20˚C
co20-cy20
Stress 28˚C
co20-st28
Constant regime
Constant 20˚C

Figure 4.2

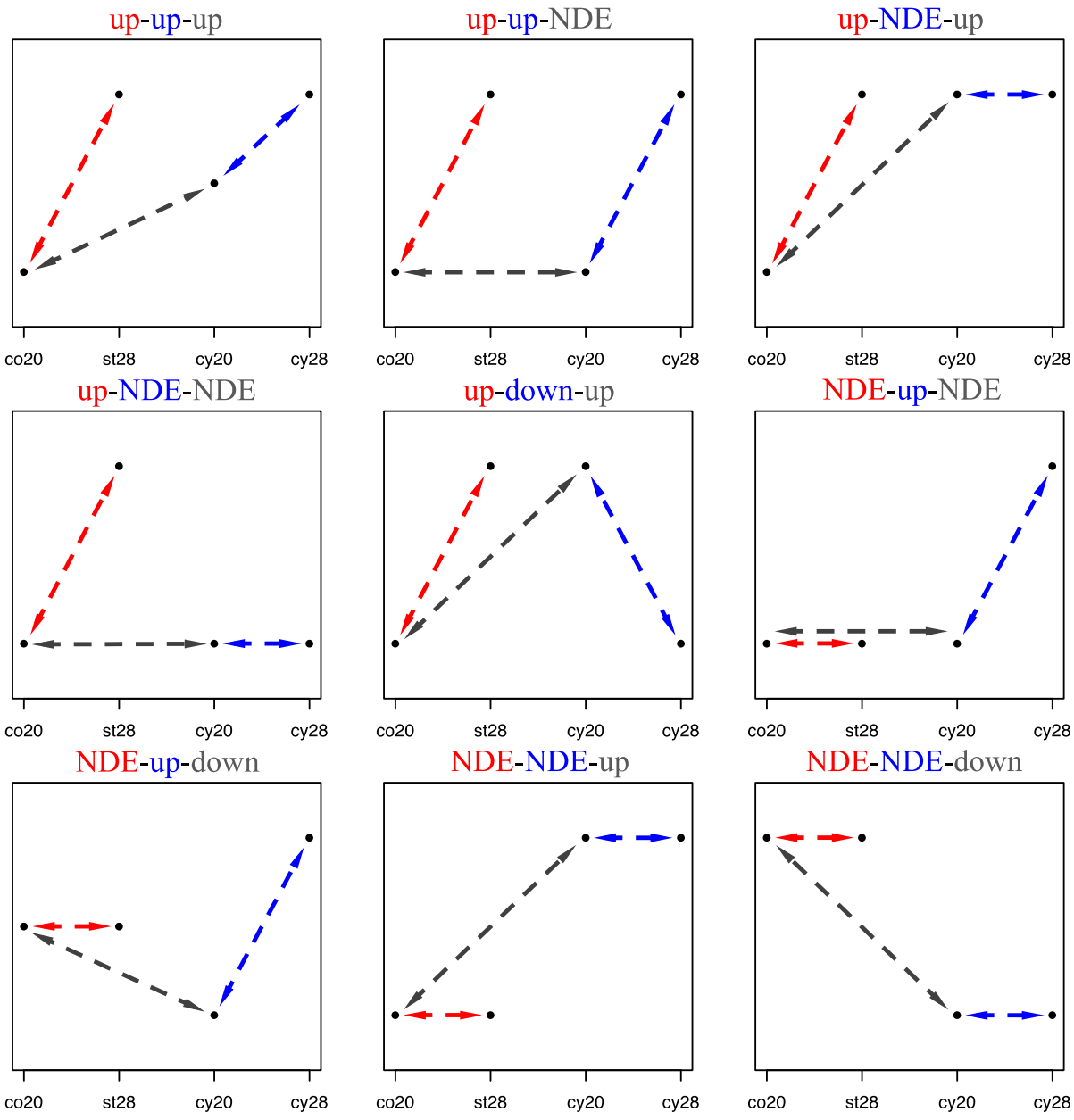
up-up-up
up-up-NDE
up-NDE-up
up-NDE-NDE
up-down-up
NDE-up-NDE
NDE-up-down
NDE-NDE-up
NDE-NDE-down
co20
st28
cy20
cy28

Figure 4.3

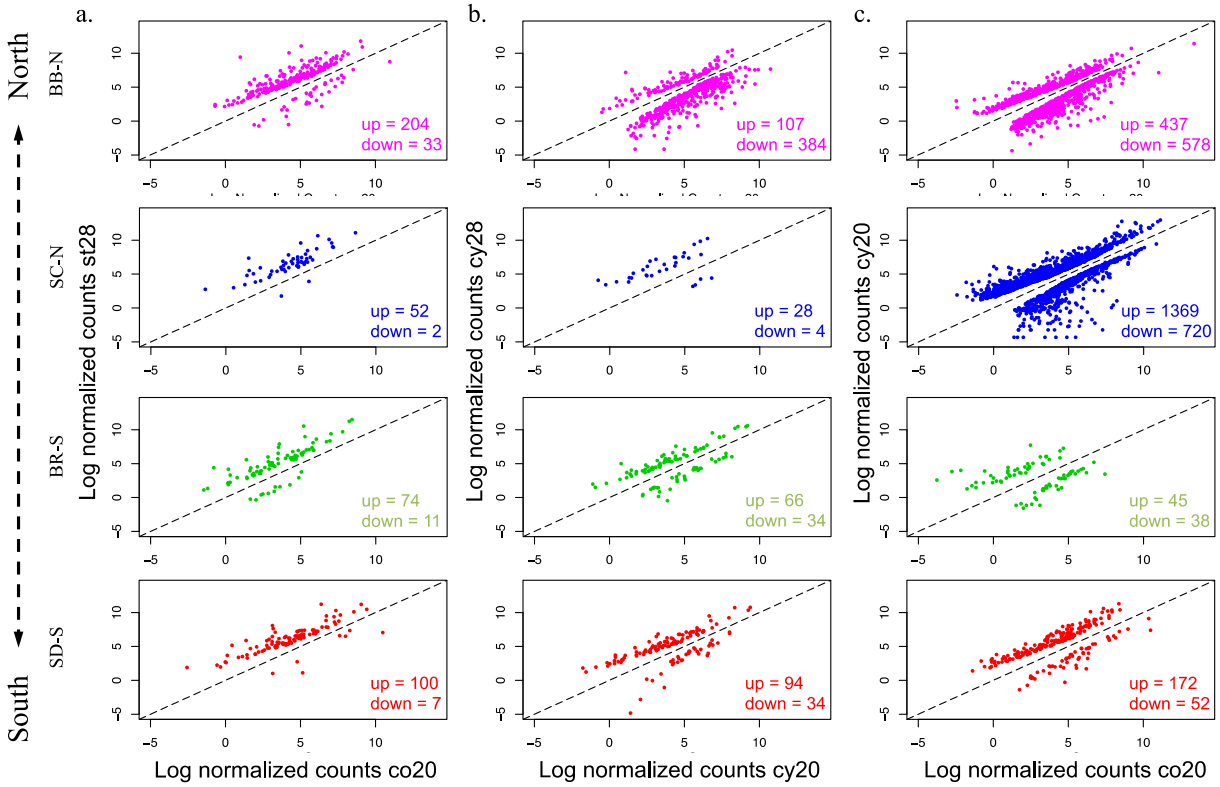
a.
b.
c.
North
South
BB-N
SC-N
BR-S
SD-S
up = 204
down = 33
up = 107
down = 384
up = 437
down = 578
up = 52
down = 2
up = 28
down = 4
up = 1369
down = 720
up = 74
down = 11
up = 66
down = 34
up = 45
down = 38
up = 100
down = 7
up = 94
down = 34
up = 172
down = 52
Log normalized counts st28
Log normalized counts cy28
Log normalized counts cy20
Log normalized counts co20
Log normalized counts cy20
Log normalized counts co20

CHAPTER V: CONCLUSION

The chapters in this dissertation contribute new insights both into the genetic basis of intrinsic postzygotic isolation in a species that lacks sex chromosomes and to our understanding of how differences in local adaptation contribute to a population's ability to deal with increases in thermal variability. In chapter 2, I use predictions from the "two rules of speciation" (Haldane's rule and the Large-X effect), to develop hypotheses regarding how the strength of intrinsic postzygotic isolation will increase as populations/species diverge with varying amounts of sex chromosome heteromorphism in the different taxa. Using data from the literature from a wide range of taxa, I determined that higher levels of sex chromosome heteromorphism is associated with higher levels of intrinsic postzygotic isolation for a given amount of divergence between the hybridizing taxa. This result supports previous assertions that sex chromosomes are important for the formation of intrinsic postzygotic reproductive barriers (Presgraves 2008). Another important finding stemming from this chapter is the observation that as sex chromosome heteromorphism decreases, differences in the strength of intrinsic postzygotic isolation between males and females also decreases. Therefore, both Haldane's rule and the Large-X effect are stronger with higher levels of sex chromosome heteromorphism.

The results from chapter 2 indicate species that lack sex chromosomes should remain compatible until reaching much higher levels of genetic differentiation (considering only intrinsic postzygotic isolation), and that no one chromosome should contribute to reproductive isolation disproportionately (when hybrids from different populations/species are considered). Also, incompatibilities involving uniparentally inherited factors (such as the mitochondrial

genome), should play an important role for the evolution of intrinsic postzygotic isolation in these systems.

In chapter 3 we begin to address some of these points, by looking at hybrid inviability at a genome-wide scale for three crosses between different populations of the copepod *Tigriopus californicus*. These crosses involve one population from Abalone Cove (AB) crossed to three others, with increasing genetic divergence between the populations in each cross. The expectation was that the most genetically divergent cross should also have a larger portion of the genome affected by hybrid inviability. This was not the case as the least divergent cross had a larger portion of its genome skewed due to hybrid inviability. While our methods do not allow us to separate individual incompatibilities and therefore we cannot determine if this is a consequence of a larger number of incompatibilities in this cross, the results are still surprising. Independent of the type of incompatibility that is causing hybrid inviability (e.g. Dobzhansky-Muller incompatibilities [DMI] or incompatibilities due to chromosomal inversion), higher genetic divergence should in general relate to more incompatibilities. The number of DMIs is predicted to increase exponentially with genetic divergence, while the number incompatibilities due to chromosomal inversions should increase linearly. The strength of incompatibilities however is not necessarily correlated with time, and it is possible the pattern we observe in the SD x AB cross is a consequence of a smaller number of large effect incompatibilities. This could be exacerbated by the positioning of certain incompatibilities to chromosomal regions where recombination is low, which would cause a larger portion of the chromosome around the incompatibility to appear skewed.

It is clear from the results in chapter 3 that none of the chromosomes contributes to hybrid inviability disproportionately in all three crosses. This was expected since this species

does have sex chromosomes and a pattern such as the Large-X effect should not apply. We did observe sex specific effects in several chromosomes in the SD x AB cross, which was somewhat surprising given the results from chapter 2. The results from chapter 2 suggest taxa without sex chromosomes should not show differences in levels of intrinsic postzygotic isolation between the sexes, but could show difference between the reciprocal crosses. In chapter 2 however only F_1 hybrids are considered, while in chapter 3 we look at F_2 hybrids. Combined, these results suggest that in the early stages of speciation while populations/species can still form second generation hybrids, sex specific incompatibilities exist in taxa without sex chromosomes. However, as these populations diverge more, incompatibilities between the nuclear genome and uniparetally inherited factors (such as mito-nuclear incompatibilities) may have a stronger effect, and ultimately contribute to complete intrinsic postzygotic isolation. Future work should focus on analyzing the reciprocal crosses of the crosses presented here to determine the impact that mito-nuclear incompatibilities have in the F_2 hybrid stage.

In chapter 4, we focus on local adaptation to moderate thermal stress and thermal variability. Transcriptome wide gene expression was measured for four *T. californicus* populations, in two thermal regimes at four temperature treatments. The cycling thermal regime elicited small changes in the more thermal tolerant populations (southern) in comparison to the constant regime, but large changes were observed in the less thermal tolerant populations (northern). This was expected since the high temperature in the cycling regime (28^{o}C) should be significantly more stressful to the northern populations. However, genetic basis of this response differed drastically between all populations, including the southern populations that are both genetically and geographically closely related. These results indicate that the response to a

variable environment cannot be predicted based on exposure to the same temperatures starting from a constant temperature environment.

APPENDIX: CHAPTER II

Appendix 2.1: Literature data for crosses. Postzygotic isolation index (IPI), postzygotic isolation index considering only inviability (Inviability), genetic distance (Nei's *D*), sex determination mechanism (by chromosome type), and condition of F_1 hybrids of each sex for the reciprocal crosses. ster = sterile; inv = inviable; fert = fertile and viable. Het = heteromorphic sex chromosomes; Hom = homomorphic sex chromosomes; NS = no sex chromosomes. References are listed in Appendix 2.7

Cross	Total IPI	Inviability	Nei's *D*	Sex Determination	1f x 2m	2f x 1m	References
Drosophila melanogaster x *D. sechellia*	1.00	0.50	0.620	Het	f: ster; m: inv	f:inv; m:ster	[2–4]
D. yakuba x *D. santomea*	0.50	0.00	0.300	Het	f:fert; m: ster	f:fert; m: ster	[2,5]
D. p. pseudoobscura x *D. p. bogotana*	0.25	0.00	0.194	Het	f: fert; m: fert	f:fert; m: ster	[2,6]
Mus m. musculus x *M. m. domesticus*	0.50	0.00	0.180	Het	f: fert; m: ster	f: fert; m:ster	[7–9]
Mus musculus x *M. caroli*	1.00	0.75	0.300	Het	f:ster; m:inv	f:inv; m:inv	[8–11]
Anopheles gambiae x *A. arabiensis*	0.50	0.00	0.150	Het	f: fert; m: ster	f: fert; m:ster	[12–14]
Papilio eurymedon x *P. glaucus*	0.25	0.25	0.418	Het	f:fert ; m: fert	f:inv ; m:fert	[15,16]
Heliconius himera x *H. erato*	0.00	0.00	0.280	Het	f: fert; m: fert	f: fert; m: fert	[15,16]
Yponomeuta cagnagellus x *Y. padellus*	0.50	0.50	0.099	Het	f: fert; m: fert	f: inv; m: inv	[15,16]
Anas platyrhynchos x *A. fulvigula*	0.00	0.00	0.011	Het	f: fert; m: fert	f: fert; m: fert	[17–19]
Hyla cinerea x *H. versicolor*	1.00	0.00	0.900	Hom	f:ster; m:ster	f: ster; m: ster	[20,21]
Rana berlanderi x *R. forreri*	0.50	0.50	0.380	Hom	f:fert; m:fert	f: inv; m: inv	[20,21]
Hyla Japonica (Tsushima) x *H. japonica* (Korea)	0.00	0.00	0.060	Hom	f: fert; m: fert	f: fert; m: fert	[20,21]
Silene latifolia x *Silene dioica*	0.00	0.00	0.038	Hom	f: fert; m: fert	f: fert; m: fert	[22–24]

Triturus cristatus x *T. marmoratus*	0.75	0.25	0.750	Hom	f: fert; m: ster	f:inv; m:ster	[25–28]
Gasterosteus aculeatus (PA) x *G. aculeatus* (JA)	0.25	0.00	0.732	Hom	f: fert; m: fert	f: fert; m:ster	[29,30]
Gasterosteus aculeatus (Limnetic) x *G. aculeatus* (Benthic)	0.00	0.00	0.018	Hom	f: fert; m: fert	f: fert; m: fert	[30–32]
Wyeomyia smithii (ON, ME) x *W. smithii* (FL)	0.00	0.00	0.330	Hom	f: fert; m: fert	f: fert; m: fert	[33–35]
Aedes triseratus x *A. hendersoni*	0.25	0.00	0.315	Hom	f: fert; m: ster	f: fert; m: fert	[36,37]
Tigriopus californicus (SD) x *T. californicus* (SC)	0.00	0.00	0.699	NS	f: fert; m: fert	f: fert; m: fert	[38,39]
Tigriopus californicus (PLA) x *T. californicus* (PMO)	0.50	0.50	1.290	NS	f: inv; m: inv	f: fert; m: fert	[38,39]
Tigriopus californicus (AB) x *T. californicus* (PLA)	1.00	0.50	1.600	NS	f: ster; m: ster	f: inv; m: inv	[38,39]
Mimulus guttatus x *M. nasutus*	0.00	0.00	0.200	NS	f: fert; m: fert	f: fert; m: fert	[40,41]
Dubautia latifolia x *D. sheriffiana*	0.00	0.00	0.473	NS	f: fert; m: fert	f: fert; m: fert	[42,43]
Xiphophorus maculatus x *X. helleri*	0.00	0.00	0.400	NS	f: fert; m: fert	f: fert; m: fert	[44–46]
Oryza sativa (japonica) x *O. sativa* (indica)	0.00	0.00	0.112	NS	f: fert; m: fert	f: fert; m: fert	[47,48]

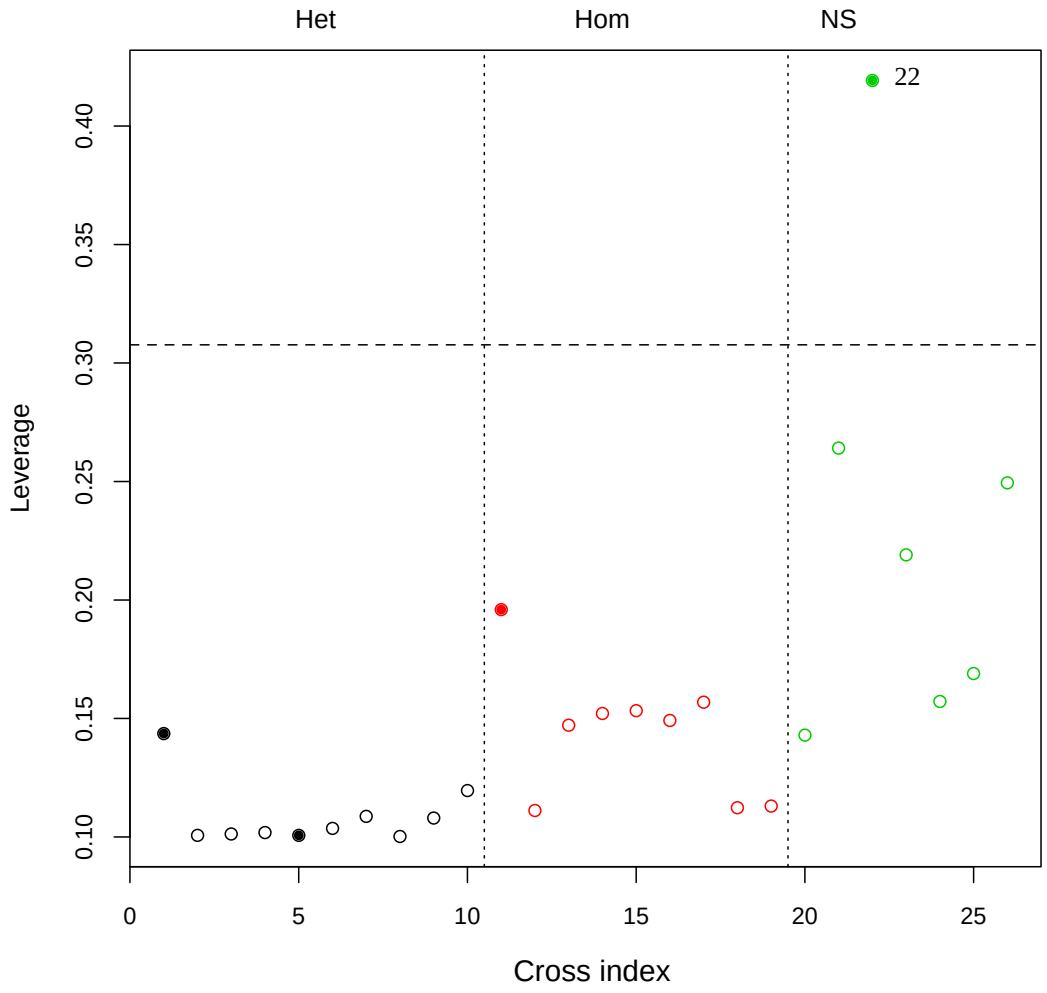

Appendix 2.2. Plot of leverage for each cross. The horizontal line is $h = \frac{2p}{n}$, where *n* is the number of crosses in the analysis and *p* is the number of parameters in the model. Observations whose leverage value is above this line have the potential to be influential. Only one cross exceeds this threshold [*Tigriopus californicus* (AB) x *T. californicus* (PLA)]. Filled circles are crosses with IPI = 1. Reference to cross indexes are in Appendix 2.6.

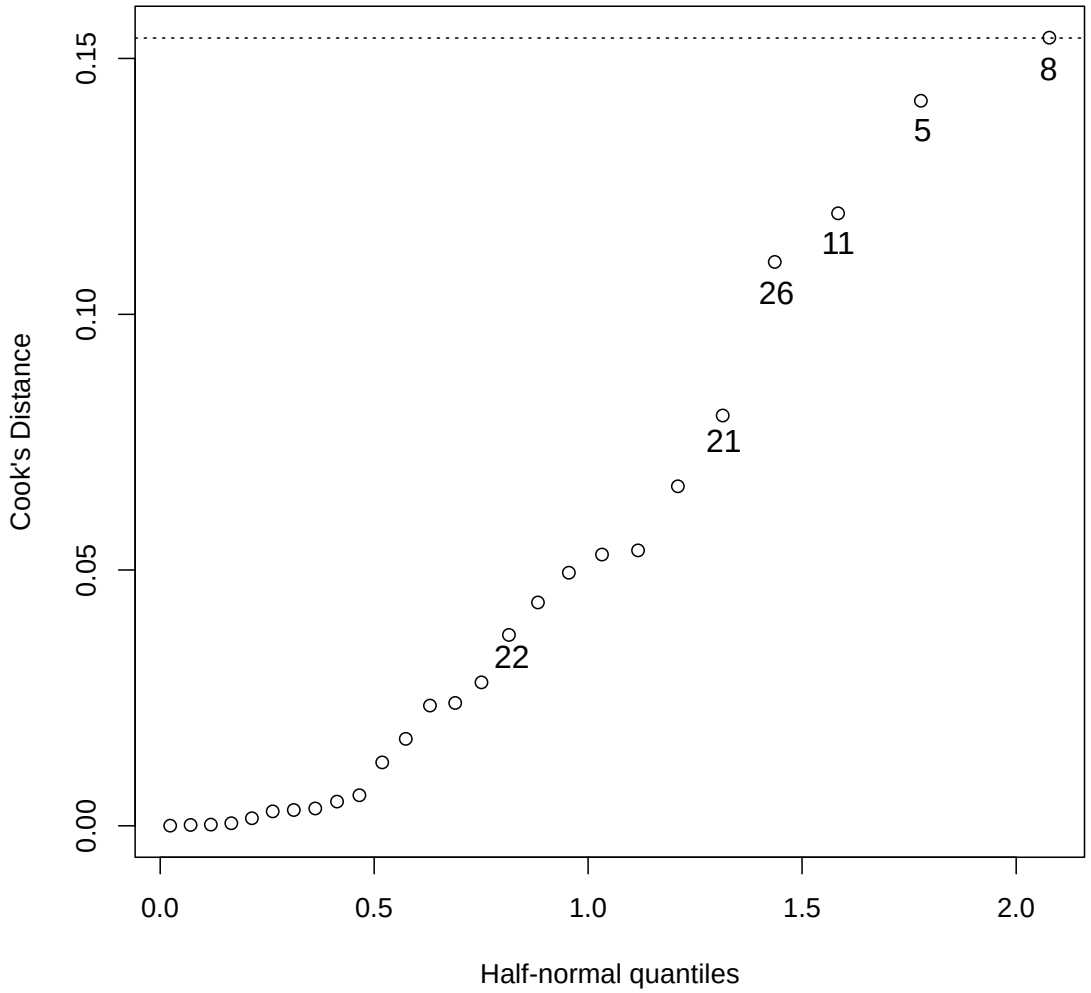

Appendix 2.3. Plot of Cook's distance over half-normal quantiles. Cook's distance measures the impact an observation has on all the regression coefficients simultaneously. One stringent recommendation to interpreting Cook's distance suggests examining values where $D_i > 4/n$ = 0.154 (indicated by the horizontal line). Numbers refer to cross indexes in Appendix 2.1. Notice that the cross *Tigriopus californicus* (AB) x *T. californicus* (PLA) [22], which has high leverage, has low Cook's *D* (0.03730), and has little influence on the fit. One cross (*Heliconius himera* x *H. erato*) [8], which has the largest Cook's D value, is right at the threshold line. The *Heliconius* cross remains compatible (at IPI = 0.25) even though it has the second highest Nei's *D* in the heteromorphic sex chromosome group. Excluding this cross leads to a stronger separation between the heteromorphic sex chromosome group and the other 2 groups. However, considering the threshold used is stringent, this observation is not very influential and is kept. All Cook's D values and cross numbers are in Appendix 2.6.

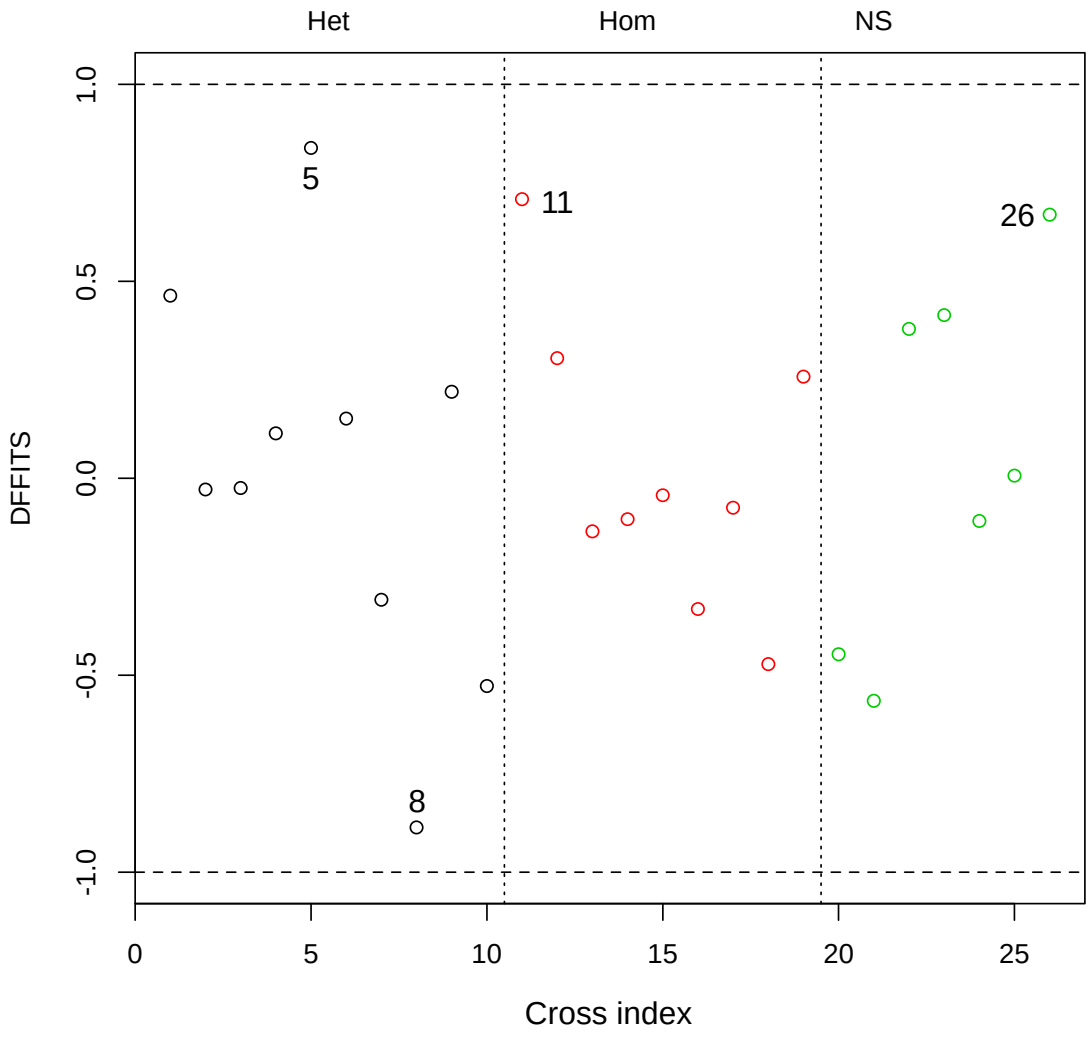

Appendix 2.4. Plot of DFFITS statistics for each cross. DFFITS is the standardized change in the predictions obtained from a regression when a given observation is included or not. For small to medium data sets, influential DFFITS statistics are those that exceed 1 (Kutner et al[1]). None of the observations exceed this threshold. The two largest DFFITS values are for the crosses between *Heliconius himera* x *H. erato* (-0.89) [8]; *Mus musculus* x *M. caroli* (0.84) [5]. The *Heliconius* cross remains compatible (at IPI = 0.25) even though it has the second highest Nei's D in the heteromorphic sex chromosome group. All DFFITS values and reference to cross indexes are in Appendix 2.6.

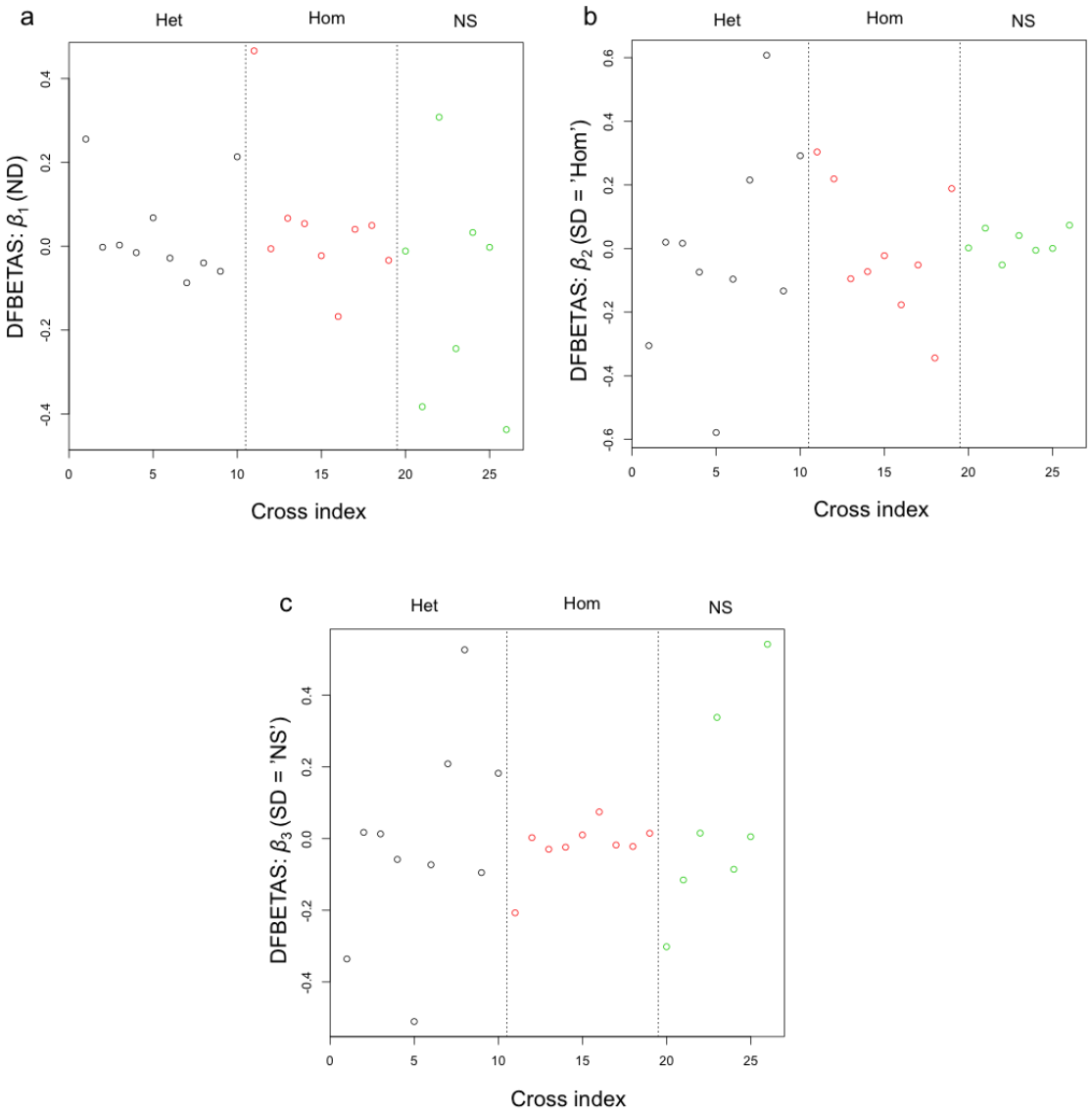

Appendix 2.5. Plot of DFBETAS for each regression coefficients. DFBETAS measures the change in each individual regression coefficient caused by an observation when it is deleted, divided by the estimated standard error of the coefficient estimate. In this case the coefficients are the following: $\mu(\text{logit } p) = \beta_0 + \beta_1\,(\text{ND}) + \beta_2\,(\text{SD} = \text{'Hom'}) + \beta_3\,(\text{SD} = \text{'NS'})$. Each panel shows the amount of influence each observation has in each of the following coefficients: a) β_1 (ND); b) β_2 (SD = 'Hom'); c) β_3 (SD = 'NS'). ND = Nei's *D* genetic distance; SD = 'Hom' is the homomorphic sex chromosome group; SD = 'NS' is the no sex chromosome group. For small to medium data sets, influential DFBETAS are those that exceed 1 (Kutner et al[1]). Note that none of the observations exceed this threshold in any of the panels. All DFBETAS values and reference to cross indices are in Appendix 2.6.

Appendix 2.6: Identification of influential observations. Intrinsic postzygotic isolation index (IPI), logit transformed IPI (logit(IPI)), Nei's *D* genetic distance (ND), sex determination mechanism (SD). Cook's distance (Cook's *D*) measures the impact an observation has on all the regression coefficients simultaneously. Observations with $D_i > 4/n = 0.154$ is considered influential. DFFITS is the standardized change in the predictions obtained from a regression when a given observation is included or not. Influential DFFITS statistics are those that exceed 1 (Kutner et al[1]). DFBETAS measures the change in each individual regression coefficient caused by an observation when it is deleted, divided by the estimated standard error of the coefficient estimate. The coefficients are the following: $\mu(\text{logit } p) = \beta_0 + \beta_1(\text{ND}) + \beta_2(\text{SD} = \text{'Hom'}) + \beta_3(\text{SD} = \text{'NS'})$. The effects on three coefficients are shown separately. Values above 1 should be considered influential (Kutner et al[1]).

Cross index	Cross	IPI	logit(IPI)	ND	SD	Cook's *D*	DFFITS	DFBETAS β_1 (ND)	DFBETAS β_2 (HOM)	DFBETAS β_3 (NS)
1	*Drosophila melanogaster* x *D. sechellia*	1.00	6.907	0.620	Het	0.05303	0.463	0.255	-0.305	-0.336
2	*D. yakuba* x *D. santomea*	0.50	0.000	0.300	Het	0.00021	-0.029	-0.002	0.020	0.017
3	*D. p. pseudoobscura* x *D. p. bogotana*	0.25	-1.096	0.194	Het	0.00016	-0.025	0.003	0.016	0.013
4	*Mus m. musculus* x *M. m. domesticus*	0.50	0.000	0.180	Het	0.00338	0.114	-0.015	-0.074	-0.058
5	*Mus musculus* x *M. caroli*	1.00	6.907	0.300	Het	0.14172	0.838	0.068	-0.578	-0.511
6	*Anopheles gambiae* x *A. arabiensis*	0.50	0.000	0.150	Het	0.00596	0.152	-0.028	-0.096	-0.073
7	*Papilio eurymedon* x *P. glaucus*	0.25	-1.096	0.418	Het	0.02401	-0.308	-0.087	0.215	0.209
8	*Heliconius himera* x *H. erato*	0.00	-6.907	0.280	Het	0.15406	-0.887	-0.040	0.608	0.527
9	*Yponomeuta cagnagellus* x *Y. padellus*	0.50	0.000	0.099	Het	0.01239	0.220	-0.060	-0.133	-0.095
10	*Anas platyrhynchos* x *A. fulvigula*	0.00	-6.907	0.011	Het	0.06638	-0.527	0.213	0.292	0.183
11	*Hyla cinerea* x *H. versicolor*	1.00	6.907	0.900	Hom	0.11972	0.708	0.466	0.304	-0.207
12	*Rana berlanderi* x *R. forreri*	0.50	0.000	0.380	Hom	0.02349	0.305	-0.006	0.219	0.003
13	*Hyla Japonica* (Tsushima) x *H. japonica* (Korea)	0.00	-6.907	0.060	Hom	0.00474	-0.135	0.067	-0.095	-0.030
14	*Silene latifolia* x *Silene dioica*	0.00	-6.907	0.038	Hom	0.00282	-0.104	0.054	-0.073	-0.024
15	*Triturus cristatus* x *T. marmoratus*	0.75	1.096	0.750	Hom	0.00048	-0.043	-0.023	-0.022	0.010
16	*Gasterosteus aculeatus* (PA) x *G. aculeatus* (JA)	0.25	-1.096	0.732	Hom	0.02802	-0.332	-0.168	-0.177	0.074
17	*Gasterosteus aculeatus* (Limnetic) x *G. aculeatus* (Benthic)	0.00	-6.907	0.018	Hom	0.00146	-0.075	0.040	-0.052	-0.018
18	*Wyeomyia smithii* (ON, ME) x *W. smithii* (FL)	0.00	-6.907	0.330	Hom	0.05384	-0.472	0.050	-0.344	-0.022
19	*Aedes triseratus* x *A. hendersoni*	0.25	-1.096	0.315	Hom	0.01698	0.258	-0.034	0.188	0.015

20	*Tigriopus californicus* (SD) x *T. californicus* (SCN)	0.00	-6.907	0.699	NS	0.04946	-0.447	-0.012	0.002	-0.302
21	*Tigriopus californicus* (PLA) x *T. californicus* (PMO)	0.50	0.000	1.290	NS	0.08021	-0.565	-0.383	0.064	-0.115
22	*Tigriopus californicus* (AB) x *T. californicus* (PLA)	1.00	6.907	1.600	NS	0.03730	0.379	0.308	-0.052	0.015
23	*Mimulus guttatus* x *M. nasutus*	0.00	-6.907	0.200	NS	0.04364	0.414	-0.244	0.041	0.338
24	*Dubautia latifolia* x *D. sheriffiana*	0.00	-6.907	0.473	NS	0.00308	-0.109	0.033	-0.005	-0.086
25	*Xiphophorus maculatus* x *X. helleri*	0.00	-6.907	0.400	NS	0.00001	0.007	-0.003	0.000	0.005
26	*Oryza sativa* (japonica) x *O. sativa* (indica)	0.00	-6.907	0.112	NS	0.11022	0.669	-0.437	0.073	0.542

Appendix 2.7: Supplementary References

1. Kutner, M. H., Nachtsheim, C. J., Neter, J. & Li, W. *Applied linear statistical models*. (McGraw-Hill, 2005).

2. Coyne, J. A. & Orr, H. A. Patterns of Speciation in *Drosophila*. *Evolution* **43,** 362–381 (1989).

3. Lemeunier, F. & Ashburner, M. Relationships within the melanogaster species subgroup of the genus *Drosophila* (Sophophora). *Chromosoma* **89,** 343–351 (1984).

4. Carvalho, A. Origin and evolution of the *Drosophila* Y chromosome. *Curr. Opin. Genet. Dev.* **12,** 664–668 (2002).

5. Lachaise, D. *et al.* Evolutionary novelties in islands: *Drosophila santomea*, a new *melanogaster* sister species from São Tomé. *Proc. R. Soc. Biol. Sci.* **267,** 1487–1495 (2000).

6. Bachtrog, D. Y-chromosome evolution: emerging insights into processes of Y-chromosome degeneration. *Nat. Rev. Genet.* **14,** 113–24 (2013).

7. Britton-davidian, E. J. *et al.* Postzygotic isolation between the two European subspecies of the house mouse: estimates from fertility patterns in wild and laboratory-bred hybrids. *Biol. J. Linn. Soc.* **84,** 379–393 (2005).

8. Ohno, S. *Sex chromosomes and sex-linked genes (Monographs on endocrinology, Vol. 1)*. (Springer, 1967).

9. Bonhomme, F. *et al.* Biochemical diversity and evolution in the genus *Mus*. *Biochem. Genet.* **22,** 275–303 (1984).

10. West, B. J. D., Frels, W. I., Papaioannou, V. E., Karr, J. P. & Chapman, V. M. Development of interspecific hybrids of *Mus*. *J. Embryol. Exp. Morphol.* **41,** 233–243 (1977).

11. West, J. D., Frels, W. I. & Chapman, V. M. *Mus musculus* x *Mus caroli* hybrids: mouse mules. *J. Hered.* **69,** 321–6 (1978).

12. Slotman, M., della Torre, A. & Powell, J. R. The genetics of inviability and male sterility in hybrids between *Anopheles gambiae* and *An . arabiensis*. *Genetics* **167,** 275–287 (2004).

13. Kitzmiller, J. B. & Mason, G. F. in *Genet. insect vectors Dis.* (Wright, J. W. & Pal, R.) 3–16 (Elsevier Publishing Company, 1967).

14. Kamau, L. *et al.* Use of short tandem repeats for the analysis of genetic variability in sympatric populations of *Anopheles gambiae* and *Anopheles arabiensis*. *Heredity* **80,** 675–682 (1998).

15. Presgraves, D. C. Patterns of postzygotic isolation in Lepidoptera. *Evolution* **56,** 1168–83 (2002).

16. Traut, W. & Marec, F. Sex Chromatin in Lepidoptera. *Q. Rev. Biol.* **71,** 239–256 (1996).

17. Mccarthy, E. M. *Handbook of Avian Hybrids of the World*. (Oxford University Press, Inc., 2006).

18. Clinton, M. & Haines, L. C. in *Genes Mech. Vertebr. sex Determ.* (Scherer, G. & Schmid, M.) 97–115 (Birkhäuser, 2001).

19. Tegelström, H. & Gelter, H. P. Haldane's rule and sex biassed gene flow between two hybridizing flycatcher species (*Ficedula albicollis* and *F. hypoleuca*, Aves: Muscicapidae). *Evolution* **44,** 2012–2021 (1990).

20. Sasa, M. M., Chippindale, P. T. & Johnson, N. A. Patterns of postzygotic isolation in frogs. *Evolution* **52,** 1811–1820 (1998).

21. Hillis, D. M. & Green, D. M. Evolutionary changes of heterogametic sex in the phylogenetic history of amphibians. *J. Evol. Biol.* **3,** 49–64 (1990).

22. Brothers, A. N. & Delph, L. F. Haldane's rule is extended to plants with sex chromosomes. *Evolution* **64,** 3643–8 (2010).

23. Nicolas, M. *et al.* A gradual process of recombination restriction in the evolutionary history of the sex chromosomes in dioecious plants. *PLoS Biol.* **3,** e4 (2005).

24. Goulson, D. & Jerrim, K. Maintenance of the species boundary between *Silene dioica* and *S. latifolia* (red and white campion). *Oikos* **79,** 115–126 (1997).

25. Lantz, L. A. & Callan, H. G. Phenotypes and spermatogenesis of interspecific hybrids between *Triturus cristatus* and *T. marmoratus*. *J. Genet.* **52,** 165–185 (1954).

26. Arntzen, J. W. & Wallis, G. P. Restricted gene flow in a moving hybrid zone of the newts *Triturus cristatus* and *T. marmoratus* in Western France. *Evolution* **45,** 805–826 (1991).

27. Arntzen, J. W., Jehle, R., Bardakci, F., Burke, T. & Wallis, G. P. Asymmetric viability of reciprocal-cross hybrids between crested and marbled newts (*Triturus cristatus* and *T. Marmoratus*). *Evolution* **63,** 1191–202 (2009).

28. Schmid, M. & Steinlein, C. in *Genes Mech. Vertebr. sex Determ.* (Scherer, G. & Schmid, M.) 143–76 (Birkhäuser, 2001).

29. Kitano, J., Mori, S. & Peichel, C. L. Phenotypic divergence and reproductive isolation between sympatric forms of Japanese threespine sticklebacks. *Biol. J. Linn. Soc.* **91,** 671–685 (2007).

30. Peichel, C. L. *et al.* The master sex-determination locus in threespine sticklebacks is on a nascent Y chromosome. *Curr. Biol.* **14,** 1416–1424 (2004).

31. McPhail, J. D. in *Evol. Biol. threespine stickleback* (Bell, M. A. & Foster, S. A.) 399–437 (Oxford University Press, Inc., 1994).

32. Mckinnon, J. S. & Rundle, H. D. Speciation in nature : the threespine stickleback model systems. *Trends Ecol. Evol.* **17,** 480–488 (2002).

33. Armbruster, P., Bradshaw, W. E. & Holzapfel, C. M. Evolution of the genetic architecture underlying fitness in the pitcher-plant mosquito, *Wyeomyia smithii*. *Evolution* **51,** 451–458 (1997).

34. Mathias, D., Jacky, L., Bradshaw, W. E. & Holzapfel, C. M. Quantitative trait loci associated with photoperiodic response and stage of diapause in the pitcher-plant mosquito, *Wyeomyia smithii*. *Genetics* **176,** 391–402 (2007).

35. Armbruster, P., Bradshaw, W. E. & Holzapfel, C. M. Effects of postglacial range expansion on allozyme and quantitative genetic variation of the pitcher-plant mosquito, *Wyeomyia smithii*. *Evolution* **52,** 1697–1704 (1998).

36. Taylor, D. B. Genetic compatibility of *Aedes* (*Protomacleaya*) *triseriatus* with *A.* (*P.*) *brelandi* and *A.* (*P.*) *hendersoni* (Diptera: Culicidae). *Ann. Entomol. Soc. Am.* **80,** 109–117 (1987).

37. Bhalla, S. C. & Craig, G. B. Linkage analysis of chromosome I of *Aedes aegypti*. *Can. J. Genet. Cytol.* **12,** 425–435 (1970).

38. Ganz, H. H. & Burton, R. S. Genetic differentiation and reproductive incompatibility among Baja California populations of the copepod *Tigriopus californicus*. *Mar. Biol.* **123,** 821–827 (1995).

39. Voordouw, M. J. & Anholt, B. R. Environmental sex determination in a splash pool copepod. *Biol. J. Linn. Soc.* **76,** 511–520 (2002).

40. Fishman, L. & Willis, J. H. Evidence for Dobzhansky-Muller incompatibilites contributing to the sterility of hybrids between *Mimulus guttatus* and *M. nasutus*. *Evolution* **55,** 1932–42 (2001).

41. Ritland, C. & Ritland, K. Variation of sex allocation among eight taxa of the *Mimulus guttatus* species complex (Scrophulariaceae). *Am. J. Bot.* **76,** 1731–1739 (1989).

42. Carr, G. D. & Kyhos, D. W. Adaptive Radiation in the Hawaiian Silversword Alliance (Compositae- Madiinae). II . Cytogenetics of Artificial and Natural Hybrids. *Evolution* **40,** 959–976 (1986).

43. Witter, M. S. & Carr, G. D. Adaptive radiation and genetic differentiation in the Hawaiian Silversword Alliance (Compositae : Madiinae). *Evolution* **42,** 1278–1287 (1988).

44. Gordon, M. Hereditary basis of melanosis in hybrid fishes. *Am. J. Cancer* **15,** 1495–1523 (1931).

45. Bull, J. J. *Evolution of sex determining mechanisms.* (The Benjamin/Cummings Publishing Company, 1983).

46. Morizot, D. C. & Siciliano, M. J. Protein polymorphisms, segregation in genetic crosses and genetic distances among fishes of the genus *Xiphophorus* (Poeciliidae). *Genetics* **102,** 539–56 (1982).

47. Guiderdoni, E., Galinato, E., Luistro, J. & Vergara, G. Anther culture of tropical japonica × indica hybrids of rice (*Oryza sativa* L .). *Euphytica* **62,** 219–224 (1992).

48. Xiao, J., Li, J., Yuan, L. & McCouch, S. R. Genetic diversity and its relationship to hybrid performance and heterosis in rice as revealed by PCR-based markers. *Theor. Appl. Genet.* **92,** 637–643 (1996).

APPENDIX: CHAPTER III

Appendix 3.1. Primers' names and sequences for the 16 markers at which 227 individuals (87 males and 137 females) were genotyped

Primer	Chromosome	Sequence (5' to 3')
c1_1718_c3_sdf	1	GAACGTACGTATTTCTGAGGCC
c1_1718_c3_ABf	1	AGCGTGACCTTCAAATGCTCG
c1_1718_c3_conr	1	CGGCAAATGTACAGGACCACA
c4_left_SD.f2	1	AGATTTTTGCACTGAGTTTACTTC
c4_left_AB.f2	1	CGTTTGCCACTACGGTCATAT
c4_left_con.r2	1	ACTCGGATGACAAACAGCCCA
c2_5_AB.f	2	GAACTACATTTGGAGGTACAGACA
c2_5_SD.f	2	ACTCTCAATGTATCAGCCTAATCC
c2_5_con.r	2	GCCACCGTGAGTTTTGAGTTC
3QCR8p_AB.f	3	TTCTCATGGGGAGGCCCGAA
3QCR8p_SD.f	3	TGAAATGAACCTAGCTTAGCTGCC
3QCR8p_con.r	3	TTTGAACTTACGGGGCACCACG
3FBLRR_con.f	3	CCTGGCACGGTTCCCAATCTGTTC
3FBLRR_ABspec.r	3	CAATGATCTTCCACGAGTGCGGGA
3FBLRR_SDspec.r	3	AGCGGCCAATGTCTCTTATCATAATAAACC
c4_right_SD.f	4	TTTGAAACTCGCCTTCCATGTTAT
c4_right_AB.f	4	TTCCTACTTTTTTTGCTACCTTCG
c4_right_con.r	4	GATAAAGTCTGGCATCTTAGAGC
P5CexD.fwd	5	TTCGCCGCAAAAGATCCAAGC
TcP5Cex11.fwd	5	TCACGAGGATCTGCTCAAGAC
P5Cs-SD.rev	5	GAATCGGCGTACTGATACAAATCC
P5Cs-AB.rev	5	GCTTCTTTGACGATGTTCATCAACA
Cyt 14.r	6	GGAATGTACTTTTTGGGGTTCG
ccSD.f	6	CCACAAAATGCCCCTCGCTCG
ccAB.F	6	CCGACAGACGGGCAAGGCCTCT
c7_2276_ABf	7	TAATTTGTTTTGTGCCGGCGATTT
c7_2276_SDf	7	TTAAGGAGATAATCTACGACGCTA
c7_2276_conr	7	CCCTGGCTGCTGAGCTGCTAG
c7_37_SD.f	7	TGCGTTTTTGTCGAATTTTGAATC

c7_37_AB.f	7	ACAACTCGTACACCCGTTTG
c7_37_con.r	7	TTGCTTCATATGAACCGGGG
Ch8_3336_AB.f	8	CGGTGATTGGAACACAAATATGAGC
Ch8_3336_SD.f	8	CAACTACTTGACGTTTCAAAAAAGGGA
Ch8_3336_cons.r	8	CTCTGTGCCAATGTGGTCAGTTATT
Ch9_2203_SD.f	9	TAATCATCTACAAAACGCTCTGAAG
Ch9_2203_AB.f	9	TTGGCATGTTCTGTTTGATCAC
Ch9_2203_cons.r	9	AGGTTTCGGTGGAGGATCAA
Ch10_1464_SD.f	10	CATCGTGCAATTTTTGGCAGGT
Ch10_1464_AB.f	10	CAGTTTGACATTGGTCACCCTT
Ch10_1464_cons.r	10	GGATGGAAAACATAAGCAGGTG
c11_left_SD.f	10	CTTGAAAATGTAACTATGAATATGAGG
c11_left_AB.f	10	GTTCCAAGCTACCGAATAAGTAC
c11_left_con.r	10	CCATGTACATCTTGGGCCTC
11sep_tub_con.f	11	CTCAGACAGCTCCTTGTGCT
11sep_tub_SD.r	11	ACAATCTCTGATCAACTAACATCG
11sep_tub_AB.r	11	CACATGTTGAAATCATCCGGATAA
MEpro1con.f	12	GGAATGTACTTTTCTCACGGAGATCG
ME1_SD.r	12	ATATCAAGAACCTGTGCCACAC
ME1_ab.r	12	CTAGAGCATCCTACGCATTCC

Appendix 3.2. Genotypic ratios for 16 loci across the 12 chromosomes and tests for deviations from Mendelian ratios. AB and SD refer to the number of homozygous individuals for these alleles; H refers to heterozygous individuals.

	c1	c1-c4L	c2	3fblrr	3qcr8	c4R	C5-P5C	C6-CYC	c7-2776	c7-37	c8	c9	c10	c11-c10	c11-septub	c12-ME1
Males																
AB	27	25	13	35	39	16	11	19	18	10	12	29	21	13	21	27
H	49	51	47	50	45	49	58	49	52	55	53	39	46	50	49	36
SD	11	11	27	2	2	22	18	19	17	22	21	19	19	21	17	24
Total	87	87	86	87	86	87	87	87	87	87	86	87	86	84	87	87
χ^2 **1:2:1**	**7.276**	**7.092**	4.674	***26.977***	***32.023***	2.218	**10.793**	1.391	3.345	**9.391**	**6.535**	3.230	0.512	4.571	1.759	2.793
Females																
AB	29	27	34	33	31	46	21	49	25	16	30	36	18	10	40	21
H	84	91	76	103	105	71	81	61	75	84	75	72	74	80	81	81
SD	24	19	25	1	1	20	35	27	34	36	31	26	44	42	16	35
Total	137	137	135	137	137	137	137	137	134	136	136	134	136	132	137	137
χ^2 **1:2:1**	**7.380**	***15.715***	3.341	***49.701***	***52.036***	**10.051**	**7.423**	**8.708**	3.119	***13.412***	1.456	2.239	**11.000**	*21.455*	*12.971*	**7.423**

Note - Colored cells indicate significance at $P < 0.05$ (green) uncorrected for multiple comparisons, and following Bonferroni correction at $P < 0.003$ (yellow).

Appendix 3.3. Two and three way interactions for 16 markers distributed across the 12 chromosomes. Shown are all interactions with $P < 0.05$ for 2-way and $P < 0.01$ for 3-way interactions. None of the interactions are significant when a false discovery rate of 5% is applied to correct for multiple comparisons.

	2-way loci				3-way loci				
	Locus 1	**Locus 2**	χ^2	***P*-value (4 d.f.)**	**Locus 1**	**Locus 2**	**Locus 3**	χ^2	***P*-value (12 d.f.)**
Both sexes	3qcr8	c11_septub	13.098	0.0108	C5_P5C	C6_CYC	c8	24.996	0.0047
	c4R	c8	11.551	0.0210	c1-c4L	c10-c11	c11_septub	24.815	0.0050
	3fblrr	c1-c4L	10.029	0.0399	c2	c7_37	c9	24.631	0.0053
					c2	3fblrr	c11_septub	24.305	0.0058
					c8	c10-c11	c11_septub	22.830	0.0089
					c2	c1-c4L	c9	22.825	0.0089
					c2	3qcr8	c11_septub	22.603	0.0095
Males	c2	c8	14.654	0.0055	c1	c2	c9	26.716	0.0085
	c4R	c8	12.878	0.0119	c8	c10-c11	c11_septub	26.221	0.0099
	c2	c1-c4L	12.265	0.0155					
	c10-c11	c12_ME1	11.953	0.0177					
	c1	c2	11.696	0.0198					
	c10	c11_septub	11.480	0.0217					
	C6_CYC	c11_septub	10.158	0.0379					
	c4L	C5_P5C	10.024	0.0400					
	c2	c7_37	9.601	0.0477					
Females	c9	c10-c11	13.704	0.0083	C5_P5C	C6_CYC	c8	27.890	0.0057
	c9	c10	12.399	0.0146	C6_CYC	c9	c10-c11	26.307	0.0097
	C6_CYC	c8	11.814	0.0188					
	3qcr8	c11_septub	11.402	0.0224					
	C5_P5C	c8	11.024	0.0263					
	c2	c4R	10.322	0.0353					
	C6_CYC	c7_2776	9.621	0.0473					

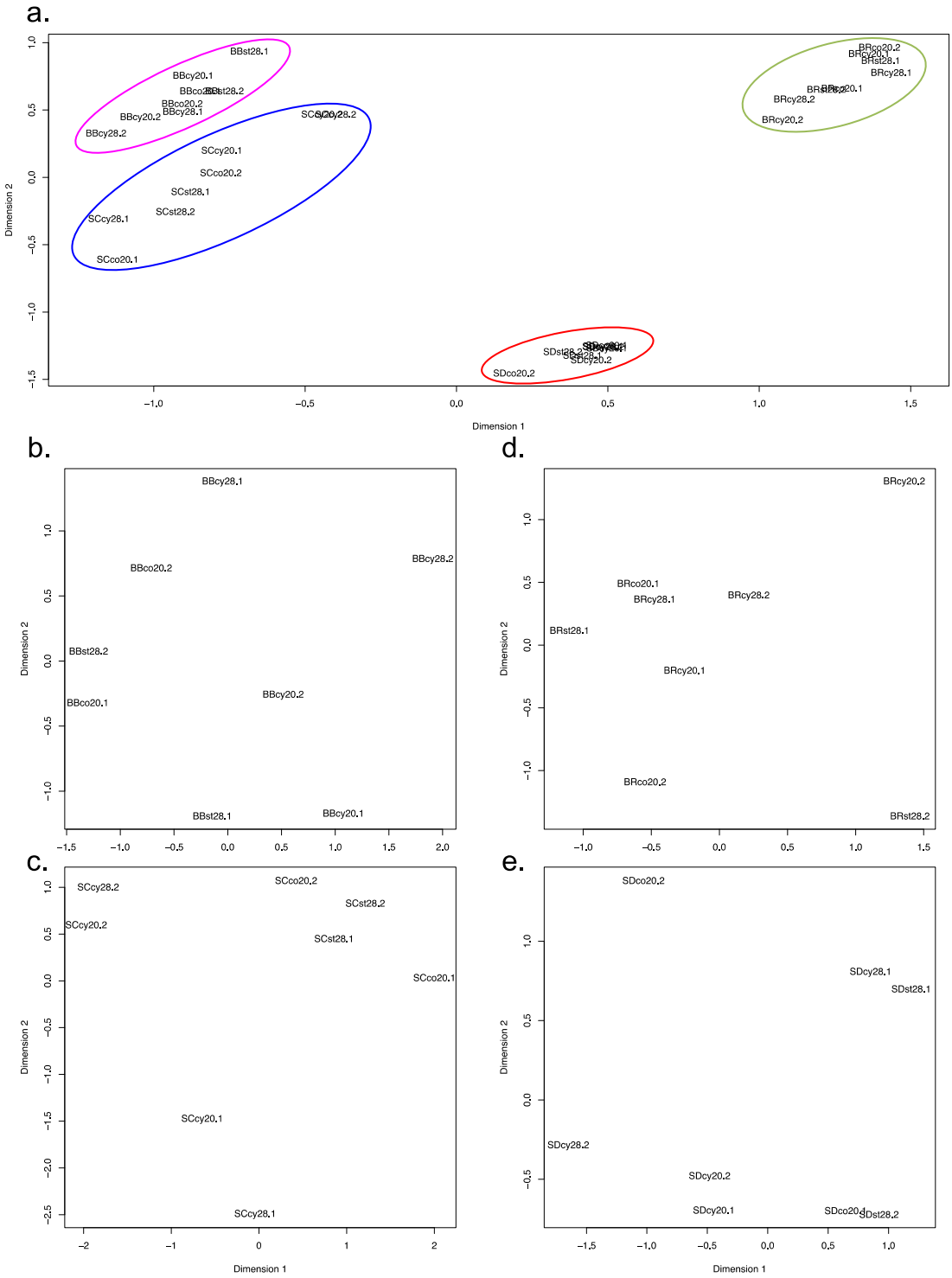

Appendix 4.1. Multidimensional scaling (MDS) plots showing the level of similarity between each RNA sample. **a.** All samples for all populations. Samples clustered by population and not by treatment or region. **b.** RNA samples from BB. **c.** RNA samples from SC. **d.** RNA samples

from BR. **e.** RNA samples from SD. Population specific MDS plots, show that many cases RNA samples that were sequenced in the same Illumina lane are more similar than they are to their replicate. This indicates a batch effect in the samples. To deal with this a generalized linear model was fit to the data, and the sample "batch" was used as a blocking factor.

Appendix 4.2. Genes that are differentially expressed in co20-st28 and cy20-cy28. FC = fold change. Fisher's tests were calculated using the normalized read counts for each treatment (co20, st28, cy20 and cy28). FDR are P-values ajusted for multiple comparisons at FDR of 5%. Bold indicates the magnitude of the fold change is significantly different between the co20-st28 and cy20-cy28.

Gene ID	Description	co20-st28 FC	cy20-cy28 FC	Fisher's test P-value	FDR	Difference	Relative FC
TCALIF_04517	heat shock protein 70	30.90	5.19	3.24E-52	**1.36E-50**	25.71	Lower in cycling
TCALIF_06728	heat shock protein 70	28.22	3.99	1.05E-08	**8.78E-08**	24.23	Lower in cycling
TCALIF_03375	---NA---	22.30	8.62	0.397	0.739	13.68	Lower in cycling
TCALIF_10081	heat shock protein beta-1	15.59	2.23	8.12E-06	**3.79E-05**	13.36	Lower in cycling
TCALIF_03376	---NA---	21.99	9.46	0.117	0.316	12.54	Lower in cycling
TCALIF_11487	heat shock protein 70	8.68	2.14	0.015	0.056	6.54	Lower in cycling
comp45224_c0_seq 1_31268	hypothetical protein DAPPUDRAFT_315459	3.86	-2.21	1.81E-09	**1.90E-08**	6.07	Lower in cycling
comp38417_c0_seq 1_22939	loc560210 protein	8.00	2.60	0.046	0.162	5.40	Lower in cycling
comp47454_c0_seq 1_35179	heat shock protein beta-1	2.57	-2.12	1.53E-06	**9.20E-06**	4.69	Lower in cycling
comp50334_c0_seq 1_42602	heat shock protein 70	5.01	1.97	0.012	0.052	3.04	Lower in cycling
comp51313_c0_seq 1_44507	---NA---	9.85	7.18	0.588	0.882	2.67	Lower in cycling
comp41377_c0_seq 2_26389	---NA---	2.74	0.53	6.66E-07	**4.66E-06**	2.21	Lower in cycling
comp46685_c0_seq 1_33583	heat shock protein 90	5.14	3.10	0.101	0.316	2.04	Lower in cycling
TCALIF_11481	---NA---	2.53	0.53	7.93E-13	**1.11E-11**	1.99	Lower in cycling
TCALIF_12922	tyrosine aminotransferase	5.41	3.42	0.186	0.410	1.99	Lower in cycling
TCALIF_01534	a chain orally active 2-amino thienopyrimidine inhibitors of the hsp90 chaperone	4.49	2.60	2.53E-16	**5.30E-15**	1.89	Lower in cycling
TCALIF_13714	heat shock protein beta-1	3.85	2.13	0.109	0.316	1.72	Lower in cycling
TCALIF_13715	heat shock protein beta-1	4.05	2.44	0.261	0.522	1.61	Lower in cycling

TCALIF_00753	78 kda glucose-regulated partial	3.89	2.40	3.85E-06	**2.02E-05**	1.49	Lower in cycling
TCALIF_09115	x-box binding protein 1	3.52	2.25	0.184	0.410	1.28	Lower in cycling
TCALIF_07011	heat shock protein beta-1	3.10	2.02	0.208	0.437	1.08	Lower in cycling
Contig10_2020	hsp70 hsp90 organizing protein homolog	2.87	1.99	0.120	0.316	0.88	Lower in cycling
TCALIF_09890	atp-dependent clp protease atp-binding subunit clpx- mitochondrial-like	5.31	4.57	0.649	0.909	0.75	Lower in cycling
comp32704_c0_seq2_17919	78 kda glucose-regulated protein precursor	3.69	2.98	1.000	1.000	0.71	Lower in cycling
TCALIF_05480	unkown protein	2.68	1.98	0.132	0.326	0.71	Lower in cycling
TCALIF_09482	heat shock protein 70	4.59	3.96	1.000	1.000	0.62	Lower in cycling
comp40436_c0_seq1_25295	---NA---	2.61	2.17	0.576	0.882	0.44	Lower in cycling
Contig20_19	---NA---	4.32	4.04	0.704	0.924	0.28	Lower in cycling
TCALIF_08135	hsp70 hsp90 organizing protein homolog	1.99	1.72	0.578	0.882	0.27	Lower in cycling
TCALIF_08964	---NA---	2.47	2.23	0.405	0.739	0.24	Lower in cycling
TCALIF_06906	---NA---	4.36	4.13	0.735	0.935	0.23	Lower in cycling
TCALIF_01587	lon peptidase n-terminal domain and ring finger protein 3 isoform x2	2.19	2.05	0.763	0.943	0.14	Lower in cycling
TCALIF_11129	protein disulfide-isomerase a6	1.99	1.86	0.685	0.924	0.13	Lower in cycling
TCALIF_02439	cd63 antigen	5.33	5.24	1.000	1.000	0.09	Lower in cycling
TCALIF_06839	set and mynd domain-containing protein 4-like	3.91	3.89	1.000	1.000	0.02	Lower in cycling
comp39174_c0_seq1_23817	protein phosphatase 1 regulatory subunit 3d	2.14	2.16	1.000	1.000	-0.02	Lower in constant
comp49397_c0_seq1_39570	---NA---	2.05	2.13	0.787	0.945	-0.09	Lower in constant
TCALIF_09316	galactosylgalactosylxylosylprotein 3-beta-glucuronosyltransferase s	2.17	2.29	1.000	1.000	-0.13	Lower in constant
TCALIF_00461	---NA---	3.17	3.77	0.612	0.886	-0.60	Lower in constant
TCALIF_08840	---NA---	2.98	3.81	0.494	0.830	-0.83	Lower in constant
Contig298_2287	gamma-crystallin a	3.52	4.54	1.000	1.000	-1.01	Lower in constant
TCALIF_12219	cuticle protein	2.65	5.07	0.463	0.810	-2.42	Lower in constant

Appendix 4.3. Genes that are differentially expressed in co20-st28 and cy20-cy28 in BR. FC = fold change. Fisher's tests were calculated using the normalized read counts for each treatment (co20, st28, cy20 and cy28). FDR are P-values adjusted for multiple comparisons at FDR of 5%. Bold indicates the magnitude of the fold change is significantly different between the co20-st28 and cy20-cy28.

Gene ID	Description	co20-st28 FC	cy20-cy28 FC	Fisher's test P-value	FDR	Difference	Relative FC
TCALIF_04517	heat shock protein 70	42.41	6.55	1.42E-24	**3.84E-23**	35.86	Lower in cycling
TCALIF_06728	heat shock protein 70	19.63	4.33	6.08E-06	**2.35E-05**	15.30	Lower in cycling
TCALIF_10081	heat shock protein beta-1	18.03	5.96	0.571	0.848	12.07	Lower in cycling
comp42136_c0_seq1_27295	general transcription factor iih subunit 4-like	15.29	5.25	0.253	0.489	10.04	Lower in cycling
TCALIF_03376	---NA---	14.99	6.61	0.155	0.349	8.38	Lower in cycling
TCALIF_01877	serine protease	3.60	-3.00	1.38E-09	**7.44E-09**	6.60	Lower in cycling
comp48306_c0_seq1_36978	cuticle protein 7	2.81	-3.11	1.43E-08	**6.42E-08**	5.92	Lower in cycling
comp47559_c0_seq5_35364	---NA---	8.85	3.14	0.042	0.113	5.71	Lower in cycling
TCALIF_12674	cuticle protein 7	2.87	-2.79	1.82E-17	**1.23E-16**	5.66	Lower in cycling
comp46685_c0_seq1_33583	heat shock protein 90	8.34	3.76	8.04E-23	**1.09E-21**	4.59	Lower in cycling
TCALIF_01534	a chain orally active 2-amino thienopyrimidine inhibitors of the hsp90 chaperone	8.04	3.61	4.31E-20	**3.88E-19**	4.44	Lower in cycling
comp51313_c0_seq1_44507	---NA---	13.18	9.06	0.231	0.479	4.12	Lower in cycling
TCALIF_00753	78 kda glucose-regulated partial	5.13	2.96	5.33E-05	**1.80E-04**	2.17	Lower in cycling
TCALIF_09890	atp-dependent clp protease atp-binding subunit clpx-mitochondrial-like	8.22	6.51	0.659	0.848	1.71	Lower in cycling
TCALIF_01814	adhesion lipoprotein	4.02	2.62	1.64E-04	**4.92E-04**	1.40	Lower in cycling
TCALIF_02439	cd63 antigen	4.49	3.12	0.645	0.848	1.37	Lower in cycling
TCALIF_09115	x-box binding protein 1	3.11	2.09	0.114	0.279	1.03	Lower in cycling
comp40436_c0_seq1_25295	---NA---	2.66	2.01	0.491	0.799	0.65	Lower in cycling
TCALIF_12922	tyrosine aminotransferase	2.57	2.31	0.741	0.870	0.26	Lower in cycling

TCALIF_01587	lon peptidase n-terminal domain and ring finger protein 3 isoform x2	2.26	2.16	0.914	1.000	0.10	Lower in cycling
comp49509_c0_seq3_39872	rhomboid family member 1	3.79	3.80	1.000	1.000	-0.01	Lower in constant
TCALIF_06802	aael017225- partial	2.96	2.98	1.000	1.000	-0.02	Lower in constant
comp48270_c0_seq1_36905	beta-lactamase domain-containing protein	2.77	2.96	0.735	0.870	-0.19	Lower in constant
Contig6926_8381	---NA---	2.88	3.88	1.000	1.000	-1.00	Lower in constant
Contig20_19	---NA---	3.37	4.57	0.503	0.799	-1.20	Lower in constant
TCALIF_12758	copine-9-like isoform x2	-3.86	-2.41	0.433	0.779	-1.46	Lower in constant
comp29011_c1_seq1_15625	---NA---	2.62	4.46	0.638	0.848	-1.84	Lower in constant

Appendix 4.4. Genes that are differentially expressed in co20-st28 and cy20-cy28 in SC-N. FC = fold change. Fisher's tests were calculated using the normalized read counts for each treatment (co20, st28, cy20 and cy28). FDR are P-values ajusted for multiple comparisons at FDR of 5%. Bold indicates the magnitude of the fold change is significantly different between the co20-st28 and cy20-cy28.

Gene ID	Description	co20-st28 FC	cy20-cy28 FC	Fisher's test P-value	FDR	Difference	Relative FC
TCALIF_06728	heat shock protein 70	54.94	14.18	0.126	0.361	40.76	Lower in cycling
comp38417_c0_seq1_22939	loc560210 protein	24.16	12.69	0.016	0.072	11.47	Lower in cycling
TCALIF_04517	heat shock protein 70	22.90	12.55	6.00E-04	**0.005**	10.35	Lower in cycling
TCALIF_03375	---NA---	16.15	9.22	1.000	1.000	6.93	Lower in cycling
TCALIF_13715	heat shock protein beta-1	12.47	7.23	0.366	0.599	5.24	Lower in cycling
TCALIF_03376	---NA---	10.44	7.87	1.000	1.000	2.56	Lower in cycling
TCALIF_13523	small heat shock protein	6.63	4.29	0.140	0.361	2.34	Lower in cycling
TCALIF_11866	kda small heat shock protein	8.02	6.34	0.365	0.599	1.68	Lower in cycling
comp32704_c0_seq2_17919	78 kda glucose-regulated protein precursor	5.20	3.91	0.575	0.862	1.28	Lower in cycling
TCALIF_04918	heat shock protein hsp16-	5.00	4.25	1.000	1.000	0.75	Lower in cycling
TCALIF_10081	heat shock protein beta-1	6.78	6.73	1.000	1.000	0.05	Lower in cycling
comp46685_c0_seq1_33583	heat shock protein 90	9.72	11.08	0.752	1.000	-1.36	Lower in constant
TCALIF_13893	short-chain dehydrogenase	2.39	3.79	0.279	0.599	-1.39	Lower in constant
TCALIF_02439	cd63 antigen	6.25	8.28	0.331	0.599	-2.03	Lower in constant
comp51313_c0_seq1_44507	---NA---	9.21	12.65	0.013	0.072	-3.44	Lower in constant
TCALIF_00461	---NA---	4.09	8.01	0.026	0.094	-3.92	Lower in constant
comp50110_c0_seq1_41582	conserved hypothetical protein	2.79	17.89	6.15E-07	**1.11E-05**	-15.10	Lower in constant
TCALIF_05177	na+ k+ 2cl- cotransporter isoform partial	10.06	29.52	1.000	1.000	-19.46	Lower in constant

Appendix 4.5. Genes that are differentially expressed in co20-st28 and cy20-cy28 in BB-N. FC = fold change. Fisher's tests were calculated using the normalized read counts for each treatment (co20, st28, cy20 and cy28). FDR are P-values ajusted for multiple comparisons at FDR of 5%. Bold indicates the magnitude of the fold change is significantly different between the co20-st28 and cy20-cy28.

Gene ID	Description	co20-st28 FC	cy20-cy28 FC	Fisher's test P-value	FDR	Difference	Relative FC
TCALIF_06728	heat shock protein 70	333.38	4.75	1.70E-19	**6.23E-19**	328.63	Lower in cycling
TCALIF_04873	ferric-chelate reductase 1 homolog	10.50	-122.56	1.03E-07	**2.28E-07**	133.06	Lower in cycling
TCALIF_07916	c-type lectin	13.87	-78.11	4.22E-33	**2.35E-32**	91.97	Lower in cycling
TCALIF_02545	---NA---	14.79	-50.98	8.84E-191	**2.83E-189**	65.77	Lower in cycling
TCALIF_04517	heat shock protein 70	67.36	4.85	2.71E-74	**3.15E-73**	62.52	Lower in cycling
comp38417_c0_seq1_22939	loc560210 protein	56.94	4.60	3.65E-37	**2.22E-36**	52.34	Lower in cycling
TCALIF_01526	e-selectin precursor	8.80	-41.00	6.56E-96	**9.33E-95**	49.80	Lower in cycling
comp56926_c0_seq1_44704	c-type lectin - galactose binding	13.03	-30.97	3.26E-13	**9.06E-13**	44.01	Lower in cycling
TCALIF_13700	---NA---	12.22	-25.89	4.80E-27	**1.98E-26**	38.11	Lower in cycling
comp49814_c4_seq1_40728	---NA---	9.64	-27.63	9.38E-10	**2.35E-09**	37.27	Lower in cycling
TCALIF_01412	---NA---	8.00	-21.31	8.81E-66	**8.68E-65**	29.31	Lower in cycling
comp43208_c1_seq1_28628	---NA---	3.73	-19.31	2.22E-258	**1.42E-256**	23.04	Lower in cycling
TCALIF_09501	c-type lectin 5 precursor	5.63	-14.41	4.08E-85	**5.22E-84**	20.05	Lower in cycling
comp38805_c0_seq1_23397	c-type lectin	5.70	-14.32	4.71E-17	**1.55E-16**	20.02	Lower in cycling
comp45224_c0_seq1_31268	hypothetical protein DAPPUDRAFT_315459	4.74	-13.95	2.33E-115	**4.25E-114**	18.70	Lower in cycling
TCALIF_10126	cuticle protein 7	2.82	-15.46	5.43E-15	**1.66E-14**	18.29	Lower in cycling
comp50829_c0_seq1_44470	---NA---	4.06	-12.62	1.52E-155	**3.89E-154**	16.68	Lower in cycling
TCALIF_10081	heat shock protein beta-1	18.74	2.20	1.65E-05	**3.36E-05**	16.54	Lower in cycling
comp24610_c0_seq1_13069	flexible cuticle protein 12 precursor	4.32	-11.78	4.31E-38	**2.76E-37**	16.10	Lower in cycling
comp41096_c0_seq1_26055	cuticular protein analogous to peritrophins 3-d1 precursor	5.00	-10.17	2.01E-05	**4.02E-05**	15.16	Lower in cycling

comp51184_c0_seq1_44497	domon domain-containing protein cg14681 precursor	3.98	-10.13	2.09E-08	**4.87E-08**	14.10	Lower in cycling
TCALIF_11866	kda small heat shock protein	16.00	1.90	1.56E-29	**7.39E-29**	14.10	Lower in cycling
TCALIF_01463	cuticular protein analogous to peritrophins 3-d1 precursor	4.21	-9.69	5.59E-19	**1.99E-18**	13.90	Lower in cycling
TCALIF_00939	domon domain-containing protein cg14681 precursor	3.34	-9.26	3.43E-153	**7.33E-152**	12.60	Lower in cycling
comp46685_c0_seq1_33583	heat shock protein 90	14.89	2.30	2.39E-05	**4.63E-05**	12.59	Lower in cycling
comp41824_c0_seq1_26913	---NA---	4.38	-7.32	1.00E-16	**3.20E-16**	11.70	Lower in cycling
TCALIF_03376	---NA---	14.61	3.05	0.006	**0.010**	11.56	Lower in cycling
TCALIF_13775	---NA---	4.67	-6.59	5.86E-12	**1.53E-11**	11.26	Lower in cycling
TCALIF_03695	glucose-dependent insulinotropic receptor-like	3.59	-7.42	1.12E-46	**8.44E-46**	11.01	Lower in cycling
TCALIF_10789	isoform a	3.41	-7.33	2.27E-25	**9.06E-25**	10.74	Lower in cycling
TCALIF_06039	cuticle protein 7	2.67	-8.03	4.93E-68	**5.26E-67**	10.70	Lower in cycling
TCALIF_08785	flexible cuticle protein 12 precursor	3.28	-7.34	0.00E+00	**0.00E+00**	10.63	Lower in cycling
TCALIF_13715	heat shock protein beta-1	12.95	2.46	3.23E-08	**7.25E-08**	10.49	Lower in cycling
TCALIF_11487	heat shock protein 70	13.52	3.06	1.24E-03	**2.12E-03**	10.45	Lower in cycling
TCALIF_08009	at-rich interactive domain-containing protein 1a-like	4.14	-6.22	4.17E-32	**2.23E-31**	10.36	Lower in cycling
TCALIF_11051	bcs-1 protein	3.12	-7.21	9.29E-05	**1.70E-04**	10.33	Lower in cycling
TCALIF_07845	sodium-dependent glucose transporter partial	3.83	-6.24	9.83E-04	**1.70E-03**	10.06	Lower in cycling
comp24528_c0_seq1_12991	---NA---	2.34	-7.55	1.28E-39	**9.10E-39**	9.89	Lower in cycling
TCALIF_07462	solute carrier family 22 member 5	4.60	-5.26	1.91E-04	**3.45E-04**	9.86	Lower in cycling
TCALIF_04682	aminopeptidase n	-6.88	-16.58	1.000	1.000	9.71	Lower in cycling
TCALIF_04700	phospholipase a2 homolog 1-like	4.31	-5.23	0.002	**0.003**	9.54	Lower in cycling
TCALIF_02751	conserved hypothetical protein	4.92	-4.60	0.080	0.113	9.52	Lower in cycling
comp38456_c0_seq1_22985	---NA---	3.55	-5.85	3.49E-17	**1.18E-16**	9.40	Lower in cycling
TCALIF_03375	---NA---	16.14	7.08	0.379	0.466	9.06	Lower in cycling
TCALIF_05329	hypothetical protein	2.19	-6.78	1.94E-57	**1.77E-56**	8.96	Lower in cycling

	DAPPUDRAFT_316261						
comp41129_c0_seq1_26085	---NA---	2.72	-5.74	1.47E-28	**6.27E-28**	8.46	Lower in cycling
Contig3210_4929	endoprotease furin	3.54	-4.84	0.005	**0.008**	8.38	Lower in cycling
TCALIF_08344	---NA---	2.74	-5.45	3.41E-29	**1.56E-28**	8.19	Lower in cycling
TCALIF_01705	mical-like protein 2	1.98	-5.74	9.08E-49	**7.26E-48**	7.73	Lower in cycling
TCALIF_04494	---NA---	3.26	-4.39	3.91E-208	**1.67E-206**	7.65	Lower in cycling
TCALIF_04637	n -dimethylarginine dimethylaminohydrolase 1-like	3.63	-3.97	0.016	**0.024**	7.60	Lower in cycling
TCALIF_12300	morn repeat protein	3.29	-4.15	6.22E-05	**1.15E-04**	7.45	Lower in cycling
TCALIF_01856	endoprotease furin	3.39	-4.00	2.07E-05	**4.08E-05**	7.39	Lower in cycling
TCALIF_13523	small heat shock protein	9.39	2.09	6.99E-22	**2.63E-21**	7.30	Lower in cycling
comp51313_c0_seq1_44507	---NA---	10.42	3.23	2.17E-08	**4.97E-08**	7.19	Lower in cycling
comp52007_c0_seq1_44551	---NA---	3.22	-3.96	1.86E-08	**4.41E-08**	7.18	Lower in cycling
comp47559_c0_seq5_35364	---NA---	9.14	1.96	9.52E-04	**1.67E-03**	7.18	Lower in cycling
comp38371_c0_seq1_22889	serine threonine-protein kinase rio1	2.43	-4.69	1.13E-110	**1.81E-109**	7.11	Lower in cycling
TCALIF_04918	heat shock protein hsp16-	9.13	2.07	0.011	**0.016**	7.06	Lower in cycling
comp47671_c1_seq12_35628	mical-like protein 2	2.30	-4.72	1.31E-13	**3.74E-13**	7.01	Lower in cycling
TCALIF_02785	peptidyl-prolyl cis-trans isomerase	2.90	-4.02	1.18E-53	**1.00E-52**	6.93	Lower in cycling
TCALIF_04305	---NA---	2.47	-4.19	1.16E-28	**5.14E-28**	6.66	Lower in cycling
TCALIF_07889	flexible cuticle protein 12 precursor	3.36	-2.93	1.01E-33	**5.89E-33**	6.28	Lower in cycling
TCALIF_13714	heat shock protein beta-1	7.80	1.99	4.68E-05	**8.80E-05**	5.82	Lower in cycling
TCALIF_13855	---NA---	3.00	-2.79	5.83E-19	**2.02E-18**	5.79	Lower in cycling
TCALIF_09482	heat shock protein 70	8.88	3.09	0.034	**0.050**	5.79	Lower in cycling
TCALIF_02710	restin homolog isoform x1	2.25	-3.47	1.60E-30	**8.19E-30**	5.72	Lower in cycling
TCALIF_10840	somatomedin-b and thrombospondin type-1 domain-containing protein	2.29	-3.39	3.38E-24	**1.31E-23**	5.68	Lower in cycling
Contig4521_6158	isoform c	2.72	-2.85	4.83E-09	**1.17E-08**	5.57	Lower in cycling

TCALIF_04086	chorion peroxidase-like	2.25	-3.19	2.29E-06	**4.73E-06**	5.43	Lower in cycling
TCALIF_10398	hypothetical protein EAG_12595	2.30	-3.08	6.82E-15	**2.03E-14**	5.38	Lower in cycling
TCALIF_10399	chitin deacetylase-like partial	2.56	-2.79	4.31E-05	**8.23E-05**	5.35	Lower in cycling
TCALIF_06491	hypothetical protein DAPPUDRAFT_47496	2.37	-2.92	1.16E-16	**3.62E-16**	5.29	Lower in cycling
comp24701_c0_seq1_13144	---NA---	2.74	-2.25	4.28E-13	**1.16E-12**	4.99	Lower in cycling
TCALIF_06906	---NA---	13.80	8.82	0.671	0.740	4.98	Lower in cycling
comp49275_c0_seq1_39258	chitin deacetylase-like partial	2.12	-2.79	1.71E-38	**1.15E-37**	4.91	Lower in cycling
TCALIF_07501	moxd1-like protein 2	2.31	-2.45	6.06E-14	**1.76E-13**	4.76	Lower in cycling
TCALIF_02287	---NA---	2.58	-2.03	1.39E-11	**3.57E-11**	4.62	Lower in cycling
TCALIF_09019	notum-like protein	2.22	-2.06	2.94E-07	**6.37E-07**	4.28	Lower in cycling
TCALIF_09395	bag domain-containing protein samui-like isoform x3	5.93	1.84	7.09E-07	**1.49E-06**	4.08	Lower in cycling
TCALIF_02439	cd63 antigen	7.11	3.40	0.102	0.138	3.72	Lower in cycling
TCALIF_13287	chorion peroxidase	1.97	-1.57	4.17E-07	**8.90E-07**	3.54	Lower in cycling
comp654839_c0_seq1_48400	---NA---	5.80	2.82	0.630	0.707	2.98	Lower in cycling
TCALIF_09115	x-box binding protein 1	5.81	3.04	0.013	**0.019**	2.77	Lower in cycling
comp32136_c0_seq1_17426	beta-ig-h3 fasciclin	7.31	4.67	0.355	0.442	2.64	Lower in cycling
TCALIF_13962	hypothetical protein	-2.18	-4.38	0.019	**0.029**	2.21	Lower in cycling
TCALIF_00753	78 kda glucose-regulated partial	4.91	2.73	2.88E-09	**7.08E-09**	2.18	Lower in cycling
TCALIF_05614	heat shock protein 40	3.88	1.81	3.63E-04	**6.46E-04**	2.07	Lower in cycling
comp32704_c0_seq2_17919	78 kda glucose-regulated protein precursor	4.57	2.51	0.002	**0.003**	2.06	Lower in cycling
TCALIF_01814	adhesion lipoprotein	7.37	5.49	0.007	**0.011**	1.88	Lower in cycling
comp49814_c3_seq5_40727	heat shock protein 40	3.37	1.68	0.009	**0.013**	1.69	Lower in cycling
TCALIF_00461	---NA---	9.86	8.23	0.735	0.796	1.63	Lower in cycling
TCALIF_08840	---NA---	4.58	2.97	0.760	0.804	1.60	Lower in cycling
TCALIF_04449	---NA---	3.67	2.46	0.552	0.637	1.20	Lower in cycling
TCALIF_13893	short-chain dehydrogenase	3.24	2.05	0.602	0.682	1.19	Lower in cycling

TCALIF_11129	protein disulfide-isomerase a6	3.41	2.28	0.005	**0.008**	1.13	Lower in cycling
Contig20_19	---NA---	5.10	4.00	1.000	1.000	1.10	Lower in cycling
comp33548_c0_seq1_18708	isoform a	2.52	1.55	0.087	0.121	0.97	Lower in cycling
comp40436_c0_seq1_25295	---NA---	2.61	1.67	0.147	0.194	0.93	Lower in cycling
Contig1623_1622	origin recognition complex subunit 4	2.76	1.84	0.045	0.065	0.92	Lower in cycling
comp38150_c0_seq1_22653	metalloreductase steap3	2.57	1.78	0.154	0.201	0.79	Lower in cycling
TCALIF_01598	dnaj homolog subfamily b member 9	2.50	1.72	0.157	0.203	0.77	Lower in cycling
comp32472_c0_seq1_17716	---NA---	2.37	1.62	0.107	0.145	0.75	Lower in cycling
TCALIF_09316	galactosylgalactosylxylosylprotein 3-beta-glucuronosyltransferase s	2.73	2.00	0.546	0.637	0.73	Lower in cycling
comp46868_c0_seq1_33965	bla g 5 allergen	2.29	1.60	0.117	0.156	0.69	Lower in cycling
TCALIF_06995	isoform a	2.46	1.80	0.048	0.068	0.66	Lower in cycling
TCALIF_11041	oxidoreductase htatip2	2.17	1.54	0.093	0.127	0.62	Lower in cycling
TCALIF_05273	metalloreductase steap3	2.39	1.82	0.557	0.637	0.57	Lower in cycling
TCALIF_13101	denn domain-containing protein 2a	2.78	2.21	1.000	1.000	0.57	Lower in cycling
Contig768_2701	---NA---	2.71	2.23	1.000	1.000	0.48	Lower in cycling
TCALIF_06802	aael017225- partial	4.30	3.89	0.724	0.792	0.41	Lower in cycling
TCALIF_05274	eh domain-containing protein 1	2.01	1.61	0.167	0.212	0.40	Lower in cycling
comp40104_c0_seq1_24896	---NA---	2.56	2.19	0.843	0.878	0.37	Lower in cycling
TCALIF_04976	esterase fe4-like	2.19	1.87	0.553	0.637	0.32	Lower in cycling
Contig449_448	---NA---	2.33	2.10	0.851	0.878	0.22	Lower in cycling
TCALIF_08964	---NA---	2.16	1.94	0.497	0.590	0.22	Lower in cycling
TCALIF_10390	cuticle protein 7	-2.35	-2.45	0.768	0.806	0.11	Lower in cycling
comp45359_c0_seq1_31481	histone h1-delta	2.56	2.80	0.745	0.796	-0.24	Lower in constant
TCALIF_01587	lon peptidase n-terminal domain and ring finger protein 3 isoform x2	2.20	2.45	0.639	0.712	-0.25	Lower in constant

TCALIF_03706	endocuticle structural glycoprotein bd-8-like	-2.22	-1.90	0.430	0.515	-0.32	Lower in constant
comp42764_c0_seq1_28045	---NA---	-2.25	-1.81	0.410	0.495	-0.44	Lower in constant
TCALIF_09890	atp-dependent clp protease atp-binding subunit clpx-mitochondrial-like	3.72	4.27	0.747	0.796	-0.54	Lower in constant
TCALIF_08504	heme-binding protein 3	2.04	2.59	0.167	0.212	-0.55	Lower in constant
TCALIF_06172	hypothetical protein	-2.82	-1.85	1.28E-03	**0.002**	-0.97	Lower in constant
TCALIF_07288	---NA---	-3.50	-2.06	0.399	0.486	-1.43	Lower in constant
comp44811_c0_seq1_30716	---NA---	-2.43	2.28	4.93E-12	**1.31E-11**	-4.72	Lower in constant
TCALIF_02781	---NA---	-2.41	3.68	3.75E-30	**1.85E-29**	-6.09	Lower in constant
TCALIF_13494	---NA---	-14.81	-4.66	0.281	0.353	-10.15	Lower in constant

LITERATURE CITED

Alexander, H. J., J. M. L. Richardson, and B. R. Anholt. 2014. Multigenerational response to artificial selection for biased clutch sex ratios in *Tigriopus californicus* populations. J. Evol. Biol. 27:1921–1929.

Angilletta, M. J. 2009. Thermal adaptation: a theoretical and empirical synthesis. Oxford University Press.

Ashburner, M., C. a Ball, J. a Blake, D. Botstein, H. Butler, J. M. Cherry, a P. Davis, K. Dolinski, S. S. Dwight, J. T. Eppig, M. a Harris, D. P. Hill, L. Issel-Tarver, A. Kasarskis, S. Lewis, J. C. Matese, J. E. Richardson, M. Ringwald, G. M. Rubin, and G. Sherlock. 2000. Gene ontology: tool for the unification of biology. Nat. Genet. 25:25–29.

Baack, E., M. C. Melo, L. H. Rieseberg, and D. Ortiz-barrientos. 2015. The origins of reproductive isolation in plants. New Phytol.

Bachtrog, D. 2013. Y-chromosome evolution: emerging insights into processes of Y-chromosome degeneration. Nat. Rev. Genet. 14:113–24. Nature Publishing Group.

Barshis, D. J., J. T. Ladner, T. a Oliver, F. O. Seneca, N. Traylor-Knowles, and S. R. Palumbi. 2013. Genomic basis for coral resilience to climate change. Proc. Natl. Acad. Sci. U. S. A. 110:1387–1392.

Benjamini, Y., and Y. Hochberg. 1995. Controlling the false discovery rate: a practical and powerful approach to multiple testing. J. R. Stat. Soc. 57:289–300.

Brown, J. D., and R. J. O'Neill. 2010. Chromosomes, conflict, and epigenetics: chromosomal speciation revisited. Annu. Rev. Genomics Hum. Genet. 11:291–316.

Bull, J. J. 1983. Evolution of sex determining mechanisms. The Benjamin/Cummings Publishing Company.

Burke, M. K., G. Liti, and a. D. Long. 2014. Standing Genetic Variation Drives Repeatable Experimental Evolution in Outcrossing Populations of Saccharomyces cerevisiae. Mol. Biol. Evol. 31:3228–3239.

Burton, R. S. 1987. Differentiation and integration of the genome in populations of the marine copepod *Tigriopus californicus*. Evolution. 41:504–513.

Burton, R. S. 1997. Genetic evidence for long term persistence of marine invertebrate populations in an ephemeral environment. Evolution. 51:993–998.

Castresana, J. 2000. Selection of conserved blocks from multiple alignments for their use in phylogenetic analysis. Mol. Biol. Evol. 17:540–552.

Charlesworth, B., J. A. Coyne, and N. H. Barton. 1987. The relative rates of evolution of sex chromosomes and autosomes. Am. Nat. 130:113–146.

Charron, G., J. B. Leducq, and C. R. Landry. 2014. Chromosomal variation segregates within incipient species and correlates with reproductive isolation. Mol. Ecol. 4362–4372.

Conesa, A., S. Götz, J. M. García-Gómez, J. Terol, M. Talón, and M. Robles. 2005. Blast2GO: a universal tool for annotation, visualization and analysis in functional genomics research. Bioinformatics 21:3674–3676.

Coyne, J. A., and H. A. Orr. 1989a. Patterns of Speciation in *Drosophila*. Evolution. 43:362–381.

Coyne, J. A., and H. A. Orr. 1997. "Patterns of Speciation in *Drosophila*" Revisited. Evolution. 51:295–303.

Coyne, J. A., and H. A. Orr. 2004. Speciation. Sinauer Associates, Sunderland, Ma.

Coyne, J. A., and H. A. Orr. 1989b. Two rules of speciation. Pp. 180–207 *in* J. A. Endler and D. Otte, eds. Speciation and its Consequences. Sinauer Associates, Sunderland, Ma.

Dobzhansky, T. 1936. Studies on hybrid sterility. II. Localization of sterility factors in *Drosophila pseudoobscura* hybrids. Genetics 21:113–135.

Dong, Y. W., T. T. Ji, X. L. Meng, S. L. Dong, and W. M. Sun. 2010. Difference in thermotolerance between green and red color variants of the Japanese Sea Cucumber, *Apostichopus japonicus* Selenka: Hsp70 and heat-hardening effect. Biol. Bull. 218:87–94.

Edmands, S. 1999. Heterosis and outbreeding depression in interpopulation crosses spanning a wide range of divergence. Evolution. 53:1757–1768.

Ellison, C. K., and R. S. Burton. 2008. Interpopulation hybrid breakdown maps to the mitochondrial genome. Evolution. 62:631–638.

Feder, J. H., J. M. Rossi, J. Solomon, N. Solomon, and S. Lindquist. 1992. The consequences of expressing hsp70 in *Drosophila* cells at normal temperatures. Genes Dev. 6:1402–1413.

Foley, B. R., C. G. Rose, D. E. Rundle, W. Leong, and S. Edmands. 2013. Postzygotic isolation involves strong mitochondrial and sex-specific effects in *Tigriopus californicus*, a species lacking heteromorphic sex chromosomes. Heredity (Edinb). 111:391–401. Nature Publishing Group.

Foley, B. R., C. G. Rose, D. E. Rundle, W. Leong, G. W. Moy, R. S. Burton, and S. Edmands. 2011. A gene-based SNP resource and linkage map for the copepod *Tigriopus californicus*. BMC Genomics 12:568. BioMed Central Ltd.

Folguera, G., D. a Bastías, J. Caers, J. M. Rojas, M.-D. Piulachs, X. Bellés, and F. Bozinovic. 2011. An experimental test of the role of environmental temperature variability on ectotherm molecular, physiological and life-history traits: implications for global warming. Comp. Biochem. Physiol. A. Mol. Integr. Physiol. 159:242–246. Elsevier Inc.

Ganz, H. H., and R. S. Burton. 1995. Genetic differentiation and reproductive incompatibility among Baja California populations of the copepod *Tigriopus californicus*. Mar. Biol. 123:821–827.

Gleason, L. U., and R. S. Burton. 2015. RNA-seq reveals regional differences in transcriptome response to heat stress in the marine snail *Chlorostoma funebralis*. Mol. Ecol. 24:610–627.

Good, J. M., M. D. Dean, and M. W. Nachman. 2008. A complex genetic basis to X-linked hybrid male sterility between two species of house mice. Genetics 179:2213–28.

Haldane, J. B. 1922. Sex ratio and unisexual sterility in hybrid animals. J. Genet. 12:101–109.

Hillis, D. M., and D. M. Green. 1990. Evolutionary changes of heterogametic sex in the phylogenetic history of amphibians. J. Evol. Biol. 3:49–64.

Hoffmann, A. a, and C. M. Sgrò. 2011. Climate change and evolutionary adaptation. Nature 470:479–485.

Hoffmann, A. a., and L. H. Rieseberg. 2008. Revisiting the impact of inversions in evolution: from population genetic markers to drivers of adaptive shifts and speciation? Annu. Rev. Ecol. Evol. Syst. 39:21–42.

Huelsenbeck, J. P., and F. Ronquist. 2001. MRBAYES: Bayesian inference of phylogenetic trees. Bioinformatics 17:754–755.

Kawecki, T. J., and D. Ebert. 2004. Conceptual issues in local adaptation. Ecol. Lett. 7:1225–1241.

Kelly, M. W., E. Sanford, and R. K. Grosberg. 2012. Limited potential for adaptation to climate change in a broadly distributed marine crustacean. Proc. R. Soc. Biol. Sci. 279:349–56.

Kofler, R., P. Orozco-terWengel, N. De Maio, R. V. Pandey, V. Nolte, A. Futschik, C. Kosiol, and C. Schlötterer. 2011a. PoPoolation: a toolbox for population genetic analysis of next generation sequencing data from pooled individuals. PLoS One 6:e15925.

Kofler, R., R. V. Pandey, and C. Schlötterer. 2011b. PoPoolation2: Identifying differentiation between populations using sequencing of pooled DNA samples (Pool-Seq). Bioinformatics 27:3435–3436.

Kuo, E. S. L., and E. Sanford. 2009. Geographic variation in the upper thermal limits of an intertidal snail: implications for climate envelope models. Mar. Ecol. Prog. Ser. 388:137–146.

Levin, D. A. 2012. The long wait for hybrid sterility in flowering plants. New Phytol. 196:666–670.

Li, H. 2011. A statistical framework for SNP calling, mutation discovery , association mapping and population genetical parameter estimation from sequencing data. Bioinformatics 27:2987–2993.

Li, H., and R. Durbin. 2009. Fast and accurate short read alignment with Burrows-Wheeler transform. Bioinformatics 25:1754–1760.

Li, H., B. Handsaker, A. Wysoker, T. Fennell, J. Ruan, N. Homer, G. Marth, G. Abecasis, and R. Durbin. 2009. The Sequence Alignment/Map format and SAMtools. Bioinformatics 25:2078–9.

Lima, T. G. 2014. Higher levels of sex chromosome heteromorphism are associated with markedly stronger reproductive isolation. 1–8.

Lowry, D. B., and J. H. Willis. 2010. A widespread chromosomal inversion polymorphism contributes to a major life-history transition, local adaptation, and reproductive isolation. PLoS Biol. 8.

Loytynoja, A. 2014. Phylogeny-aware alignment with PRANK. Pp. 155–170 *in* D. J. Russel, ed. Multiple Sequence Alignment Methods. Humana Press.

Mank, J. E., B. Vicoso, S. Berlin, and B. Charlesworth. 2009. Effective population size and the faster-X effect: empirical results and their interpretation. Evolution. 64:663–674.

Masly, J. P., and D. C. Presgraves. 2007. High-resolution genome-wide dissection of the two rules of speciation in *Drosophila*. PLoS Biol. 5:e243.

Matute, D. R., I. a Butler, D. a Turissini, and J. a Coyne. 2010. A test of the snowball theory for the rate of evolution of hybrid incompatibilities. Science (80-.). 329:1518–1521.

Mayr, E. 1942. Systematics and the origin of species, from the viewpoint of a zoologist. Harvard University Press.

Meisel, R. P., and T. Connallon. 2013. The faster-X effect : integrating theory and data. Trends Genet. 29:537–544. Elsevier Ltd.

Moyle, L. C., and E. B. Graham. 2005. Genetics of hybrid incompatibility between *Lycopersicon esculentum* and *L. hirsutum*. Genetics 169:355–73.

Moyle, L. C., and T. Nakazato. 2010. Hybrid incompatibility “snowballs” between Solanum species. Science (80-.). 329:1521–1523.

Muller, H. J. 1942. Isolating mechanisms, evolution, and temperature. Biol. Symp. 6:71–125.

Nei, M. 1972. Genetic distance between populations. Am. Nat. 106:283–292.

Noor, M. a, K. L. Grams, L. a Bertucci, and J. Reiland. 2001. Chromosomal inversions and the reproductive isolation of species. Proc. Natl. Acad. Sci. U. S. A. 98:12084–12088.

Orr, H. A. 1993a. A mathematical model of Haldane's rule. Evolution. 47:1606–1611.

Orr, H. A. 1997. Haldane's rule. Annu. Rev. Ecol. Syst. 28:195–218.

Orr, H. A. 1993b. Haldane's rule has multiple genetic causes. Nature 361:532–533.

Orr, H. A. 1995. The population genetics of speciation: the evolution of hybrid incompatibilities. Genetics 139:1805–1813.

Orr, H. A., and S. Irving. 2005. Segregation distortion in hybrids between the Bogota and USA subspecies of *Drosophila pseudoobscura*. Genetics 169:671–682.

Orr, H. A., J. P. Masly, and D. C. Presgraves. 2004. Speciation genes. Curr. Opin. Genet. Dev. 14:675–679.

Petavy, G., J. R. David, V. Debat, P. Gibert, and B. Moreteau. 2004. Specific effects of cycling stressful temperatures upon phenotypic and genetic variability of size traits in *Drosophila melanogaster*. Evol. Ecol. Res. 6:873–890.

Peterson, D. L., K. B. Kubow, M. J. Connolly, L. R. Kaplan, M. M. Wetkowski, W. Leong, B. C. Phillips, and S. Edmands. 2013. Reproductive and phylogenetic divergence of tidepool copepod populations across a narrow geographical boundary in Baja California. J. Biogeogr. 40:1664–1675.

Phillips, B. C., and S. Edmands. 2012. Does the speciation clock tick more slowly in the absence of heteromorphic sex chromosomes? Bioessays 34:166–9.

Podrabsky, J. E., and G. N. Somero. 2004. Changes in gene expression associated with acclimation to constant temperatures and fluctuating daily temperatures in an annual killifish Austrofundulus limnaeus. J. Exp. Biol. 207:2237–2254.

Presgraves, D. C. 2002. Patterns of postzygotic isolation in Lepidoptera. Evolution 56:1168–83.

Presgraves, D. C. 2008. Sex chromosomes and speciation in *Drosophila*. Trends Genet. 24:336–343.

Presgraves, D. C. and H. A. Orr. 1998. Haldane's rule in taxa lacking a hemizygous X. Science 282:952-954.

Price, T. D., and M. M. Bouvier. 2002. The evolution of F1 postzygotic incompatibilities in birds. Evolution 56:2083–9.

Pritchard, V. L., L. Dimond, J. S. Harrison, C. C. S Velázquez, J. T. Zieba, R. S. Burton, and S. Edmands. 2011. Interpopulation hybridization results in widespread viability selection across the genome in *Tigriopus californicus*. BMC Genet. 12:54. BioMed Central Ltd.

Rieseberg, L. H. 2001. Chromosomal rearrangements and speciation. Trends Ecol. Evol. 16:351–358.

Robinson, M. D., D. J. McCarthy, and G. K. Smyth. 2010. edgeR: a Bioconductor package for differential expression analysis of digital gene expression data. Bioinformatics 26:139–140.

Robinson, M. D., and A. Oshlack. 2010. A scaling normalization method for differential expression analysis of RNA-seq data. Genome Biol. 11:R25.

Sambrook, J., and D. W. Russel. 2006. Purification of nucleic acids by extraction with phenol:chloroform. Cold Spring Harb. Protoc. pdb–prot4455.

Sasa, M. M., P. T. Chippindale, and N. A. Johnson. 1998. Patterns of postzygotic isolation in frogs. Evolution. 52:1811–1820.

Schaefer, J., and A. Ryan. 2006. Developmental plasticity in the thermal tolerance of zebrafish *Danio rerio*. J. Fish Biol. 69:722–734.

Schilthuizen, M., M. Giesbers, and L. W. Beukeboom. 2011. Haldane ' s rule in the 21st century. Heredity (Edinb). 107:95–102.

Schlötterer, C., R. Tobler, R. Kofler, and V. Nolte. 2014. Sequencing pools of individuals — mining genome-wide polymorphism data without big funding. Nat. Rev. Genet. 15:749–763. Nature Publishing Group.

Schoville, S. D., F. S. Barreto, G. W. Moy, A. Wolff, and R. S. Burton. 2012. Investigating the molecular basis of local adaptation to thermal stress : population differences in gene expression across the transcriptome of the copepod *Tigriopus californicus*. BMC Evol. Biol. 12:1–17. BMC Evolutionary Biology.

Slotman, M., A. della Torre, and J. R. Powell. 2004. The genetics of inviability and male sterility in hybrids between *Anopheles gambiae* and *An . arabiensis*. Genetics 167:275–287.

Somero, G. N. 2010. The physiology of climate change: how potentials for acclimatization and genetic adaptation will determine "winners" and "losers". J. Exp. Biol. 213:912–920.

Sorensen, J. G., M. M. Nielsen, M. Kruhøffer, J. Justesen, and V. Loeschcke. 2005. Full genome gene expression analysis of the heat stress response in *Drosophila melanogaster*. Cell Stress Chaperones 10:312–328.

Städler, T., A. M. Florez-Rueda, and M. Paris. 2012. Testing for “snowballing” hybrid incompatibilities in Solanum: impact of ancestral polymorphism and divergence estimates. Mol. Biol. Evol. 29:31–34.

Tao, Y., S. Chen, D. L. Hartl, and C. C. Laurie. 2003. Genetic dissection of hybrid incompatibilities between *Drosophila simulans* and *D. mauritiana*. I. Differential accumulation of hybrid male sterility effects on the X and autosomes. Genetics 164:1383–97.

Tao, Y., and D. L. Hartl. 2003. Genetic dissection of hybrid incompatibilities between *Drosophila simulans* and *D . mauritiana*. III. Heterogeneous accumulation of hybrid incompatibilities, degree of dominance, and implications for Haldane’s rule. Evolution. 57:2580–2598.

Tao, Y., D. L. Hartl, and C. C. Laurie. 2001. Sex-ratio segregation distortion associated with reproductive isolation in *Drosophila*. Proc. Natl. Acad. Sci. U. S. A. 98:13183–13188.

Tomanek, L. 2010. Variation in the heat shock response and its implication for predicting the effect of global climate change on species’ biogeographical distribution ranges and metabolic costs. J. Exp. Biol. 213:971–979.

Tomanek, L., and G. N. Somero. 1999. Evolutionary and acclimation-induced variation in the heat-shock responses of congeneric marine snails (genus *Tegula*) from different thermal habitats: implications for limits of thermotolerance and biogeography. 202:2925–2936.

Turelli, M., and D. J. Begun. 1997. Haldane’s Rule and X-chromosome Size in *Drosophila*. Genetics 147:1799–1815.

Turelli, M., and H. A. Orr. 2000. Dominance, epistasis and the genetics of postzygotic isolation. Genetics 154:1663–79.

Turelli, M., and H. A. Orr. 1995. The dominance theory of Haldane’s Rule. Genetics 140:389–402.

Voordouw, M. J., and B. R. Anholt. 2002. Environmental sex determination in a splash pool copepod. Biol. J. Linn. Soc. 76:511–520.

Watson, E. T., and J. P. Demuth. 2012. Haldane’s rule in marsupials: what happens when both sexes are functionally hemizygous? J. Hered. 103:453–8.

Willett, C. S. 2011. Complex deleterious interactions associated with malic enzyme may contribute to reproductive isolation in the copepod *Tigriopus californicus*. PLoS One 6:e21177.

Willett, C. S. 2006. Deleterious Epistatic Interactions Between Electron Transport System Protein-Coding Loci in the Copepod Tigriopus californicus. 1477:1465–1477.

Willett, C. S. 2008a. No evidence for faster male hybrid sterility in population crosses of an intertidal copepod (*Tigriopus californicus*). Genetica 133:129–36.

Willett, C. S. 2010. Potential fitness trade-offs for thermal tolerance in the intertidal copepod *Tigriopus californicus*. Evolution. 64:2521–34.

Willett, C. S. 2008b. Significant variation for fitness impacts of ETS loci in hybrids between populations of Tigriopus californicus. J. Hered. 99:56–65.

Willett, C. S., and J. N. Berkowitz. 2007. Viability effects and not meoitic drive cause dramatic departures from Mendelian inheritance for malic enzyme in hybrids of *Tigriopus californicus* populations. J. Evol. Biol. 20:1196–205.

Willett, C. S., and J. T. Ladner. 2009. Investigations of fine-scale phylogeography in *Tigriopus californicus* reveal historical patterns of population divergence. BMC Evol. Biol. 9:139.

Yang, Z. 2007. PAML 4: Phylogenetic analysis by maximum likelihood. Mol. Biol. Evol. 24:1586–1591.

Yukilevich, R. 2013. Tropics accelerate the evolution of hybrid male sterility in Drosophila. Evolution 67:1805–14.

Zhao, L., J. Wit, N. Svetec, and D. J. Begun. 2015. Parallel Gene Expression Differences between Low and High Latitude Populations of Drosophila melanogaster and D. simulans. PLOS Genet. 11:e1005184.